Aus dem Institut für Anatomie
der Medizinischen Fakultät Charité
der Humboldt-Universität zu Berlin

DISSERTATION

Kir2 potassium channels in rat striatum are strategically localized to control basal ganglia function

Zur Erlangung des akademischen Grades
Doctor medicinae (Dr. med.)

vorgelegt der Medizinischen Fakultät Charité
der Humboldt-Universität zu Berlin

von
Harald Prüß
aus Güstrow

Dekan: Prof. Dr. Joachim W. Dudenhausen

Gutachter: 1. Prof. Dr. A. Karschin
2. Prof. Dr. R. W. Veh
3. Prof. Dr. J. Roeper

eingereicht: 16.07.2003
Datum der Promotion: 15. 03 2004

1 INTRODUCTION 6

1.1 Kir2 channels 6

1.1.1 Potassium channels 6
1.1.2 Kir – inward rectifier potassium channels 7
1.1.2.1 Kir subfamilies 9
1.1.3 Kir2 subfamily 9
1.1.3.1 Electrophysiology 10
1.1.3.2 Basic principles of inward rectification 10
1.1.3.3 Modulation 12
1.1.3.4 Distribution of Kir2 channels in the brain 13

1.2 Basal ganglia 14

1.2.1 Principle neuron and interneurons 14
1.2.1.1 Kir current in striatal spiny neurons 15
1.2.1.2 Cholinergic interneurons 15
1.2.2 Patch and matrix 16
1.2.3 Understanding the basal ganglia circuitry 17
1.2.4 Striatal regulation of movements 19
1.2.5 The therapeutic dilemma 20
1.2.6 Intention of the research 21

2 MATERIALS AND METHODS 23

2.1 Cloning 23

2.1.1 Selection of sequences 23
2.1.2 Polymerase chain reaction (PCR) 24
2.1.3 Restriction 25
2.1.4 Agarose gel electrophoresis 25
2.1.5 Determination of DNA concentration 25
2.1.6 Ligation 26
2.1.7 Generation of competent cells 26
2.1.8 Transformation 26
2.1.9 Preparation of plasmid DNA 26

2.2 Protein expression and purification 27

2.2.1 Overexpression of fusion proteins 27
2.2.2 Protein purification 27
2.2.3 SDS-Polyacrylamide gel electrophoresis (SDS-PAGE) 28
2.2.4 Preparative electrophoresis 29
2.2.5 Determination of protein content 29
2.2.5.1 BCA (Bicinchoninic acid) assay 29
2.2.5.2 Bradford assay 29

2.3 Raising of antibodies in rabbits 30

2.3.1 Immunization and blood taking 30
2.3.2 Determination of antibody titer, ELISA 30
2.3.3 Competitive ELISA 31

2.4 Purification of antibodies 31

2.4.1 Removal of IgM 31
2.4.2 Removal of cross reactivity 32
2.4.3 Affinity purification 33
2.4.4 Chromatofocussing 33
2.4.5 Concentration of antibodies 33

2.5 Characterization of antibodies 34

2.5.1 Analysis of specificity in Western Blots 34
2.5.1.1 Preparation of brain homogenates 34
2.5.1.2 Western Blotting 34
2.5.1.3 Immune detection 35
2.5.1.4 Visualization by use of alkaline phosphatase (aP) 35
2.5.2 Analysis of specificity by transfected cells 36
2.5.2.1 Liposome-mediated transfection 36
2.5.2.2 Detection of transfected cells by immunofluorescence 36

2.6 Immunocytochemistry 37

2.6.1 Perfusion fixation of rat brains 37
2.6.2 Rat brain slices for light microscopy 37
2.6.3 Rat brain slices for fluorescence microscopy 38
2.6.4 Coating of slides 38
2.6.5 Cresyl violet staining 39
2.6.6 Electron microscopy 39
2.6.6.1 Immunoreaction 39
2.6.6.2 Staining with the avidin-biotin method 39
2.6.6.3 Gold-silver-enhancement 40
2.6.6.4 Araldite embedding 40
2.6.6.5 Contrasting the ultrathin sections 41
2.6.6.6 Toluidin blue staining 41
2.6.7 Histological analysis 41

3 RESULTS 42

3.1 Preparation of monospecific and affinity-purified antibodies 42

3.1.1 Comparison of the amino acid sequences 42
3.1.2 Recombinant fusion proteins 44
3.1.3 Removal of IgM antibodies by gel-filtration 44
3.1.4 Affinity purification 45

3.2 Specificity of purified antibodies 47

3.2.1 Cross reactivity 47
3.2.2 Competitive ELISA 47
3.2.3 Western blot of fusion proteins 48
3.2.4 Western blot of rat brain homogenates 49
3.2.5 Specificity of anti-Kir2.4 antibodies 50
3.2.6 Antibody specificity in brain sections 52

3.3 Distribution of Kir2 channels in the rat brain 54

3.3.1 Olfactory system 54
3.3.2 Hippocampus 56
3.3.3 Neocortex 56
3.3.4 Basal ganglia and amygdala 59
3.3.5 Thalamus 61
3.3.6 Hypothalamus and habenula 61
3.3.7 Substantia nigra, ventral tegmental area (VTA), superior colliculus 63
3.3.8 Cerebellum and spinal medulla 63

3.4 Distribution of Kir2 channels in the striatum 68

3.4.1 Kir2 subunits are differentially distributed in the rat striatum 69
3.4.2 Anti-Kir2.2 antibodies stain striatal fiber bundles 71
3.4.3 Kir2.3 channels are predominantly localized in the matrix compartment 73
3.4.4 Kir2.4 channel subunits are localized at cholinergic interneurons 75

4 DISCUSSION 79

4.1.1 Kir2 channel proteins are differentially expressed throughout the rat brain 80
4.1.2 The Kir2.3 subunit is preferentially expressed in striatal matrix neurons 82
4.1.3 Kir2.4 immunoreactivity in the striatum is most prominently displayed by the giant cholinergic interneurons 84
4.1.4 Can Kir channel subunits be targets for novel therapeutic strategies? 85

Summary 88

References 89

Curriculum vitae 98

Publications 100

Danksagung 101
Eidesstattliche Erklärung 102

Abbreviations

aca	anterior commissure, anterior part
AcbC	core part of the nucleus accumbens
AcbSh	shell part of the nucleus accumbens
ACh	acetylcholine
aP	alkaline phosphatase
BSA	bovine serum albumin
CA1-CA3	cornu ammonis 1-3
cc	corpus callosum
CG	central gray
ChAT	choline acetyltransferase
cp	cerebral peduncle
CPu	caudate-putamen
cu	cuneate fasciculus
Cx	cortex
DA	dopamine
DAB	3,3-diaminobenzidine
DG	dentate gyrus
ELISA	enzyme-linked immunosorbent assay
Enk	Leu-enkephalin
EPl	external plexiform layer
fi	fimbria of the hippocampus
GABA	γ-amino butyric acid
Gl	glomerular layer
Glu	glutamate
GP	globus pallidus
GPe	external segment of the GP
GPi	internal segment of the GP
Gr	granule cell layer
IG	induseum griseum
ic	internal capsule
IP	interpeduncular nucleus

IPl	internal plexiform layer
ISH	*in situ* hybridization
Kir	inwardly rectifying K^+ channels
LHb	lateral habenula
lfu	lateral funiculus
LOT	lateral olfactory tract nucleus
MG	medial geniculate
MHb	medial habenula
Mi	mitral cell layer
NGS	normal goat serum
ox	optic chiasma
PBS	phosphate buffered saline
PCR	polymerase chain reaction
PD	Parkinson's disease
Pir	piriform cortex
Rt	reticular nucleus
SDS-PAGE	SDS-Polyacrylamide gel electrophoresis
sm	stria medullaris thalami
SNc	substantia nigra pars compacta
SNr	substantia nigra pars reticulate
SO	supraoptic nucleus
STN	subthalamic nucleus
STR	striatum
SubP	substance P
SuC	superior colliculus
TAN	tonically active neuron
Thal	thalamus
Tu	olfactory tubercle
vfu	ventral funiculus
VP	ventral pallidum
VTA	ventral tegmental area

1 Introduction

1.1 Kir2 channels

1.1.1 Potassium channels

The diversity of potassium-(K^+-)specific channels far exceeds any other group of ion channels. The importance of this superfamily of eucaryotic channels is underlined by the responsibility for many regulatory processes[1].

Potassium channels contain alpha subunits and in some cases auxiliary beta subunits. The alpha subunit represents the integral membrane protein responsible for the conduction of potassium ions across the lipid bilayer[2]. Based on their molecular architecture different channel classes are distinguished (Fig. 1). Most channels are referred to as voltage-gated channels (Kv). They are composed of six transmembrane (TM) helices (S1-S6) and one pore-region (P-region), resulting in the 6TM/1P class. Furthermore, the Ca^{2+}-dependent potassium channels with their additional helix, S0, belong to this class. The simplest structural plan of potassium channels is visible in the 2TM/1P class, named after their typical composition of two TM helices and one P-region and represented by the inward rectifier potassium channels (see next chapter). The class of the so-called 'background' or 'leakage' channels is made up of two P-regions, hence structurally referred to as 4TM/2P type.

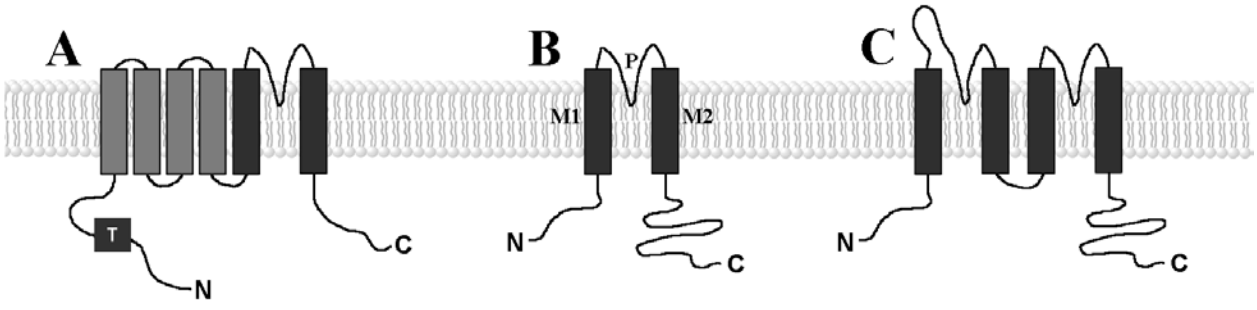

Fig. 1: Alpha-subunits of distinct potassium channel classes. A) voltage-gated (Kv) K^+ channels, B) inward rectifier (Kir) potassium channels (M1, M2: transmembrane helices, P: pore-forming region), C) 'background' or 'leakage' channels

[1] SANGUINETTI, M.C. 1997
[2] BIGGIN, P.C. 2000; MINOR, D.L. 1999

All potassium channels require a tetrameric arrangement of four P-regions to make up a K^+-selective filter. In contrast to the tetrameric association formed by the assembly of four 1P channel subunits in the plasma membrane[3], the 4TM/2P type only needs to dimerize to construct a pore.

The structural key causing potassium selectivity of potassium channels is a highly conserved stretch of eight amino acids (TXXTXGYG)[4]. This K^+ channel signature sequence with a GYG (Gly-Tyr-Gly) motif plays an essential role to selectively allow K^+ ions to pass through the pore[5]: The carbonyl oxygen atoms of the channel pore are in the precise position to substitute for the oxygen of solvating water molecules. Thus, the entering K^+ ion can strip its hydration shell at reasonably balanced energy cost. In K^+ channels, however, the carbonyl oxygen atoms of the selectivity filter are not narrow enough to allow dehydration of the smaller Na^+ ion.

1.1.2 Kir – inward rectifier potassium channels

Inwardly **r**ectifying **K**$^+$ (Kir) channels represent the minimal requirement for a potassium channel, however, it is involved centrally in physiological functions. The Kir current was first observed electrophysiologically in frog sceletal muscle by KATZ in 1949[6] and named an anomalous rectifier due to its unique properties, which were in contrast to the known voltage-dependent delayed-rectifier K^+ channels. In recent years K^+ channel genes were discovered encoding channels whose properties verify his original measurement[7]. In 1993, the primary sequence of Kir channels was identified by HO et al. who cloned the ROMK gene transcribed from an mRNA sequence from rat kidney cells.

The Kir superfamily contains at least 15 members in six distinct subfamilies (Kir1, Kir2, Kir3, Kir5, Kir6, Kir7) that respond to many types of regulation. In the usual terminology, members are designated Kirx.y, whereas „x“ determines the subfamily and „y“ names the subtype within the subfamily[8]. Kir subunit cDNAs encode proteins between 327 and 501

[3] GLOWATZKI, E. 1995
[4] ISOMOTO, S. 1997; MINOR, D.L. 1999; MACKINNON, R. 1998
[5] REIMANN, F. 1999; DOYLE, D.A. 1998; TAGLIALATELA, M. 1994
[6] KATZ, B. 1949; HODGKIN, A.L., HUXLEY, A.F., KATZ, B. 1952
[7] DOUPNIK, C.A. 1995; ISOMOTO, S. 1997
[8] MINOR, D.L. 1999; CHANDY and GUTMAN 1995; JAN, L.Y. 1997

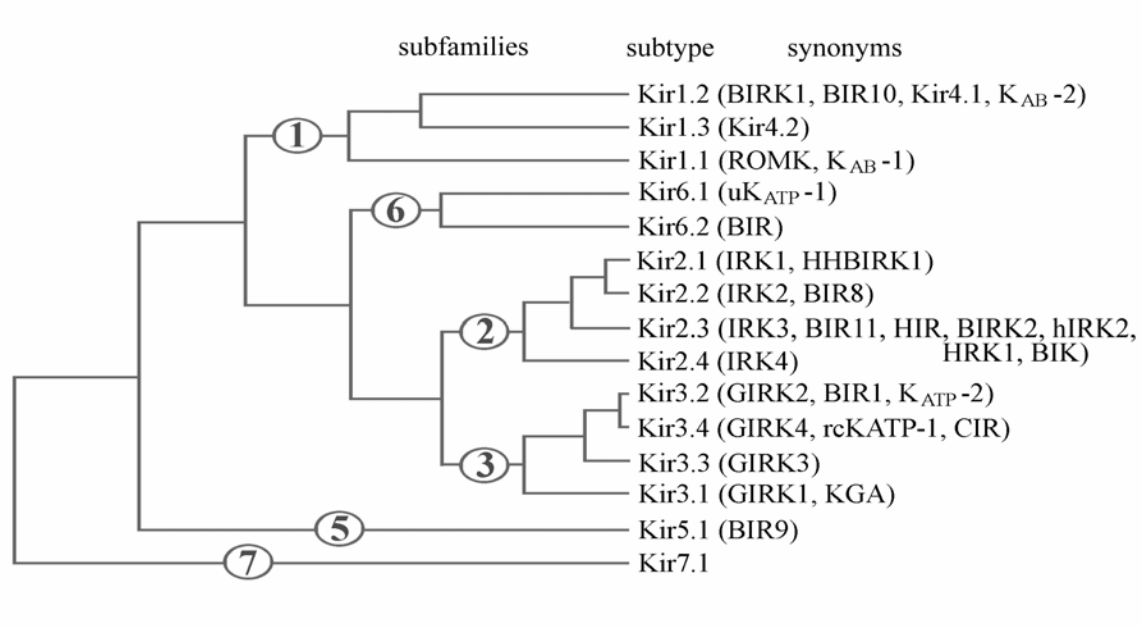

Fig. 2: Dendrogram of the Kir family. Subfamilies, subtypes and former names. (modified from Reimann and Ashcroft 1999)

amino acids in length. As shown in the dendrogram (Fig. 2), the channel proteins share about 30-40% homology among the Kir subfamilies and >60% within the subfamilies.

The electrophysiological properties of Kir channels include the conduction of more current in the inward than in the outward direction. This is due to a reduced open probability in a depolarized membrane. Hyperpolarization above the K^+ equilibrium potential hardly occurs under physiological conditions at the mammalian plasmamembrane. Consequently, despite their name, Kir channels primarily conduct outward potassium currents.

Due to their peculiar properties in a particular cell, Kir channels have a key role in stabilizing the resting membrane potential. The Kir-mediated outward fluxes prevent action potential firing by small electrical stimuli. In case of strong electrical stimuli, however, these channels close and allow action potentials, thereby preventing massive K^+ loss. Furthermore, modulation of these channels can alter the membrane potential, cellular excitability and heart rate, information processing and secretion of neurotransmitters or hormones[9].

[9] CHUANG, H. 1997; ISOMOTO, S. 1997, REIMANN, F. 1999

1.1.2.1 Kir subfamilies

Very different physiological functions are assigned to Kir channels originating in the diversity of these proteins. Aside from differential cellular expression the diverse subset of Kir channel subtypes determines the pattern of electrical properties.

The Kir1 subtype is a Kir channel with weak inward rectifying properties that is involved in transepithelial membrane transport, predominantly in the kidney, where it is important in homeostasis by conducting large amounts of potassium. Kir3 channels are the predominant mediators of metabotropic inhibition and are activated directly by Gβγ subunits. They influence electrical activity in neuronal, cardial and neurosecretory cells[10]. Kir4 is known to control K^+ homeostasis in glial cells and the inner ear[11]. ATP-sensitive Kir6 (K_{ATP}) channels play an important role in the pancreas; they influence the control of insulin secretion[12] in interaction with SUR (sulphonylurea receptor) subunits. Moreover, this channel may contribute to the cell survival during anoxia or hypoglycaemia in neuronal and cardiac structures.

1.1.3 Kir2 subfamily

Recent investigations produced extensive information about the molecular structure, electrophysiology, modulation and localization of the Kir2 inward rectifier potassium channels. They form tetramers of four identical (homomeric) or related (heteromeric) subunits that each contains two putative membrane spanning regions M1 and M2 (Fig. 1B). The transmembrane segments form alpha helices where M1 makes up the outer and M2 the inner helix[13]. M1 as well as M2 flank a highly conserved pore-forming region called H5 – at this side the Kir2 subfamily shows sequence differences at only one amino acid residue (Fig. 7). In addition to the common molecular motif, a homotetrameric association of subunits is a crucial structural hallmark of Kir2 channels. Kir2.1 is an exception to the rule: it forms heteromultimers if coexpressed with Kir4.1[14].

[10] DOUPNIK, C.A. 1995; KRAPIVINSKY, G. 1995
[11] ISHII, M. 1997; HIBINO, H. 1997, RUPPERSBERG, J.P. 2000
[12] SAKURA, H. 1995
[13] YANG, J. 1995; MINOR, D.L. 1999
[14] RAAB-GRAHAM, K.F. 1998; FAKLER, B. 1996

1.1.3.1 Electrophysiology

The rectification property of the "classical" inward rectifying potassium channels (Kir2) includes the following components: 1) Inwardly rectifying channels show a linear conductance below the K^+ equilibrium potential (Fig. 3). 2) The outward conductance in physiological conditions helps to stabilize the resting potential[15]. 3) Negligible outward currents during depolarization prevent massive potassium loss and allow prolonged depolarization (plateau of an action potential)[16].

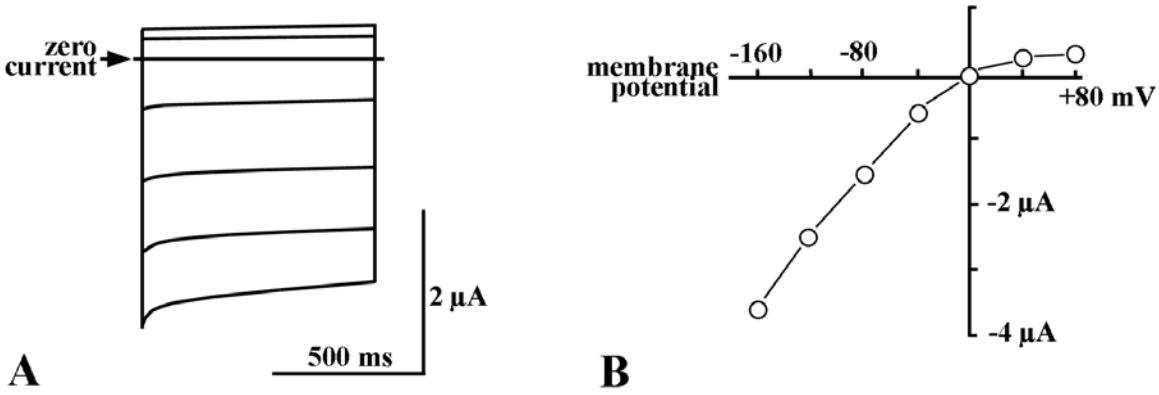

Fig. 3: Inwardly rectifying currents recorded from a Xenopus oocyte expressing a Kir channel. Experimental conditions with symmetrical K^+ concentrations. A) Current traces elicited by voltage steps from 0 mV (holding potential) to +80, +40, 0, -40, -80, -120 and –160 mV. B) Current-voltage relationship of the peak currents recorded from the same oocyte.

Therefore, in theory cells with many of these constitutively active Kir channels and no additional regulation should have a relatively constant resting membrane potential, and, in case of depolarization, they may initiate action potentials with a long-lasting plateau[17].

1.1.3.2 Basic principles of inward rectification

The ability of the strongly rectifying Kir2 channels to prevent potassium outflow was originally thought to be the effect of an intracellular Mg^{2+}-mediated blockade[18]. Cations enter the channel pore and impede K^+ efflux. Subsequent investigators postulated the intrinsic rectification caused by soluble factors different from Mg^{2+}. Detailed

[15] REIMANN, F. 1999; RAAB-GRAHAM, K.F. 1998
[16] ISOMOTO, S. 1997; KUBO, Y. 1993
[17] ISOMOTO, S. 1997
[18] KUBO, Y. 1993

characterization identified them being polyamines[19] (products of L-ornithine metabolism: putrescine, spermidine, spermine). Spermine functions in switching Kir channels off in case of significant depolarization. The Mg^{2+} block is evidently faster than the polyamine effect, thus decreasing the channel-open probability[20].

Experiments focusing on combination of Mg^{2+}-mediated block and intrinsic polyamine gating revealed a competition between these ions. The finding led to the assumption that these substances bind at the same single site of the Kir channel[21]. Mutagenesis studies have

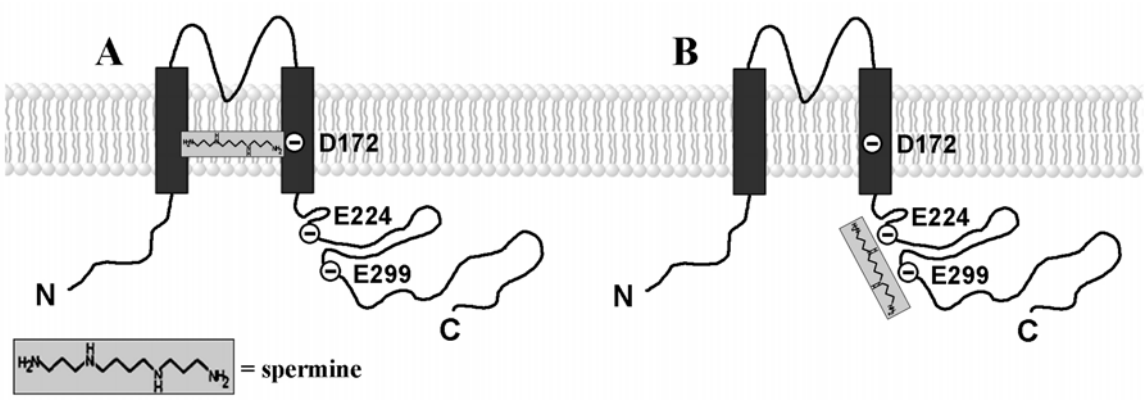

Fig. 4: Model of channel block by polyamines. A) Spermine and Mg2+ directly block the pore by binding at residue D172. B) E224 and E299 are discussed controversially: spermine binding at residue E224 leads to a high affinity blocking complex (Lee et al. 1999), or intermediate binding at E224+E299 level facilitates the entry of spermine but does not plug the pore (Kubo and Murata 2001).

characterized at least two negatively charged amino acid residues as regulators of inward rectification (Fig. 4, 5). Aspartic acid D172 in the second transmembrane domain (M2) as well as the widely separated aspartic acid D260, glutamate E224 and E299 in the C-terminal region seem to be key positions in the strong inward rectifier Kir2[22].

A recent X-ray crystallography analysis reveals many amino acids lining the pore yet to be altered by mutagenesis[23]. Their further conclusions display the voltage-dependent rectification in a simple fashion: The lining of the cytoplasmic pore contains polar, negatively charged amino acid side chains interspersed with hydrophobic amino acid side chains. These amino acids exactly match with polyamines, which are long chains of positive amino groups separated by hydrophobic spacers.

---

[19] LOPATIN, A. 1994; FAKLER, B. 1995
[20] DOUPNIK, C.A. 1995; RUPPERSBERG, J.P. 2000
[21] YAMASHITA, T. 1996
[22] YANG, J. 1995; LU, Z. and MACKINNON, R. 1994; STANFIELD, P.R. 1994, LEE, J.-K. 1999, KUBO, Y. and MURATA, Y. 2001
[23] NISHIDA, M. AND MACKINNON, R. 2002

1.1.3.3 Modulation

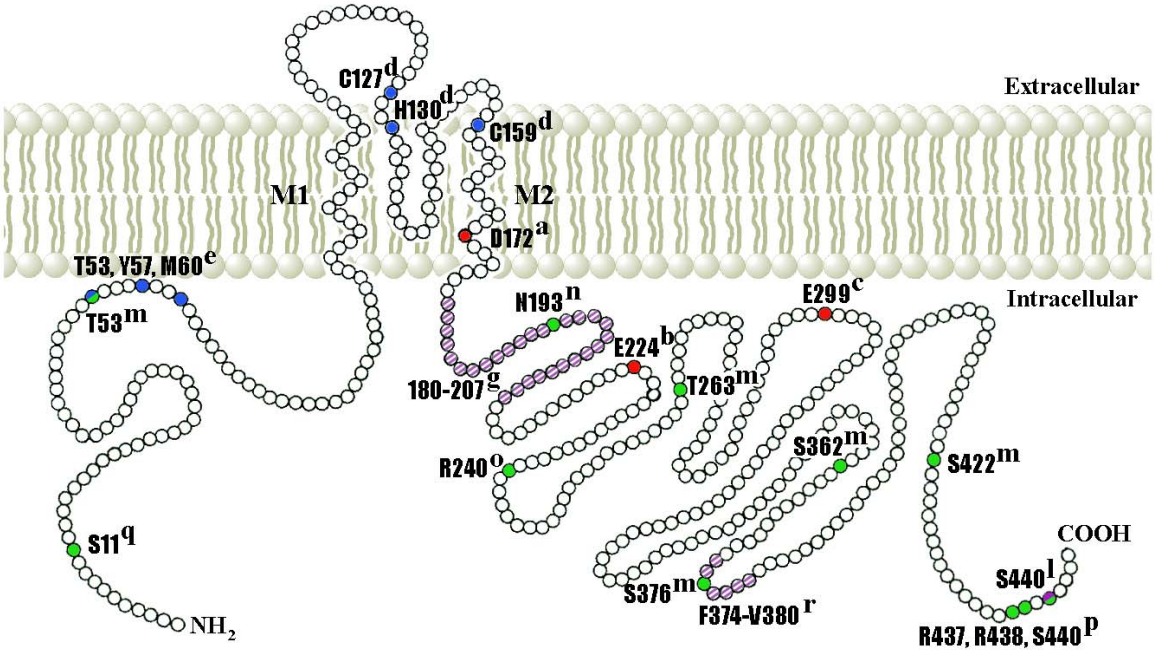

Fig. 5: Synopsis of Kir2 channel modulations. For detailed explanation of (a) to (r) see table 1.

Despite their rather simple structure, members of the Kir2 subfamily play a central role in many physiological processes. They depend prominently on multiple regulators[24] such as pH, G-proteins, kinases, polyamines, nucleotides and phospholipids, but also on pharmaceutical products like the immunosuppressant cyclosporin A[25]. Due to the complexity of modulators, a synopsis is given (Fig. 5) summarizing the most important factors with their site of interaction. Moreover, it underlines the extraordinary significance of this information with respect to normal and pathophysiological conditions.

[24] ISOMOTO, S. 1997; REIMANN, F. 1999; QU, Z. 1999/2000; COHEN, N.A. 1996; ZHU, G. 1999; HUANG, C.-L. 1998; COULTER, K.L. 1995; NAMBA, N. 1996; WISCHMEYER, E. 1998
[25] CHEN, H. 1998

Table 1: Kir2 channel modulators.

modulator	channel effect	Kir2.1	Kir2.2	Kir2.3	Kir2.4	reference
$Mg2^+$, spermine	inward rectification	+ (r)				Yang 1995, Lee 1999 Lee 1999 Kubo 2001
pH extracellular	inhibition			+ (r)	+ (h)	Hughes 2000
pH intracellular	inhibition	– (r)		+ (r)		Qu 1999, Qu 2000
ATP	inhibition	–		+		Collins 1996
PIP_2	activation	+ (r)				Huang 1998
G-protein	suppression	–		+		Cohen 1996b
M1 ACh receptor	inhibition	–		+		Chuang 1997
$5HT_{1A}$	inhibition	+				Cohen 1996a
Substance P	suppression					Stanfield 1985
PSD-95 binding	cytosceletal binding	+		+		Cohen 1996a
PKC phosphorylation	decreased activity	+		+ (r)	+ (h)	Kir2.1: Doupnik 1995, Kir2.3: Zhu 1999b, Kir2.4: Hughes 2000
Asn glycosylation	glycosylation				+ (h)	Hughes 2000
tyrosine kinase	phosphorylation				+ (h)	Hughes 2000
cAMP/cGMP dependent	phosphorylation			+ (r)	+ (h)	Kir2.3: Cohen 1996a Kir2.4: Hughes 2000
endoplasmic reticulum	ER-export consensus sequence FxYENEV	+ (r)				Stockklausner 2001

+ = effect, – = no effect, (r) = rat, (h) = human

1.1.3.4 Distribution of Kir2 channels in the brain

Kir2 channels are expressed by diverse cells including neuronal cells, myocytes, blood cells, sceletal muscle fibers, macrophages, osteoclasts, endothelial and placental cells[26]. Most information about distribution of Kir channels is based on *in situ* hybridization experiments[27]. In general, Kir2 mRNAs are widely distributed throughout the rat brain. Kir2.1, Kir2.2 and Kir2.3[28] are expressed in dentate gyrus, olfactory bulb, caudate putamen, and piriform cortex (see discussion). Kir2.1 and Kir2.3 are less prominent in thalamus, cerebellum and brainstem, where Kir2.2 displays a prominent expression pattern. The Kir2.4 subunit[29] seems to be strongly expressed in several nuclei of medulla and brainstem.

[26] DOUPNIK, C.A. 1995; PERILLAN, P.R. 2000; RAAB-GRAHAM, K.F. 1998; FALK, T. 1995; KARSCHIN, C. 1999; KOYAMA, H. 1994
[27] MORISHIGE, K.-I. 1993; HORIO, Y. 1996; KARSCHIN, C. 96; BREDT, D.S. 95; TÖPERT, C. 98; FALK, T. 95
[28] KARSCHIN, C. 1999; KARSCHIN, C. 1996; HORIO, Y. 1996; FALK, T. 1995
[29] TÖPERT, C. 1998; TÖPERT, C. 2000

So far, only few studies investigated the distribution of Kir proteins in the mammalian brain by using specific antibodies[30]. Up to date, available data are largely restricted to brain nuclei at the cellular level. Consequently, a more detailed localization at the subcellular and regional level in cells linked to physiological or clinical questions are to the fore.

1.2 Basal ganglia

The basal ganglia are a major neural system of subcortical telencephalic brain nuclei. They are involved in movement disorders, motivated behavior and drug addiction; they are strongly interconnected with each other as well as linked to most elements of the mammalian brain. The main structures are the striatum (STR, caudate nucleus and putamen), pallidum (GP), substantia nigra (pars compacta (SNc) and pars reticulata (SNr)), ventral tegmental area (VTA) and subthalamic nucleus (STN). The pallidum is further divided into an external pallidum (GPe, corresponding to the globus pallidus in rat) and an internal segment (GPi, corresponding to the entopeduncular nucleus in rat).

1.2.1 Principle neuron and interneurons

Simple neuroanatomical techniques (cresyl violet) characterize the homogeneous structure of the striatum, predominantly composed of medium-sized spiny neurons and perforated by numerous fiber bundles. Using axon tracing and immunocytochemistry, the neostriatum seems to be a complex mosaic of connections, cell morphologies and neurochemical markers. Aside from spiny projection neurons, at least four classes of interneurons contribute to the neuronal framework.

The principal *medium-sized spiny neuron* represents over 90% of neurons in the rodent neostriatum[31]. The cell bodies range from 12-20 μm in size and these projection cells show the highest spine density in the brain and have highly collateralized axons. Since the

[30] RAAB-GRAHAM, K.F. 1998; COHEN, N.A. 1996; PERILLAN, P.R. 2000
[31] KAWAGUCHI, Y. 1995, WILSON, C. 1998

spiny neurons are the main output of the striatum, the principal neuron is the primary circuit element. In addition, most of the incoming axons target their spines.

After identification as projection cells in the 1970s, the projections of spiny neurons were examined. Approximately one half of these cells forms the *direct pathway* (see chapter 1.2.3.), while the remaining neurons project via the *indirect pathway*[32]. Both subpopulations form GABAergic synapses, but these two classes of spiny neurons are different in their cytochemical profile containing either enkephalin or substance P[33]. No preferential distribution is present in the striatum.

1.2.1.1 Kir current in striatal spiny neurons

Medium spiny neurons move between two membrane states, referred to as the down-state and the up-state[34]. During the down-state, the membrane potential remains at relatively hyperpolarized potentials (-85 mV) and the spiny cells do not generate action potentials. In contrast, during the episodes of depolarization (up-state) the membrane potential resides just below threshold (-60 mV) and action potential discharge may occur[35]. The transition to the depolarized state depends on temporally coherent activity.

The membrane conductance in the hyperpolarized down-state is mainly determined by inwardly rectifying Kir2 potassium channels[36]. These channels help to hold the neuron close to the K^+ equilibrium potential. Thus, the Kir current reduces the effect of temporally or spatially isolated excitatory synaptic input and acts like a barrier for asynchronous excitatory potentials. In up-states, the influence of Kir channels is minimal due to their inward rectification properties.

1.2.1.2 Cholinergic interneurons

Up to 60 µm in length, *cholinergic interneurons* are the main source of the high acetylcholine (ACh) levels in the striatum and neurotransmission of these cells is of central importance for the final striatal output. The giant interneurons account for less than

---

[32] PARENT, A. 2000; GERFEN, C. 1992; AIZMAN, O. 2000
[33] PENNY, G.R. 1986; KITA, H. 1988; GROENEWEGEN, H.J. 1996; KAWAGUCHI, Y. 1990
[34] WILSON AND KAWAGUCHI 1996; NICOLA 2000
[35] NISENBAUM, E.S. 1995; WILSON, C. 1993
[36] NICOLA, S.M. 2000; MERMELSTEIN, P.G. 1998

2% of cells in the striatum. They can be identified by staining for choline acetyltransferase (ChAT)[37], the enzyme for synthesis of the transmitter acetylcholine from acetyl-CoA and choline. Communication between the striatal compartments (see chapter 1.2.2.) is thought to be performed by very extensive axonal fields and widespread dendritic trees of cholinergic interneurons. Due to their tendency to preferentially arborize in the matrix, the cholinergic cells seem to transmit information from the patch to the spiny projection neurons in the matrix[38] that represent the main synaptic target of cholinergic interneurons. Aside from some dopaminergic input, cholinergic interneurons are mainly innervated by cortical and thalamic projections[39].

The capability of firing irregularly in a spontaneous tonic pattern named these cells tonically active neurons (TANs). In contrast to spiny neurons, the cholinergic cells integrate the effects of only a small numbers of afferent axons[40]. TANs exhibit a pause in firing, which is thought to represent the physiological correlate of motor learning and rewarded movements[41]. Therefore, cholinergic neurons play a pivotal role for striatal output and learning in normal and pathophysiological conditions.

1.2.2 Patch and matrix

Both in the primate and rodent neostriatum, two compartments can be distinguished. The so-called *cell islands* in primates correspond to *striosomes = patches* in the rat, where they occupy approximately 10% of striatal space[42]. The areas surrounding the patches are called *matrix*. The compartmental organization can be distinguished using biochemical markers such as transmitters, related enzymes or metabolites, and transmitter binding and uptake sites. The patchy organization of μ-opiate receptors as first reported by PERT et al. in 1976 provided an excellent and constant marker of the patch compartment in the embryonic, young and adult rat, and throughout both the dorsal and ventral striatum[43]. Another marker is acetylcholinesterase (AChE) that is more intensively detectable in the

[37] BOLAM, J.P. 1984
[38] VAN VULPEN, E.H.S. 1998; KAWAGUCHI, Y. 1995
[39] CALABRESI, P. 2000; WILSON, C.J. 1998
[40] WILSON, C. 1998; KAWAGUCHI, Y. 1995
[41] BENNETT, B.D. 2000; WATANABE, K. 1998; KAWAGUCHI, Y. 1995; RAZ, A. 1996
[42] TRYTEK, E.S. 1996; WILSON, C. 1998; BOLAM, J.P. 1988
[43] PERT, C.B. 1976; HERKENHAM, M. and PERT, C.B. 1981; DESBAN, M. 1993; CABOCHE, J. 1991

matrix. The AChE-poor striosomes form three-dimensional labyrinths and correspond to the μ-opiate receptor patches[44].

With respect to the neurochemical differences of patch and matrix, it seems plausible to assume functional heterogeneity. Separate sets of dopamine midbrain neurons target the two compartments, respectively. Dopaminergic afferents from part of the SN project to striosomes, whereas much of cell group A8 (retrorubral area) projects to the matrix[45]. It suggests a differential regulation between striosome-related versus matrix-related basal ganglia circuits.

Outputs are as distinct as inputs: neurons from the matrix project to the SNr via direct and indirect pathway. In contrast, patches preferentially project to dopaminergic nigrostriatal neurons in the SNc (Fig. 6). They may either inhibit dopaminergic neurons in SNc, or disinhibit them through inhibition of GABAergic interneurons.

The local axon collaterals of spiny neurons as well as their dendrites are restricted to the compartment of their parent cell body[46]. In contrast, dendrites of cholinergic interneurons cross the compartments. Their axon collaterals are denser in the matrix, whereas cell bodies and dendrites are approximately equally distributed[47].

1.2.3 Understanding the basal ganglia circuitry

Observations of humans afflicted with degenerative diseases of basal ganglia were essential for the understanding of the basic circuitry. Diseases related to basal ganglia include Parkinson's disease (PD), Tourette's syndrome, schizophrenia, Huntington's chorea and hemiballism.

Parkinson's disease is the most frequent disorder of the basal ganglia caused by loss of dopaminergic neurons and resulting depigmentation in the substantia nigra. Typical features are extreme underactivity, poverty of movement (hypokinesia), infrequency of swallowing, abnormal postural reflexes, absence of arm swing in walking and reduced velocity of movement (bradykinesia) up to inability to walk forwards (freezing). Also firm

[44] GRAYBIEL, A. 1990
[45] DAHLSTROM, A. and FUXE, K. 1964; GRAYBIEL, A. 1990; EBLEN, F. 1995; SURMEIER, D.J. 1996
[46] GERFEN, C. 1992; WILSON, C. 1998
[47] KAWAGUCHI, Y. 1995; GRAYBIEL, A. 1990

and tense muscles (rigidity) and a low-frequency resting tremor are seen in many patients, often beginning in one limb and spreading to one side[48].

Both the features of the disease and the success of available therapies can be understood to a remarkable degree, when the neuronal circuits are considered, on which movements are based. Cerebral cortex and basal ganglia are the main structures of movement planning and program selection (Fig. 6).

Neuronal transmission through the basal ganglia is performed in circuits. Beginning at the cerebral cortex most information enters the basal ganglia at the level of the striatal projection neurons. The axons form asymmetrical excitatory glutamatergic synapses primarily on the head of dendritic spines. Afterwards, the circuit continues to the GABAergic neurons located in GPi (entopeduncular nucleus in rats) and SNr. This so-called *direct pathway* facilitates a certain movement. Another half of spiny projection neurons make use of an alternative route also including GPe and STN (*indirect pathway*). It suppresses a movement in contrast to the direct pathway. Glutamatergic projections from the subthamalic nucleus to GPi/SNr are thought to excite the GPi, consequently increasing pallidal inhibition of the thalamus[49]. Both GPe and STN influence all striatal structures and are affected by cortical and thalamic projections[50].

From GPi/SNr the circuit proceeds to the output nuclei of basal ganglia, i.e. ventral anterior, ventromedial and mediodorsal thalamic nuclei and superior colliculus. These structures are under tonic GABAergic inhibition by pallidal and nigral spontaneous firing. Finally, the cortex receives excitatory input from this complex circuit.

This model of circuitry contains multiple parallel basal ganglia-thalamocortical circuits (motor, oculomotor, dorsolateral prefrontal, lateral orbitofrontal and anterior cingulate). Depending on the cortical input, three striatal territories were distinguished (motor, associative and limbic or ventral striatum)[51]. Neither the striatal subdivision nor the specific loops are supposed to be considered as strictly bordered or without neuronal interactions. Recent studies[52] suggest an information flow through the basal ganglia not by segregated parallel circuits, but by an ascending spiral interconnecting different functional regions.

---

[48] BERGMANN, H. 1998
[49] GROENEWEGEN, H.J. 1996; KAWAGUCHI, Y. 1990
[50] PARENT, A. 2000; PARENT, A. 1990; GROENEWEGEN, H.J. 1996
[51] ALEXANDER, G.E. 1986, 1990; BAEV, K.V. 1995; JOEL, D. and WEINER, I. 2000; FLAHERTY, A.W. 1991
[52] HABER, S.N. 2000

Information flow proceeds from limbic to associative, further to motor domains of the striatum via the midbrain dopamine cells. Each component disinhibits the next step in the spiral and inhibits itself by a feedback loop.

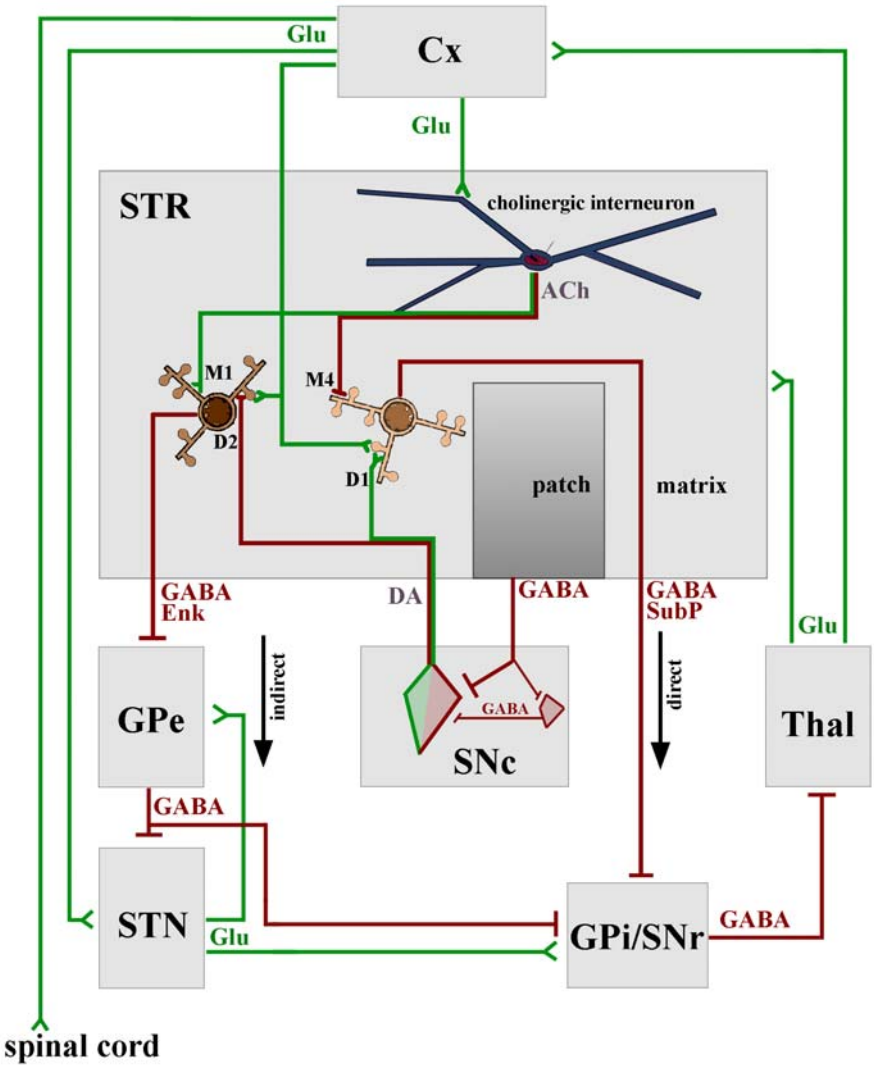

Fig. 1: Schematic representation of the neuronal circuitry underlying basal ganglia function. For details see text.

1.2.4 Striatal regulation of movements

Basal ganglia seem to play a selecting rather than initiating role in motor activity. Neuronal activity in the striatum is thought to be a "movement template" whose occurrence could become facilitated or suppressed. To perform a certain movement, inhibition of GPi/SNr is essential (Fig. 6). Therefore, activation of the direct pathway as well as suppression of the indirect pathway is required to interrupt the tonic pallidal/nigral

inhibition. Consequently, this *disinhibition* of thalamic neurons would result in excitation of the cortex and the appearance of motor action.

The efficacy of the direct and indirect pathway is regulated by two striatal key structures: the patch compartment and the cholinergic interneuron.

The dopaminergic neurons of the substantia nigra pars compacta (SNc) target spines of striatal projection neurons and are thought to control the cortical inputs synapsing on the same spine head[53]. The SNc neurons facilitate the direct pathway via D1 receptors and inhibit the indirect pathway via D2 receptors, thus synergistically favoring movements. The dopaminergic SNc neurons are controlled by the patch compartment, emphasizing the striking functional differences between the two striatal areas.

In contrast, giant cholinergic interneurons facilitate the indirect pathway via muscarinic M1 receptors and inhibit the direct pathway via M4 receptors. In animal models of Parkinson's disease, persistent oscillatory activity of cholinergic interneurons can be seen instead of normal tonic firing, underlining the functional and clinical relevance of these neurons[54].

1.2.5 The therapeutic dilemma

Effective therapies to treat the motor impediments in Parkinson´s disease described above have been available for a long time. Presently, therapeutic intervention in younger patients starts with dopamine agonists, which often improve the motor impediments. With progression of the disease addition of L-dopa (L-dihydroxy-phenylalanine) is necessary and very effective even in advanced states of the disease. The traditional choice of cholinergic antagonists is less important today and restricted to the relief of tremor. It remains essential, however, in order to achieve a marked improvement in dyskinesia during neuroleptic therapy. However, even an excellent therapeutic regime implies a medical dilemma: many side effects are the patient's price for temporary motor improvement. Dryness of the mouth, blurring of vision and constipation are the first troubles in many patients making use of anticholinergics, and nausea as well as sickness are the primary problems under L-dopa therapy.

---

[53] CEPEDA, C. 1998; GRAYBIEL, A.M. 1990; BERGMANN, H. 1998; GERFEN, C.R. 1989; GROVES, P.M. 1995
[54] RAZ, A. 1996

L-dopa application also causes more troublesome complications. Induction of involuntary movements such as grimacing, lingual-labial dyskinesia and restlessness, limits the use. Consequently, therapeutic skill is required to maintain the fine balance between a mobile patient and some degree of dyskinesia. Hallucinations, confusion and impairment of memory limit the advantages of cholinergic antagonists. Moreover, long-term treatment cannot prevent the advance of Parkinson's disease, and finally, L-dopa therapy causes severe dose-response fluctuations (on-off-phenomenon) as well as uncontrollable dyskinesia, thus terminating the pharmacological management.

1.2.6 Intention of the research

Current therapies of Parkinson's disease as described above rely on manipulation of transmission at these striatal key positions. Other targets have to be found to develop new therapeutic strategies for treating motor deficits. In principle, every step of the signal transduction cascade seems to be a possible approach for new pharmacological regimes. Special attention must be paid to those biological functions, which are performed by a variety of effector proteins in different cell types. This diversity may allow addressing individual neurons and individual neuronal circuits separately.

With respect to their enormous diversity (see chapter 1.1.3.3.), potassium channels may represent suitable targets for therapeutic intervention. The success of this type of strategy is well documented in cases like the treatment of cardiac arrhythmias and diabetes (see discussion). For the treatment of Parkinson's disease or related disorders, however, promising effects may be expected only if the channels are selectively or at least predominantly expressed in one of the key motor structures. Only in this case, selective channel activation or inhibition may specifically influence the outcome of movements.

In a first step to throw light on the possible involvement of Kir2 channels in striatal pathways, the present study aimed to:

(1) analyze the protein distribution of all members of the Kir2 channel subfamily in the rat brain.

(2) study whether members of the Kir2 channel protein family, if present in the rat basal ganglia, display a similar or distinct basal ganglia localization.

(3) learn whether any member of the Kir2 subfamily is predominantly found at the striatal key motor structures.

It may be expected that the results of this study increase the understanding of specific interactions that take place in the striatum and ultimately determine the output of the basal ganglia. The knowledge of the detailed pattern of Kir2 channel distribution is necessary to understand electrophysiological influences at the subcellular level as well as the processing within the striatum. Consequently, the study may be helpful in further examinations to clarify how a disturbed striatal circuitry causes the symptoms of diseases of the basal ganglia.

2 Materials and Methods

2.1 Cloning

2.1.1 Selection of sequences

Selection of suitable sequences of the amino acid order is necessary to produce highly specific antibodies to investigated channel proteins. I gratefully appreciate the cDNAs of Kir2.1 to Kir2.4 supplied to me by Wischmeyer (2.1), T. Falk (2.3), Kurachi (2.2) and C. Töpert (2.4).

Table 2: vectors

	Kir2.1	**Kir2.2**	**Kir2.3**	**Kir2.4**
accession code	L48490	X78461	X87635	AJ003065
species	rat	rat	rat	rat
vector of original DNA	pSVSport 1	Bluescript(SK–)	Bluescript(SK+)	pSVSport
number of amino acids	427	427	445	434

The suitable sequences were determined by comparing the homologies between the potassium channels of the Kir2 subfamily (Fig. 7). It was shown by use of the program DNASIS that the greatest difference in amino acid sequence exists at the carboxy-terminal fragments. Consequently, selection of this region is most promising for raising subtype specific antibodies. Selected 50-70 amino acids (Fig. 7) were subcloned into two different vectors. The first vector was used to produce the fusion protein for rabbit immunization and subsequent antibody production, whereas the second vector was utilized for antibody purification (see table 3).

MacDNASIS 03.02 - Hitachi Software Engineering America, USA

vectors:

pGEX-4T-1 - Pharmacia Biotech, Sweden

pQE-40, pet32b - Qiagen, Hilden

Table 3: Primer and restriction enzymes (restriction sites underlined)

	Kir2.1	Kir2.2	Kir2.3	Kir2.4
amino acid sequence	376-427	372-421	372-439	395-434
sequence 5´-Primer	TAG GAT CCC AAA GAG GAA GAG GAC AGT (27-mer)	CA TGC GGT ACC CTA GCC TTC CTG AGC (26-mer)	CA TGC GGT ACC TTG GCC CTC ATG AGC (26-mer)	TGT CAT CTC GAG GAA GGG GTG TCA (24-mer)
sequence 3´-Primer	CGC GCT CGA GTC ATA TCT CCG ATT CTC (27-mer)	TA ATT AAG CTT GTA GGG CCG CTC AAG (26-mer)	TA ATT AAG CCT GTA AGA AAT GTT GTC (26-mer)	AGA ATG GAT CCG CGC TGA GCT GCT (24-mer)
expression vector				
for immunization	pGEX-4T-1	pQE40	pQE40	pGEX-4T-1
for affinity purification	pet32b	pet32b	pet32b	
restriction sites	BamHI XhoI	Asp718 HindIII	Asp718 HindIII	XhoI BamHI

2.1.2 Polymerase chain reaction (PCR)

Polymerase chain reaction is a process of DNA amplification, where the nucleic acid helix is heated and melted into single strands. At appropriate annealing temperatures the added primers hybridize to their respective strand and act as the starting point for DNA polymerase. Multiple repetitions of this process generate amplification of the selected Kir2 DNA sequences.

PCR mixture for 100 µl:
3 µl plasmid DNA (0.5 µg)
1.5 µl 5´ primer (150 µM)
1.5 µl 3´ primer (150 µM)
1.5 µl dNTP mix (25 mM)
10 µl 10x PCR buffer
80.5 µl H_20

+ 2 µl Pfu-polymerase (2.5 U)

PCR cycle:

1. Denaturation	45 sec at 95°C
2. Hot start	addition of polymerase
3. Primer binding	45 sec at 61°C
4. Strand synthesis	20 sec at 72°C
5. Stop	45 sec at 95°C
6. Repetition from 3.	(25 cycles)
7. End	60 sec at 56°C
	10 min at 72°C

The PCR product was cleaned with the "Qiagen PCR Purification Kit". The successful amplification was further controlled by using electrophoresis on agarose gels and sequenced for confirmation of the correct nucleic acid sequence.

Thermocycler, Omn-E - Hybaid, USA

Pfu-polymerase, 10x PCR buffer - Stratagene, USA

dNTP mix(2´-Desoxyribonucleotid-5´-triphosphat, A,C,T,G) - Boehringer, Mannheim

Primer - MWG-Biotech, Ebersberg

2.1.3 Restriction

Addition of corresponding restriction enzymes to the DNA (vector and insert) results in its being cut at the available restriction sites (see table 3). Therefore, compatible "sticky ends" were generated in both vector and PCR product that become connected in the subsequent ligation. Restriction was performed at 37 °C for 90 minutes and followed by purification of DNA with "Qiagen PCR Purification Kit" / user's manual.

HindIII, Asp, BamHI - MBI Fermentas (Latvia), Boehringer, Mannheim

2.1.4 Agarose gel electrophoresis

To control the successful restriction, the PCR products were separated in 2 % and the uncut vector in 8 % agarose gel (with 0.5 µg/ml ethidium bromide) in 1x TAE. Electrophoresis was run at 100 V. During this process ethidium bromide intercalates into the DNA and thus, DNA bands can be visualized due to fluorescence under ultraviolet light.

1 x TAE: 40 mM Tris acetate, 1mM Na_2EDTA, pH 7.6 in H_2O

Agarose - Biozym, Hess.Oldendorf

Ethidium bromide - Sigma, USA

Marker - MBI Fermentas, Latvia

6 x Sample buffer - MBI Fermentas, Latvia

Electrophoresis chamber - Kreutz Laborgeräte, Reiskirchen

Power supply unit, Power Pac 200 - Bio-Rad, USA

2.1.5 Determination of DNA concentration

Concentration of DNA was calculated from the optic density OD_{260nm}, measured against water. Double stranded DNA of a 50 µg/ml concentration has a value of 1. The quotient from OD_{260nm} to OD_{280nm} indicates the purity of the DNA. Values greater than 1.8 are indicative of highly purified DNA.

UV-Photometer UV-1202 - Shimadzu, Japan

2.1.6 Ligation

Ligation was performed overnight at 15 °C mixing vector DNA and insert DNA. T4-DNA ligase was then inactivated by incubation at 65 °C for 10 minutes.

Ligation mixture:

10 µl vector DNA

12 µl insert DNA

3 µl 10 x ligase buffer - *MBI Fermentas, Latvia*

5 µl T4-DNA ligase (1 U/µl) - *MBI Fermentas, Latvia*

filled up with Millipore H_2O to 30 µl

2.1.7 Generation of competent cells

20 ml LB culture medium were incubated with competent bacteria. During the phase of logarithmical growth – at OD_{600nm} between 0.4 and 0.6 at 37 °C on a shaker – cells were extracted and centrifuged for 10 minutes at 5000 x g and 4 °C. The pellets were resolved in 20 ml ice-cold and autoclaved $CaCl_2$ solution (70 mM $CaCl_2$, 10 mM Tris, pH 8.0) and placed on ice for an hour. After new centrifugation for 10 minutes at 5000 x g and 4 °C bacteria were resolved in 2 x 1 ml $CaCl_2$ solution and stored on ice. Finally, bacteria were frozen in liquid nitrogen and stored at -80 °C.

LB-Medium - Gibco Brl, Life Technologies, GB

Centrifuge - Beckman, USA

2.1.8 Transformation

A mixture of 100 µl of competent cells with 20 µl ligated DNA was incubated on ice for 20 minutes under repeated careful shaking, followed by heating in water at 42 °C for 90 seconds and cooling down for 2 minutes on ice. This procedure led to transformation of DNA into competent cells. Afterwards 1 ml LB culture medium was added and the mixture was shaken for 45 minutes at 37 °C. The transformed cells were crossed out on LB Agar (50 µg/ml Ampicillin) in dilutions from 100-10 µl, overnight at 37 °C.

LB-Agar - Gibco Brl, Life Technologies, GB

Ampicillin sodium - Grünenthal, Stolberg Preparation of plasmid DNA

Individual grown clones on the agar plate were selected and each brought into 4 ml LB culture medium (100 µg/ml Ampicillin) and incubated at 37 °C over night. Purification was performed with the "Qiagen Qiaprep SpinPlasmid Kit" (principle of alkaline lysis). Afterwards correctness of transformation was controlled with restriction of the plasmid (same procedure as after ligation) and separation in agarose gel electrophoresis.

2.2 Protein expression and purification

2.2.1 Overexpression of fusion proteins

Successfully transformed clones grew in 6 ml LB each (+ampicillin) at 37 °C overnight on the shaker (230 rpm), were brought into 500 ml LB culture medium and matured to an OD_{600} of 0.5-1. The protein expression was induced by adding 1 mM final concentration IPTG (Isopropyl-β-D-thiogalactosid; Roth, Karlsruhe) and subsequent shaking for 4 hours. Finally, cells were harvested with the centrifuge at 5000 g for 20 minutes at 4 °C.

2.2.2 Protein purification

The pellet of expressed protein was resolved in 1 x PBS (for pGEX vector) or lysis buffer (for PQE-40 and pet32b vector) and lysed by sonification and addition of Trition X-100 (only pGEX vector) to a final concentration of 1 % while being shaken for 60 minutes. Afterwards cell debris was precipitated by centrifugation at 10000 x g for 30 minutes. Glutathione-Sepharose 4b (for pGEX vector) or Ni-NTA solution (for PQE-40 and pet32b vectors) was added to the supernatant containing the solved proteins. The suspension was incubated at room temperature for 60 minutes and then washed 5 times in PBS on a column. Eventually the proteins were eluted 5 times with 500 µl glutathione buffer (pGEX vector) or elution buffer (PQE-40 and pet32b vectors). The proteins were dialysed against PBS at 4° C overnight.

Lysis buffer:	NaH_2PO_4, pH 8	50 mM	Glutathione buffer:	
	NaCl	300 mM	Glutathione	10 mM
	Imidazol	10 mM	Tris-HCl, pH 8	50 mM

Washing buffer = Lysis buffer with 20 mM Imidazol

Elution buffer = Lysis buffer with 250 mM Imidazol

Glutathione-Sepharose 4B - Pharmacia, Sweden

Ni-NTA - Qiagen, Hilden

2.2.3 SDS-Polyacrylamide gel electrophoresis (SDS-PAGE)

The method of LAEMMLI (1970) was used for electrophoretical separation of proteins on 10 % or 12 % SDS-PAGE polyacrylamid gels. The probes were dissolved in 4 x Laemmli buffer and heated at 95 °C for 5 minutes. Gels were loaded with the probes and a marker (Fig. 8). Separation of proteins was performed at 100 V in the stacking gel and at 200 V in the separation gel in the gel chamber filled with 1 x running buffer (0,3 % Tris/HCl, 1.44 % glycine, 0.1 % SDS).

	12% separation gel	4% stacking gel
30% Acrylamid	3.88 ml	810 µl
2% Bisacrylamid	1.8 ml	375 µl
5x separation/collection gel buffer	2 ml separation gel buffer (Tris 1.88 M, SDS 0.5%, pH 8.8)	1 ml collection gel buffer (Tris 630 mM, SDS 0.5%, pH 6.8)
H_2O	2.32 ml	2.815 ml
APS (10%)	50 µl	25 µl
TEMED	10 µl	5 µl

4 x Laemmli buffer:

10 % (w/v) ß-Mercaptoethanol
4 % (w/v) SDS
2 % (w/v) Bromphenolblau
20 % (w/v) Glycerol
250 mM Tris-HCl, pH 6.8

Electrophoresis chamber Mini-Protean II - Bio-Rad, USA

LMW Standard - Pharmacia Biotech, Sweden

Power supply unit, Power Pac 200 - Bio-Rad, USA

Rainbow protein molecular weight marker - Amersham Life Science, UK

TEMED (N,N,N′,N′,-Tetramethylethylendiamin) - Bio-Rad, USA

Visualization of protein bands was done by heating the gels in Coomassie Blue for 10 minutes in the microwave and subsequent decolorization by heating in water several times until the bands demarcate.

Coomassie Blue:	Serva Blue G-250	0.025%
	Acetic acid	10%
	Ethanol	50%

2.2.4 Preparative electrophoresis

Electro elution was used for the exact purification of the proteins. Thus, protein was separated in a big preparative SDS gel and stained with Coomassie. The visualized bands were cut with a scalpel and brought into an electro elution chamber. The proteins were eluted at 100 V overnight in elution buffer (25 mM Tris, 192 mM glycine, 0.025% SDS).

Electro elution chamber, S&S Biotrap - Schleicher&Schüll, Dassel

Maxigel chamber, Protean IIxi Cell - Bio-Rad, USA

2.2.5 Determination of protein content

2.2.5.1 BCA (Bicinchoninic acid) assay

40 µl of each protein probe was mixed with 400 µl BCA solution (BCA solution A:B = 50:1) and incubated for 30 minutes at 60 °C. The same procedure was used with a standard row of BSA (bovine serum albumine, 0-200 µg/ml) in PBS. Afterwards extinctions were measured at 550 nm and the protein concentrations calculated from the standard values.

BCA solution A:	BCA-Dinatrium	25.8 mM
	Na_2CO_3	160 mM
	Na_2-Tartrat	7 mM
	NaOH	100 mM
	$NaHCO_3$	113 mM
BCA solution B:	$CuSO_4x5H_2O$	160 mM

2.2.5.2 Bradford assay

In a manner similar to that used with the BCA assay, a standard row and the protein solution were solved in 800 µl probe buffer and subsequently mixed with 200 µl 5 x

staining solution (Rotiquant). After 10 minutes the probes were measured at 595 nm in a photometer and the protein concentration calculated from the standard values.

2.3 Raising of antibodies in rabbits

2.3.1 Immunization and blood taking

For each fusion protein two 4-5 months old "New Zealand white" rabbits were immunized with either 90 or 180 µg of the produced protein. Therefore, 500 µl or 1000 µl antigen were injected intracutaneously after shaving the injection sites. To increase the immune reaction the protein solutions was mixed with an adjuvant and two booster immunizations were performed after an interval of 3-4 weeks.

Immunization solution:

Complete Freund's adjuvant (CFA)	1.25 ml	*Sigma, USA*
Antigen (360 µg) in PBS	750 µl	

Before the first injection a blood sample was taken (preimmune serum) and starting with day 35, 30 ml blood were taken weekly from the rabbit ear. The blood coagulated overnight at 4 °C and the separated serum was centrifuged at 2500 x g. The complement system was inactivated by heating for 1 hour at 56 °C and the sample was stored at –80°C. After 12 weeks the animals were killed by cervical dislocation and exsanguinated, the blood was processed as described above.

2.3.2 Determination of antibody titer, ELISA

Determination of antibody titer is mandatory to observe and follow the production of antibodies. The "enzyme-linked immunosorbent assay" (ELISA) is an adequate method. Micro titer plates are coated with antigen and subsequently incubated with the antibody whose concentration should be determined. A secondary antibody is added onto the plates after the washing process, and a staining reaction visualizes the amount of primary antibody.

Table 4: ELISA

Procedure:			
Antigen coating	100 µl	1 µg/ml in coating buffer[1]	15 h
Saturation of unspecific bindings	150 µl	saturation solution[2] pH 7.2	1 h
Primary antibody (e.g. serum)	100 µl	diluted in saturation solution	2 h
Washing (3x)	200 µl	PBS	
Secondary antibody	100 µl	peroxidase-conjugated AB goat-anti-rabbit, 1:1000 in 1mg/ml PBS-Hb	
Washing (3x)	200 µl	PBS	
Visualization	100 µl	incubation solution[3] pH 4.2	5 min
Stop	100 µl	block solution (0.1% sodium azide)	
Measurement of extinctions at 450 nm			

[1]	50 mM	Na_2CO_3 in water, pH 9.6			
[2]	50 mM	$NaH_2PO_4xH_2O$	[3]	50 mM	$NaH_2PO_4xH_2O$
	150 mM	NaCl		100 mM	$NaCH_3CO_2x3H_2O$
	0.05%	Tween 20		1 mg/ml	ABTS
	0.02%	Sodium azide		0.88 mM	H_2O_2
	1 mg/ml	Hemoglobin			

ELISA-Micro plate, Falcon3912 - Becton Dickinson, USA

ELISA Photometer, Dynatech MR 5000 - Dynatech Laboratories, USA

P-GaR (goat anti rabbit antibody) - Vector, USA

2.3.3 Competitive ELISA

This special modification of ELISA is preceded by preincubation of the antibodies for 2 hours with different antigens in varying concentrations (10 µg – 0.1 ng). The results indicate both the affinity of antibodies (decrease of extinctions, see Fig. 12) and the absent cross reactivity to other antigens.

2.4 Purification of antibodies

2.4.1 Removal of IgM

For all experiments only antibodies of the immunglobuline class G (IgG) were used, because only this class can be detected with the secondary antibodies used. Furthermore, included antibodies of the IgM class would cause undesirable background in the immunohistochemical experiments. Therefore, IgM antibodies were removed using a Superdex-200 column: 2.5 ml rabbit serum from the fractions with the highest antibody

titer were pumped through the column. The bigger IgM molecules move faster through the porous agarose beads than the smaller IgG antibodies. The resulting fractions with the highest titer were detected due to their extinctions (Fig. 9) and pooled (circa 10 x 2 ml).

Fraction collector FC 203 B - Abimed Gilson, USA

Peristalsis pump Minipuls 3 - Abimed Gilson, USA

Photometer 112, UV/VIS Detector - Abimed Gilson, USA

Column Superdex 200 prep grade - Pharmacia Biotech, Sweden

Writer BD 111 - Kipp & Zonen / Sci-Tec Instruments, Canada

2.4.2 Removal of cross reactivity

The IgM-purified serum was tested for cross reactivity to the fusion part of the immunization protein, to bacterial surfaces and to other Kir channels. In case of cross reactivity, the serum was incubated with the detected undesirable antigens.

The antibodies to the fusion part[55] and to bacterial structures were removed by applying a bacterial suspension (expression of bacteria with only the fusion part, centrifugation for 15 minutes at 4000 g, treatment with 0.5 % formaldehyde and autoclave). The bacterial suspension was added to the 1:100 in PBS-Hb diluted serum, the amount having been determined in previous experiments (Fig. 10), incubated overnight at 4 °C and centrifuged for 15 minutes at 4000 g. The supernatant contains the wanted antibodies.

After determination of cross reactivity to closely related Kir channels, these antibodies were removed. Therefore, nitrocellulose membranes were coated with the cross reacting antigen[56] overnight (2-8 µg/ml in PBS, according to previous experiments). Free binding sites were then saturated with 5 % NGS (normal goat serum) in PBS for 3 hours and the membranes incubated with the serum. Thus, the desirable antibodies were able to bind. Finally, the supernatant was checked again for cross reactivity (Fig. 11)

NGS, goat serum - PAN Systems, Aidenbach

Nitrocellulose - Schleicher & Schuell, Dassel

[55] POMPÉIA, C. 1996
[56] VEH, R.W. 1995

2.4.3 Affinity purification

Affinity purification is performed in a manner similar to that used for removing of cross reactivity by coating nitrocellulose membranes with antigen overnight (2 µg/ml in PBS). Therefore, however, the second fusion protein[57] was used which is the Kir channel fragment cloned into the pet32b vector (see table 3). The membranes were washed three times with PBS and unspecific bindings blocked with 5 % NGS in PBS for 1 hour, followed by incubation with the serum (1:100 in 5 % NGS) for 4 hours. The membranes were washed again three times with PBS and eluted for 30 minutes[1]. Finally, the elution was dialysed against 20 mM phosphate buffer (pH 6) overnight.

[1] Elution buffer (pH 2,5 with HCl) = Glycine 200 mM, NaCl 150 mM, BSA 1 mg/ml

2.4.4 Chromatofocussing

Determination of the isoelectric point of antibodies is mandatory for a pH dependent concentration of antibodies. Therefore, an anion exchange column (PBE-94 material) is used which separates different proteins according to their varying charge. The column was equilibrated above the expected isoelectric point with 10 ml loading buffer (25 mM Ethanolamine, pH 9.4) and loaded with 5 ml affinity purified antibody solution that was dialysed against loading buffer. The column was then rinsed with 10 ml loading buffer and eluted with 25 ml Polybuffer (pH 6.0). The elution was collected in 0.5 ml fractions. The pH of the fractions with the highest affinity to the antigen (ELISA) determined the isoelectric point of the antibodies.

PBE 94, Polybuffer exchanger - Pharmacia, Schweden

Polybuffer 96-CH3COOH - Pharmacia, Schweden

2.4.5 Concentration of antibodies

The antibody concentration was increased using a SP-Sepharose cation exchange column. The sulfopropyle groups of the sepharose material bind positively charged proteins above a pH of 2. The column was equilibrated with 20 ml loading buffer (20 mM phosphate

[57] PITT, J.C. 1998

buffer, pH 6.0). The column was then loaded with affinity purified antibodies that are positively charged at pH 6. Finally, 200 µl-fractions were eluted with a basic buffer (200 mM Na_2CO_3, pH 9.0) by detaching the antibodies due to the negative charge. The fractions were checked by ELISA for antibody titer and the richest were pooled and dialysed.

SP-Sepharose Fast flow - Pharmacia, Schweden

2.5 Characterization of antibodies

2.5.1 Analysis of specificity in Western Blots

2.5.1.1 Preparation of brain homogenates

Brains were rapidly dissected from deeply anesthetized (ether) adult Wistar rats (5-9 weeks) and rapidly frozen on dry ice. 2 ml of homogenization buffer were added per gram of rat brain and the solution was homogenized 10 times in a Dounce homogenizer. The homogenate was centrifuged at 4 °C for 10 minutes at 600 x g to remove cell debris and nuclei, and the supernatant was centrifuged at 100.000 x g for 10 minutes to pellet membranes. The pellet which contains cell membranes and organelles was resuspended in homogenization buffer.

Dounce homogenizer - Wheaton, USA

Homogenization buffer		added before use:	
Saccharose	250 mM	Aprotinin	2 µg/ml
Hepes; pH 7.4	4 mM	Pepstatin A	1 µg/ml
EDTA	1 mM	Leupeptin	1 µg/ml
Na-azide	5 mM	PMSF	0.5 mM

2.5.1.2 Western Blotting

Proteins were separated on an SDS gel and transferred to nitrocellulose membranes using the BioRad semidry blot device which is constructed as follows:

- anode
- 3 layers of 3 MM Whatman paper
- nitrocellulose
- SDS gel

- 3 layers of 3 MM Whatman paper
- cathode

The Whatman paper and the nitrocellulose were previously rinsed in semidry buffer. Blotting was performed at 300 mA / gel for 30 minutes. After transfer, the proteins were visualized on the membrane by using Ponceau S-solution. The nitrocellulose membranes were cut in strips containing single protein lanes and totally decolorized in PBS.

Semidry buffer	
Tris	48 mM
Glycine	390 mM
SDS	0.04% (w/v)
Methanol	20% (v/v)

Ponceau S-solution	
trichloric acid	3%
Ponceau S	400 mg/l

2.5.1.3 Immune detection

The unspecific binding sites at the membranes were saturated using 5 % low-fat milk in PBS containing 0.1 % Tween-20 for 1 hour. The primary antibody solution (anti-Kir2.1 [1:1000], anti-Kir2.2 [1:500], anti-Kir2.3 [1:500], anti-Kir2.4 [1:5000] in 5 % milk/PBS/0.1 % Tween-20) was added and incubated overnight at 4 °C. The blots were washed 5 times in PBS/0.1 % Tween-20 (1 hour in total) and the secondary antibody was added (1:500-1:1000 in PBS/0.1 % Tween-20) for 2-3 hours. Thereafter, the membranes were washed again 5 times in PBS/0.1 % Tween-20 and developed.

2.5.1.4 Visualization by use of alkaline phosphatase (aP)

The aP-conjugated secondary antibody was visualized using the substrate NBT/BCIP (Nitro Blue Tetrazolium / 5-bromo-4-chloro-3-indolyl phosphate).

Procedure:

The blots were incubated in 10 ml aP-development solution for 2-25 minutes depending on visualization intensity. The reaction was stopped by washing with PBS.

aP-development solution:	
Tris; pH 9.5	100 mM
$MgCl_2$	50 mM
NaCl	150 mM
added before use:	
NBT (75 mg/ml in 700 µl DMF + 300 µl H_2O)	50 µl/10 ml
BCIP (50 mg/ml in 1ml DMF)	37.5 µl/10 ml

2.5.2 Analysis of specificity by transfected cells

2.5.2.1 Liposome-mediated transfection

African green monkey COS-7 kidney cells were cultured at 5 % CO_2 in Dulbeccos modified Eagle medium supplemented with 10 % fetal calf-serum on 6-well-dishes containing four glass plates. At 60 % confluence cells were transiently transfected using lipofectin-DNA solution and incubated for 6 hours. After adding serum-containing medium, cells were incubated for 48-72 hours at 37 °C.

Production of lipofectin-DNA solution from solution A and B:

Solution A: 1-2 µg DNA diluted in 100 µl serum free medium per transfection

Solution B: 2-10 µl lipofectin were diluted in 100 µl SFM

Both solution were incubated for 30-45 minutes at room temperature, mixed carefully and incubated for another 10-15 minutes at room temperature. The lipofectin-DNA solution was then used for transfection.

lipofectin - Gibco Brl, Life Technologies, GB

2.5.2.2 Detection of transfected cells by immunofluorescence

Cells were washed in PBS followed by fixation in 4 % phosphate-buffered formaldehyde and three washing steps with PBS. After blocking for 1 hour at room temperature in 5 % normal goat serum (NGS) in PBS containing 2 % BSA and 0.3 % Triton-X-100, cells were incubated with the primary antibody for 2 h at 37 °C (in 5 % NGS/ 2 % BSA/ 0.3 % Triton). Subsequently, cells were washed 3 times in PBS, incubated with the secondary antibody (fluorescent Oregon Green 488-goat anti-rabbit IgG 1:200, diluted in PBS/ 2% BSA/ 0.3 % Triton) for 2 hours at room temperature and washed again with PBS. Coverslips were mounted with moviol 4-88 containing 2.5 % of 1,4-diazobicyclo-[2.2.2]-octane as anti-fading substance and viewed using fluorescence microscopy at 488 nm.

Oregon Green 488-goat anti-rabbit IgG 1:200 - Molecular Probes, USA

moviol 4-88 - Hoechst, France

1,4-diazobicyclo-[2.2.2]-octane - DABCO; Sigma, Munich

2.6 Immunocytochemistry

2.6.1 Perfusion fixation of rat brains

Adult Wistar rats were deeply anesthetized with ether, injected with muscle relaxant and coagulation inhibitor (ketamine, rompun and heparin adapted to body weight) and perfused transcardially with:

- plasma substitute (Longasteril, Fresenius) for 10 seconds at 210 torr
- PGPIC for 5 minutes at 210 torr
- PGPIC for 25 minutes at 20 torr and
- sucrose solution for 5 minutes.

Brains were dissected out, embedded in 2 % agarose in sucrose solution, and cut transversely into 2-3 mm thick sections. Brains were cytoprotected in 10 % sucrose for 1 hour and in 30 % sucrose overnight, frozen in hexane at –60 °C, attached to cork plates and stored at –80 °C until use.

PGPIC (fixation solution), pH 7.4

paraformaldehyde	4% (w/v)
$NaH_2PO_4xH_2O$	100 mM
glutaraldehyde	0.05% (w/v)
picric acid	0.37%

sucrose solution, pH 7.4

sucrose	146 mM
$NaH_2PO_4xH_2O$	100 mM

2.6.2 Rat brain slices for light microscopy

For light microscopy, frozen brain blocks were cut into 20 µm cryosections on a microtome and rinsed several times in PBS. After treatment with 1 % sodium borohydride in PBS for 15 minutes to remove excessive aldehydes and two washing steps with PBS for 15 minutes, sections were preincubated in 10 % NGS in PBS containing 0.3 % Triton-X-100 and 0.05 % phenyl hydrazine to reduce the endogenous peroxidases. Sections were washed subsequently three times in PBS, followed by incubation for 36 h at 4 °C in the primary antibody solution (rabbit anti-Kir2.1 [1:400], anti-Kir2.2 [1:100], anti-Kir2.3 [1:100], anti-Kir2.4 [1:5000] in 10 % NGS in PBS containing 0.3 % Triton-X-100, 0.1 % sodium azide and 0.01 % thimerosal). Sections were washed in PBS two times for 20 and 40 min, preincubated for 1 h in PBS-A (2 mg BSA/ ml PBS) and incubated for 16 h at room temperature in the secondary antibody solution (biotinylated goat anti-rabbit IgG 1:2000 in PBS-A containing 0.3 % Triton-X-100 and 0.1 % sodium azide). After two washing steps in PBS, preincubation for 1 hour in PBS-A and incubation in 1:1000 avidin-

biotin-complex (10 µl Elite A dissolved in 10 ml PBS-A, 10 µl Elite B added) for 6 h at RT, sections were washed three times in PBS (10, 20 and 30 minutes), followed by a preincubation in DAB-solution (0.5 mg DAB in 1 ml 50 mM Tris-buffer, pH 7.6, containing 10 mM imidazole) for 15 min. Sections were visualized by adding ammonium nickel sulfate (0.3 % final concentration) and H_2O_2 (0.015 % final concentration) for 3 min. Finally, they were washed several times in PBS, mounted onto gelatin-coated slides, dried for 30 minutes, dehydrated in increasing alcohol concentrations, brought into xylol, and coverslipped with entellan. In control experiments, the primary antibody was preabsorbed with 10 µg specific antigen per 1 ml antibody solution.

Elite A (avidin) - Vector Laboratories, USA

Elite B (biotinylated peroxidase) - Vector Laboratories, USA

DAB solution (3,3-diaminobenzidine) - Sigma, Munich

2.6.3 Rat brain slices for fluorescence microscopy

For fluorescence microscopy, frozen brain blocks were cut into 20 µm cryosections on a microtome and rinsed in PBS. After treatment with 1 % sodium borohydride in PBS for 15 minutes and two washing steps with PBS for 15 minutes, sections were incubated in 10 % NGS in PBS containing 0.3 % Triton-X-100 to saturate unspecific binding sites. Slices were incubated for 36 h at 4 °C in the primary antibody solution (rabbit anti-Kir2.4 [1:5000] in 10 % NGS in PBS containing 0.3 % Triton-X-100, 0.1 % sodium azide and 0.01 % thimerosal). Sections were washed in PBS two times for 20 and 40 min, preincubated for 1 h in PBS-A (2 mg BSA/ ml PBS) and incubated for 16 h at room temperature in the secondary antibody solution (fluorescent anti-rabbit IgG in PBS-A containing 0.3 % Triton-X-100 and 0.1 % sodium azide). Slices were washed again 3 times in PBS and, finally, coverslipped with moviol 4-88.

2.6.4 Coating of slides

Glass slides were washed thoroughly (dishwasher), dived into warm gelatine solution for 3 minutes and dried for 2-3 days at room temperature in a dust-free environment.

Production of gelatine solution:

15 g gelatine and 1.76 g potassium chromosulfate-12-hydrate were diluted at 70 °C in 630 ml H_2O. 300 ml 100 % ethanol and 70 ml acetic acid were then added and the solution filtered.

2.6.5 Cresyl violet staining

Microtome sections were coated on glass slides, dried for 30 minutes and dehydrated in 70 % ethanol overnight. The slides were washed for 2 minutes in H_2O and stained in cresyl violet solution for 20-30 minutes. Afterwards, they were washed again for 2 minutes in H_2O, dehydrated in increasing ethanol concentrations (70 %, 86 %, 96 %, 100 % I, 100% II for 5 minutes each), brought into xylol, and coverslipped with entellan.

Cresyl violet solution

cresyl violet acetate	0.2% (w/v)
acetic acid	20 mM
pH 4.0 with NaOH, always filter before use	

2.6.6 Electron microscopy

2.6.6.1 Immunoreaction

For electron microscopy, frozen brain blocks (stored at -80 °C) were thawed in 30 % sucrose in PBS. 40 µm slices were sectioned on a vibratome at 4 °C and rinsed several times in PBS. Sections were incubated with antibodies as in paragraph 2.6.2., with one exception: Triton-X-100 (0.1 % final concentration) was added only to the 0.05 % phenyl hydrazine preincubation solution. Sections were visualized for 10 min by adding 0.015 % H_2O_2 but omitting nickel ions.

Composition of secondary antibody solution:

biotinylated 2° AB	1:2000	in PBS-A with 0.1% Na-azide
0.8 nm gold-labeled 2° AB	1:40	in PBS with 0.1% BSA-C; 0.1% Tween und 0.1% NaN_3

2.6.6.2 Staining with the avidin-biotin method

After two washing steps in PBS and incubation for 1 hour in PBS-A, sections were incubated with the avidin-biotin complex for 6 hours at room temperature. Slices were washed three times in PBS (10, 20 and 30 minutes), followed by a preincubation in DAB-

solution (0.5 mg DAB in 1 ml 50 mM Tris-buffer, pH 7.6, containing 10 mM imidazole) for 10-12 minutes. Sections were visualized by adding H_2O_2 (0.015 % final concentration) for 3 minutes (without ammonium nickel sulfate). After thoroughly washing in PBS, the tissue was embedded in araldite.

2.6.6.3 Gold-silver-enhancement

In the experiments in which a gold-labeled secondary antibody was used, the slices were washed 10, 20 and 30 minutes in PBS-Tween (0.05 % Tween 20), followed by a 15 minutes fixation step in 2 % glutaraldehyde in PBS. After a short rinsing in PBS, the sections were washed 5 times in 150 mM $NaNO_3$ solution and silver-enhanced in the dark for 25 minutes. The sections were washed a few times in PBS and fixed in 2 % glutaraldehyde for 10 minutes, rinsed again in PBS and subjected to the following araldite embedding.

2.6.6.4 Araldite embedding

Slices were post-fixed with 1 % osmium tetroxide in PBS for 15-30 minutes, washed in phosphate buffer (100 mM $NaH_2PO_4xH_2O$; pH 7.4 with NaOH), dehydrated through graded ethanol and block stained with 2 % uranyl acetate in 70 % EtOH for 10 min at 4 °C. The sections were dehydrated again in graded ethanol (3 x 70 % EtOH, 2 x 95 %, 3 x 100 %), transported into propylene oxide twice for 5 minutes and incubated overnight in the propylene oxide/ araldite mixture. Afterwards, the slices were incubated 2 x 2 hours in the embedding solution and embedded in araldite between two sheets of Aclar plastic. The polymerization of the araldite was performed for 24-60 hours at 65 °C. Finally, the regions of interest were cut and glued to a carrier plastic.

Ultrathin (60-80 nm) and semithin tissue sections (800-1000 nm) were cut alternately with a diamond knife and the ultrathin sections were collected on copper grids for electron microscopy.

Aclar plastic - Ted Pella, USA

Diatome diamond knife

Araldite solution: Araldite and DDSA were intensively mixed in a ratio of 30:24.

Propylene oxide / araldite mixture: 55 g araldite solution was mixed with 1.5 ml DMP-30 and 50 ml propylene oxide.

Embedding solution: 100 g araldite solution was intensively mixed with 2 ml DMP30.

2.6.6.5 Contrasting the ultrathin sections

The sections were counterstained for 5 minutes with 5 % uranyl acetate in water, intensively washed in water, incubated for 5 minutes in lead citrate solution and washed again thoroughly in water. Thereafter the sections were examined with a transmission electron microscope.

transmission electron microscope - EM 900, Zeiss

lead citrate solution

lead citrate	1.33 g in 50 ml
sodium citrate	1,76 g auf 50 ml
pH 12.0 with NaOH	

2.6.6.6 Toluidin blue staining

The semithin tissue sections were dried on glass slides and stained for 2-5 minutes in toluidin blue solution. They were then rinsed with H_2O and and coverslipped with entellan.

Toluidin blue solution; pH 9.35

$Na_2B_4O_2 \times 10H_2O$	1% (w/v)
Toluidin blue	1% (w/v)
sucrose	40% (w/v)

2.6.7 Histological analysis

The nomenclature of Paxinos and Watson for the rat brain[58] is used throughout this report to refer to anatomical structures.

[58] PAXINOS, G. and WATSON, CH. 1998

3 Results

3.1 Preparation of monospecific and affinity-purified antibodies

3.1.1 Comparison of the amino acid sequences

Functional Kir2 channels are formed by tetrameric association of subunits. Each subunit contains two membrane-spanning regions M1 and M2. They flank a highly conserved pore-forming loop called H5. In order to produce specific antibodies against individual members of the Kir2 family, unique amino acid segments are needed. Comparison of the complete sequences of the Kir2 subfamily (Fig. 7) shows strong homology between the members in the transmembrane domains, the pore region and the adjoining cytoplasmic amino acids (shaded red). The most significant differences exist at the carboxyl terminal regions, making them the best target for antibodies. These less conserved sequences (42-68 amino acid residues, shaded gray in Fig. 7) were selected as fusion proteins for subsequent cloning and then for raising of polyclonal antibodies in rabbits.

The selected sequences were also searched for homologies with other proteins using the protein databases Swiss-Prot, NCBI-BLAST and TrEMBL. The Kir2.3 sequence contains two known domains, namely the Poly-Glu domain in amino acid position 383-390 and the Poly-Ala domain in position 391-399. There were no such domains in the sequences of the Kir2.1, Kir2.2 and Kir2.4 protein, respectively. The Poly-Ala-Poly-Glu domain or closely related domains were found in human ALMS1 protein, microtubule-associated protein EB1 (Arabidopsis thaliana), human PEG3 protein, different zinc finger proteins, mouse growth factor receptor bound protein 2-associated protein 3, NBS-LRR-like protein (Oryza sativa), human KIAA1855 protein and human mixed lineage kinase.

If there was a cross reaction to these proteins, we should detect a signal in non-transfected COS7 mammalian cells, as some of these proteins, the zinc finger domains in particular, are present in virtually all mammalian cells. However, the anti-Kir2.3 antibody only stained cells that were transfected with the Kir2.3 DNA while control cells remained unstained (not shown). This finding is confirmed by Western blots. Instead of multiple bands only a single band can be detected in the expected range of the Kir2.3 channel

protein (see Fig. 14). Thus, the affinity purified anti-Kir2.3 antibody does not detect certain domains in other proteins.

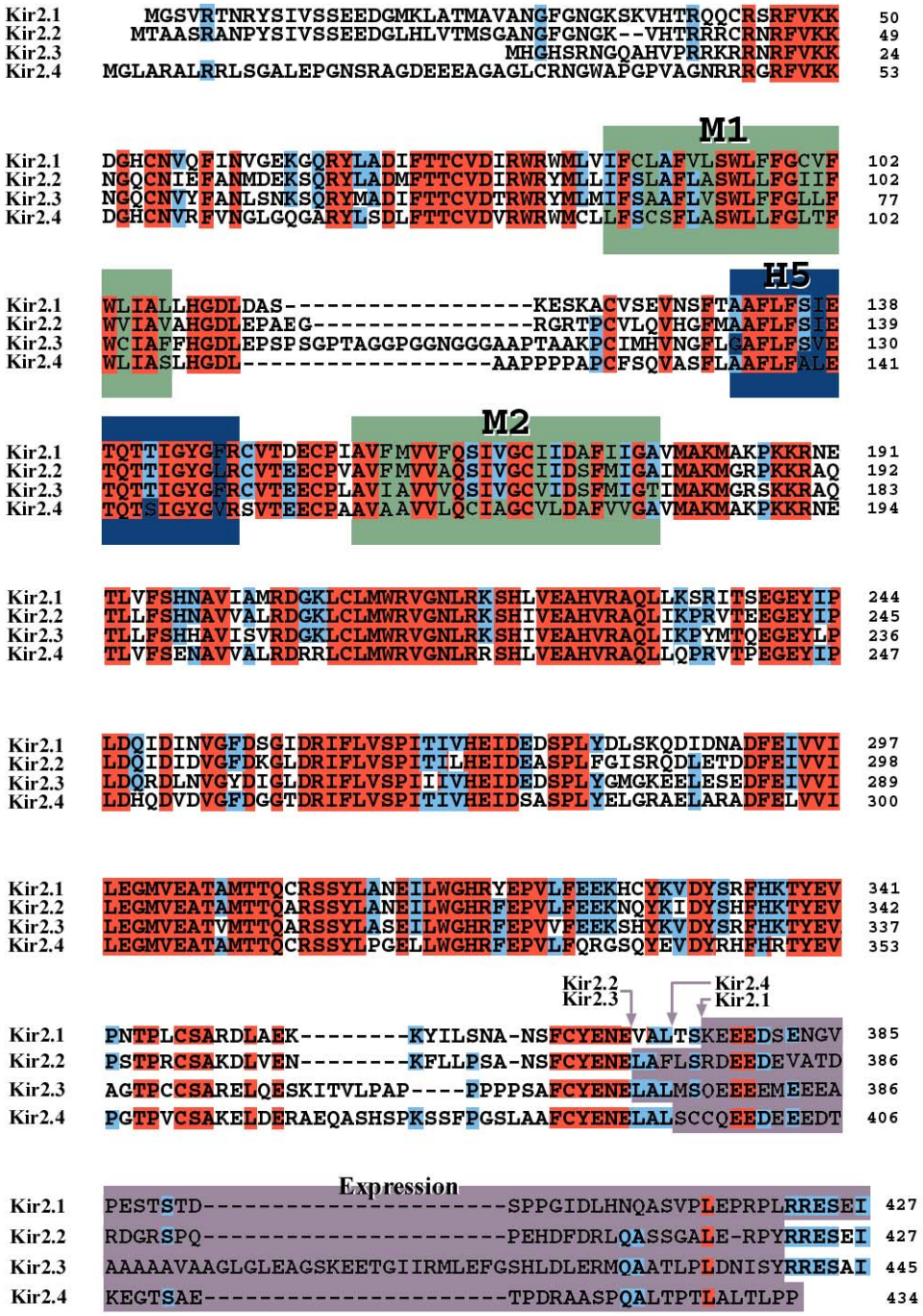

Fig. 7: Amino acid sequences of Kir2 subfamily members. The primary structures of all rat Kir2 channel subunits demonstrate that sequence conservation is lowest in the carboxyterminal area. Sequences shared by all four subfamily members are labeled in red. The carboxy terminal sequences uses for antibody production are depicted in gray. M1, M2 transmembrane regions; P5 pore-forming region (adapted from Töpert 1998)

3.1.2 Recombinant fusion proteins

After PCR amplification, the carboxyl terminal regions were cloned into the procaryotic expression vectors pQE40 and pGEX-4T-1 applying restriction enzymes. After plasmid transformation, positive clones were selected and protein expression in *E. coli* bacteria was performed. Fig. 8 displays the purified fusion proteins that were used for rabbit injections in two animals with different doses.

Fig. 8: SDS-PAGE of purified fusion proteins Kir2.1-Kir2.4

3.1.3 Removal of IgM antibodies by gel-filtration

Antibodies of the IgM class cannot be detected by applying further secondary anti-rabbit antibodies. However, they may reversibly block epitopes and prevent the binding of IgG antibodies, thereby decreasing the specific signal. Therefore these immunoglobulins need to be removed. Rabbit sera with the highest titer of specific Kir2 antibodies were pooled. Separation of IgG and IgM was performed by passage of the Superdex-column making use of the wide difference in molecular weight. The example of the Kir2.2 antibodies (Fig. 9) demonstrates the procedure of fraction selection: The protein line measured photometrically at 280nm (green line) displays the large IgM in the first peak (fractions 20-24). An ELISA measurement of the immunoreactivity to the Kir2.2 antigen (red line)

leads to the fractions with highest IgG concentration. Fractions 24-36 were pooled and used for further purification of specific antibodies and as a control of cross reactivities among the Kir family. An analogous procedure was used with remaining Kir2 subfamily members.

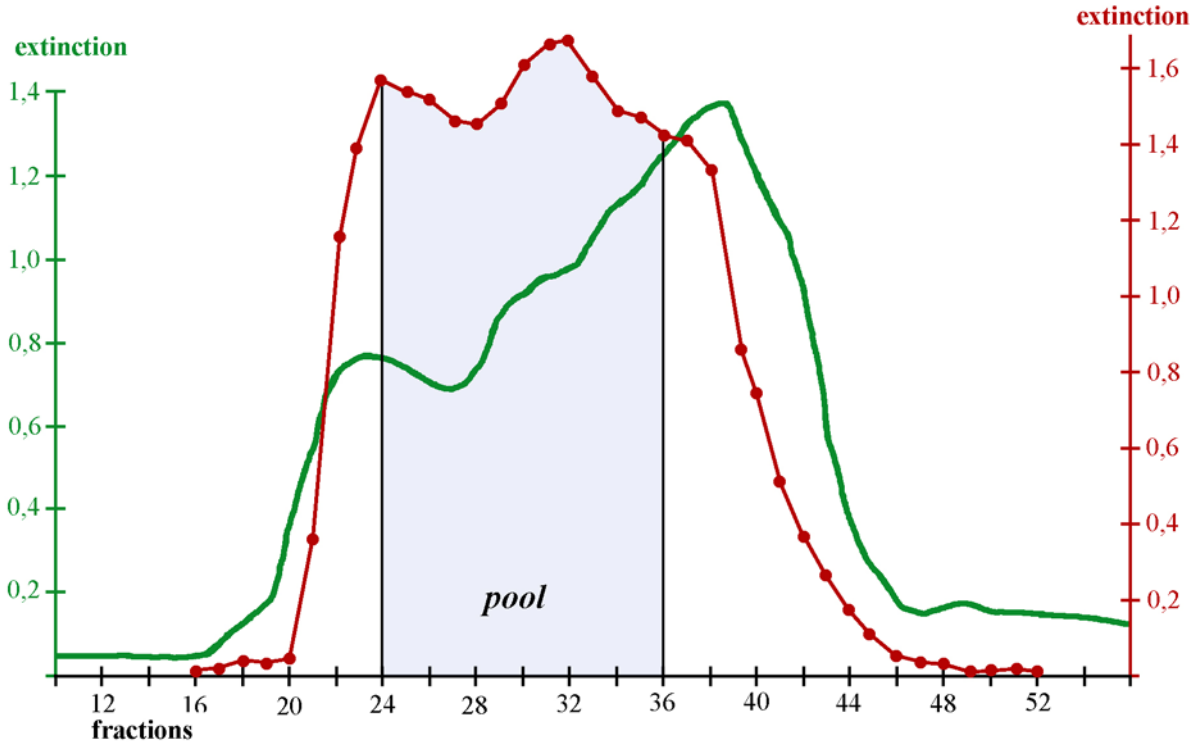

Fig. 9: Elution profile after passage through a superdex column. The green line represents the protein concentration and the red line the immunoreactivity to the corresponding Kir2 protein. Fractions selected on the basis of high antibody titer (24-36) are marked.

3.1.4 Affinity purification

The remaining solution contains antibodies specific to the Kir2 channel protein, but of course also to the rest of the fusion protein. Therefore absorption of these unintended antibodies was achieved by applying pQE40 or pGEX protein as the next step of purification. The optimal amount of protein was determined by testing the decreased cross reactivity depending on added protein concentration (Fig. 10A, arrow). Moreover, to get the anti-Kir2 antibodies, solely affinity purification was performed making use of a second expression system (pet32b); hence a different protein pattern surrounding the antigenic sequence. Nitrocellulose membranes were coated with this new fusion protein. Hence only antibodies to the Kir2 protein could bind and subsequently become washed

out (compare methods).

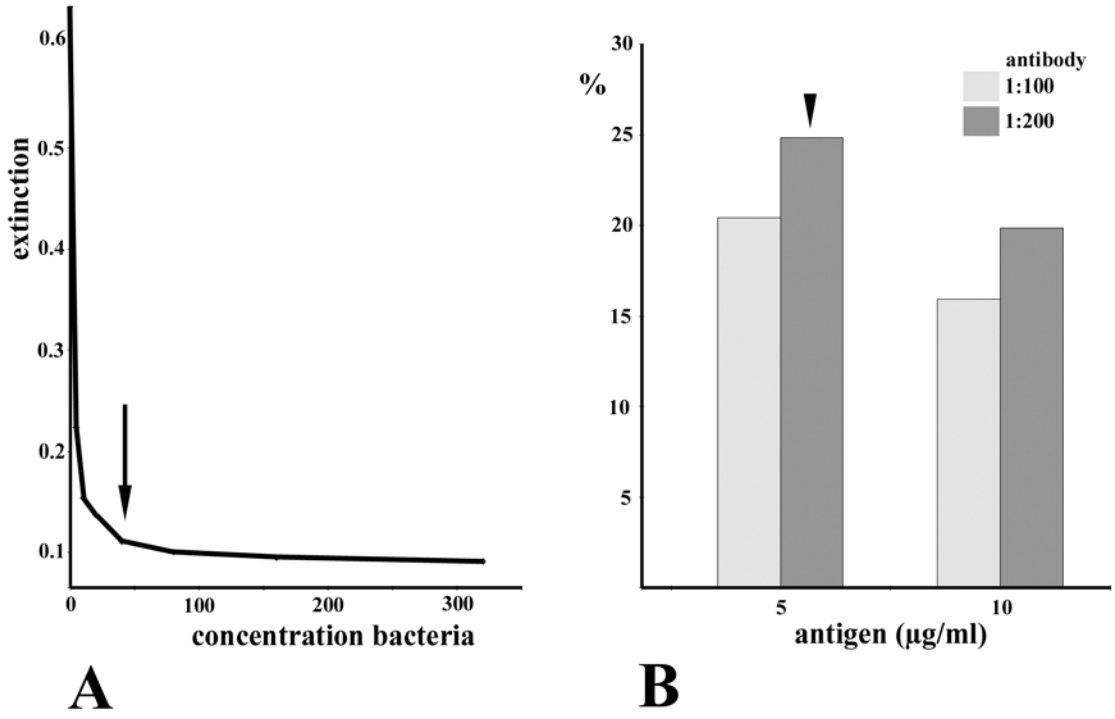

Fig. 10: Affinity purification. A) Initial application of pQE40 protein only to absorb cross reactivity to the plasmid part of the expressed antigen. B) Varying conditions to find protein concentration with best antibody quantity.

Previously, optimal conditions for affinity purification were tested to find an effective ratio between applied antigen amount and purified antibody concentration. Exemplary in the case of Kir2.2 (Fig. 10B) the highest amount of antibodies was collected using 5 µg protein/ cm^2 (arrowhead). Nevertheless only about 25% of starting activity was detectable, probably because of a high antibody affinity for the protein tethered to the membrane. Even more radical elution conditions (decreased pH) could not increase the quantity of purified antibodies. The sera of the remaining Kir2 proteins were processed using the same method and parameters.

3.2 Specificity of purified antibodies

3.2.1 Cross reactivity

Prior to affinity purification, immunoreactivity is present to the common part of the fusion protein. Afterwards all four anti-Kir2 antibodies failed to show any cross reactivity to the other subfamily members. Additionally, cross-reactivity concerning the related Kir3 subfamily was excluded (Fig. 11).

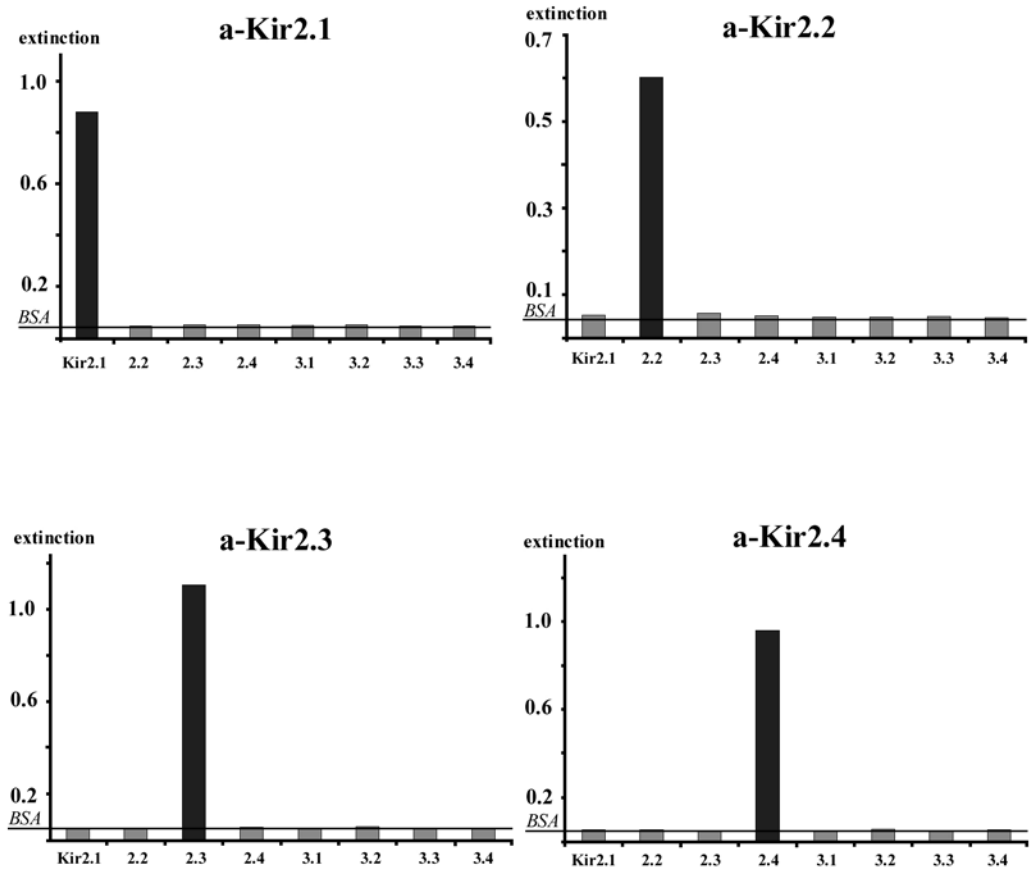

Fig. 11: No cross reactivity to other Kir subunits. Microtiter plates were coated with different proteins of Kir channels. Antibodies of the Kir2 subfamily exclusively detect their corresponding antigen and display no cross reactivity to other subunits. The horizontal line indicates extinction of BSA controls.

3.2.2 Competitive ELISA

Antibody quality was evaluated at several further levels following affinity purification. Specificity for the corresponding primary sequences is shown best in the competitive

ELISA assay (Fig. 12). It shows on the one hand that a specific polyclonal antibody cannot be blocked by proteins of other Kir2 subfamily members, on the other hand that only the distinctive protein is able to reduce the immunoreactivity depending on the concentration used. This knowledge of specific recognition of native proteins is essential for antibody application to rat brain tissue sections.

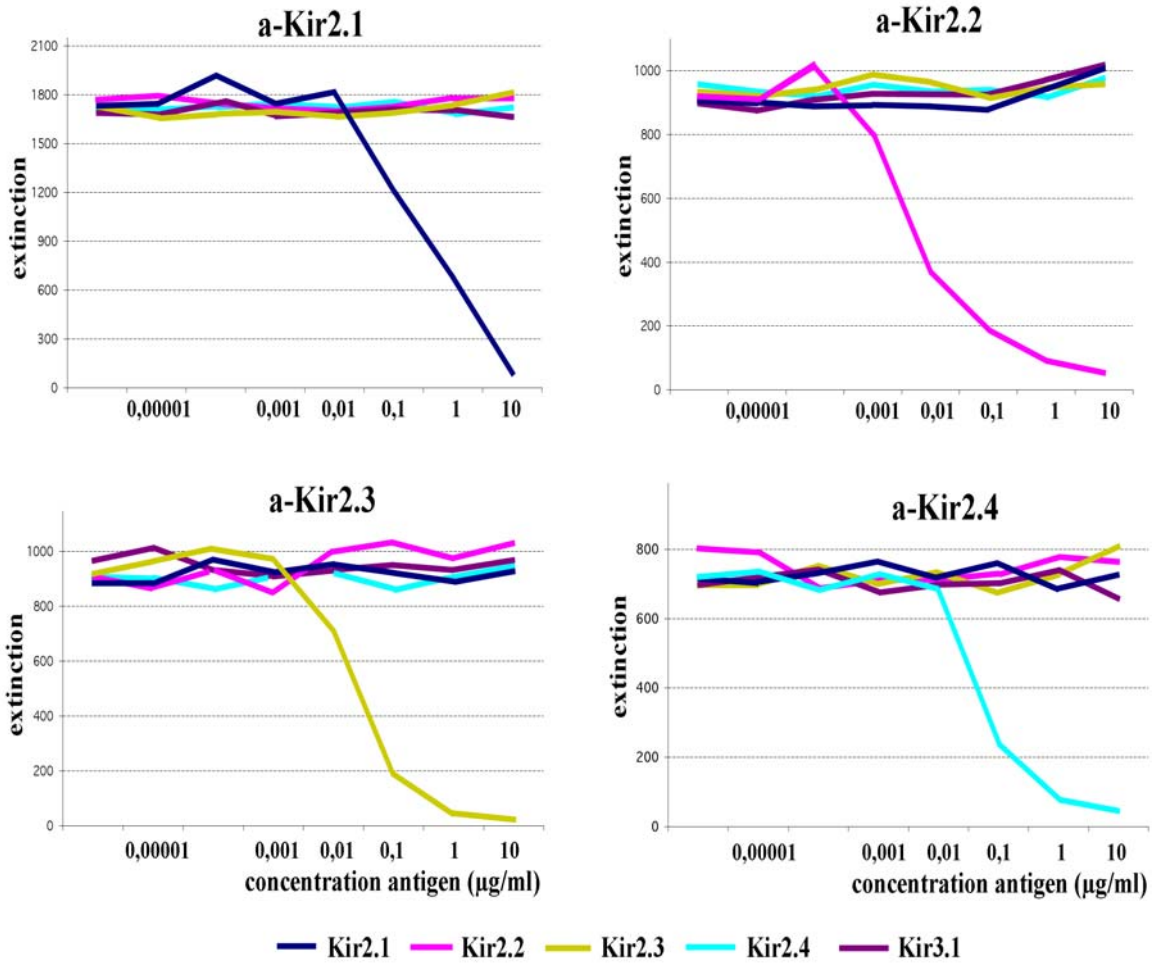

Fig. 12: ELISA assays of all members of the Kir2 subfamily. Microtiter plates were coated with the respective recombinant protein. Preincubation of antibodies with the cognate antigen only decreases the immunoreactivity in a concentration-dependent manner. Preincubation with other antigens did not show any effect.

3.2.3 Western blot of fusion proteins

A detection of denaturated fusion proteins was verified in Western blots supporting the results from the competitive ELISA. Reaction to all members of the Kir2 subfamily was examined. Again each antibody recognizes its corresponding antigen only (Fig. 13).

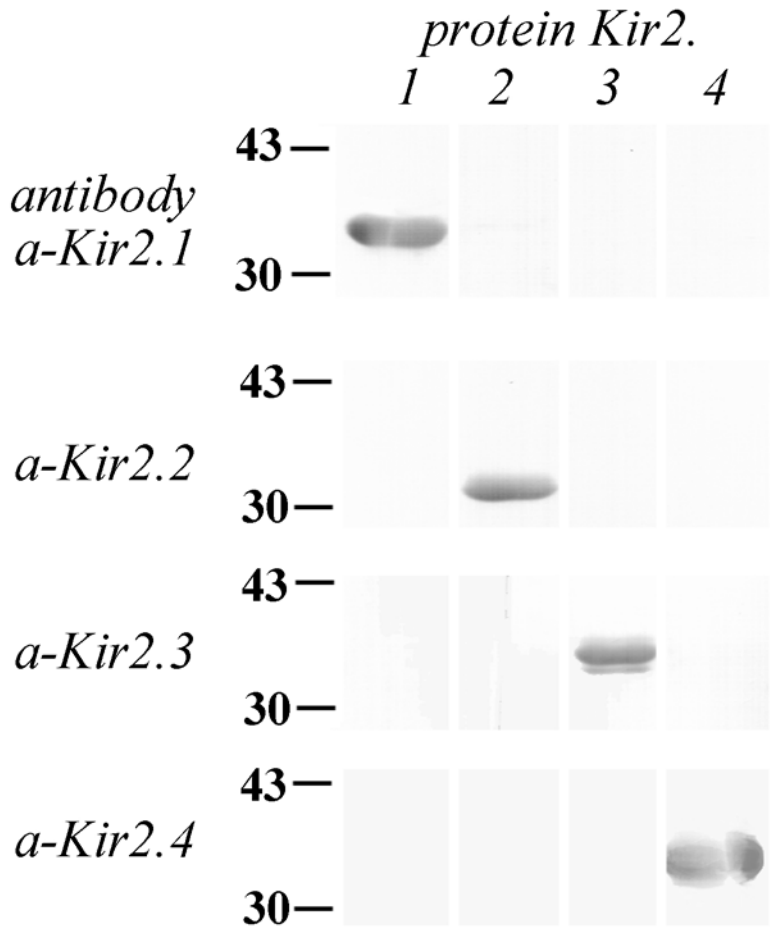

Fig. 13: Specificity of anti-Kir2 antibodies. In Western blots Kir2 antibodies recognize only their corresponding fusion protein and none of the other Kir2 subfamily members.

3.2.4 Western blot of rat brain homogenates

Competitive ELISA testing does not exclude cross reactivities with other cellular proteins. Therefore, the next step of specificity can be investigated by performing Western blot analysis of rat brain homogenates (Fig. 14). Only a single band in brain proteins suggests detection of the correct channel and the band is supposed to be located in the range of the expected molecular weight of the channel protein. All of the purified antibodies detect a specific band (left lane) that can be blocked by preincubation of the antibody with their fusion protein (right lane). In the case of Kir2.1, Kir2.2 and Kir2.3, the recognized protein displays the expected molecular weight as predicted from amino acid sequences.

Unfortunately, convincing Western blots from brain homogenates were not obtained with the anti-Kir2.4 antibodies that detect a single band with a molecular weight much higher than expected (see next paragraph).

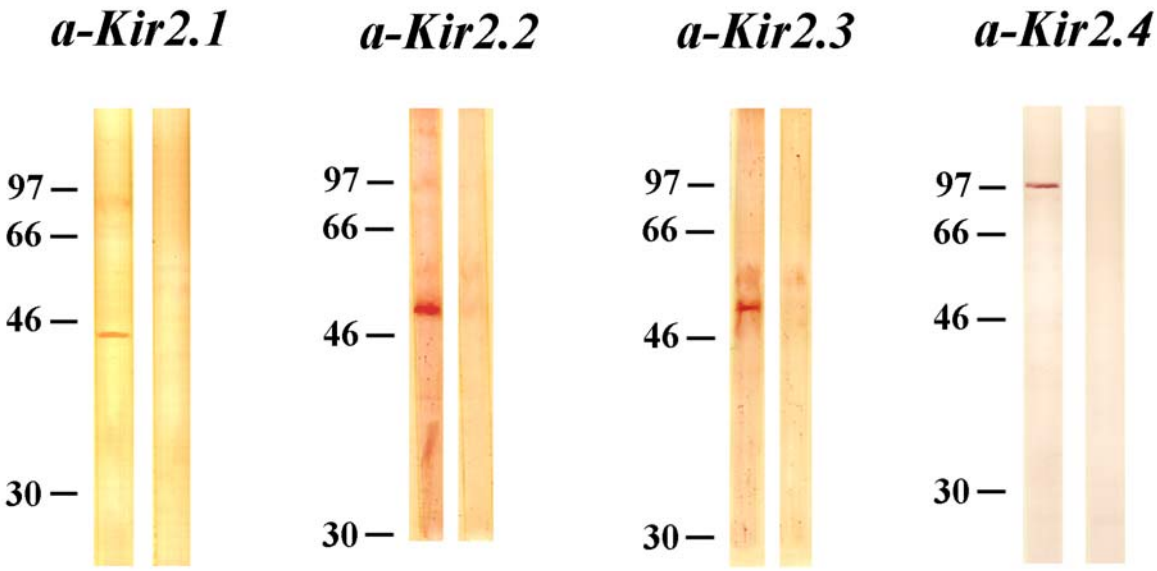

Fig. 14: Specificities of the anti-Kir2 antibodies as judged from Western blots. Homogenates from total rat brain membranes (10 µg/lane) were separated on 10% SDS-PAGE. All antibodies recognized single bands of the expected molecular weights (left lanes; with exception of Kir2.4, see next chapter) which were largely abolished subsequent to preincubation block with the cognate recombinant proteins (right lanes).

3.2.5 Specificity of anti-Kir2.4 antibodies

The surprising difference between the sizes of predicted protein versus obtained band with anti-Kir2.4 antibodies in western blot of rat brain homogenates (Fig. 14) required supplementary examination.

In order to verify the specificity of the anti-Kir2.4 antibodies, COS-7 cells were transiently transfected with Kir2.4-DNA (Fig. 15A). In contrast to untreated controls (Fig. 15B), incubation of transfected cells with anti-Kir2.4 antibodies visualized a remarkable fraction of positive cell bodies. Consequently, these antibodies recognize the correct antigen. To confirm the finding, a Western blot of homogenate of transfected cells was performed (Fig. 15C): only COS cells expressing the Kir2.4 channel display a protein band of predicted size (left lane), whereas no band is seen when blotting non-transfected

cells (right lane). Whether the fainter second band represents a phosphorylated form or a minor breakdown product remains unclear at present.

So far, there are different possibilities causing the single band in the Western blot of exact double the size of the potassium channel monomer. On the one hand the antibody might cross-react with a yet unknown brain specific protein. On the other hand the band may represent a Kir2.4 dimer that did not further dissociate during SDS-treatment before the Western blot (see also discussion in chapter 4.1.). Further examinations are required to finally rule out cross-reactivity.

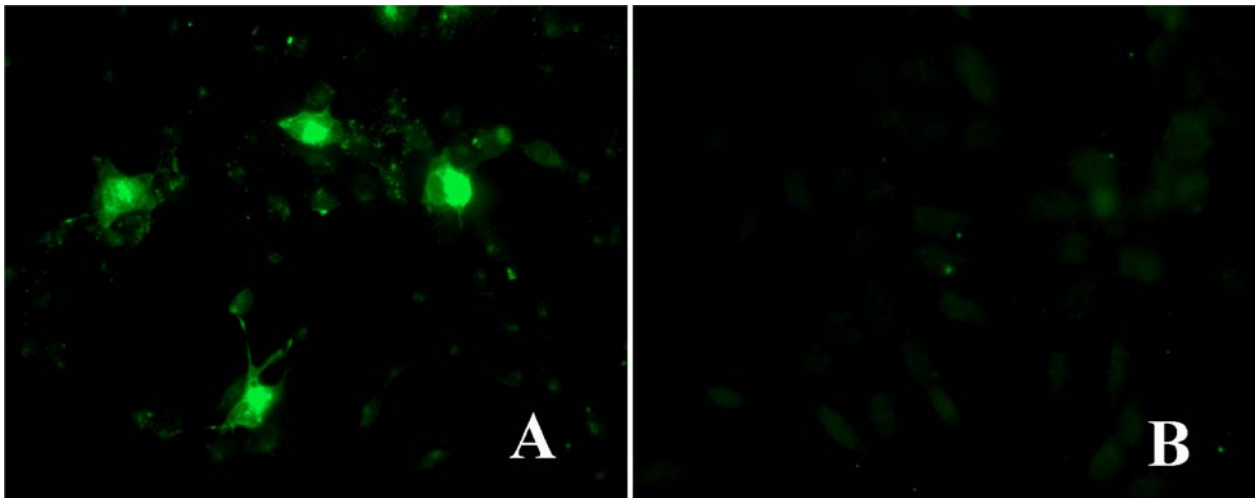

Fig. 15A,B: Specificity of anti-Kir2.4 antibodies, transfection experiments. The specificity of the Kir2.4 antibodies was further verified by the immunofluorescence obtained with Kir2.4 transfected COS-7 cells (A). Non-transfected cells were negative (B).

Since the Kir2.4 channel was reported to be expressed in the heart, an additional Western blot analysis of heart homogenate was done. It shows a protein band within the correct range (Fig. 15D), thus the anti-Kir2.4 antibodies recognize the correct protein size again. It is of remarkable interest that the Kir2.4 channel can be found only in neuronal structures of the heart[59].

[59] LIU, G.X. 2001

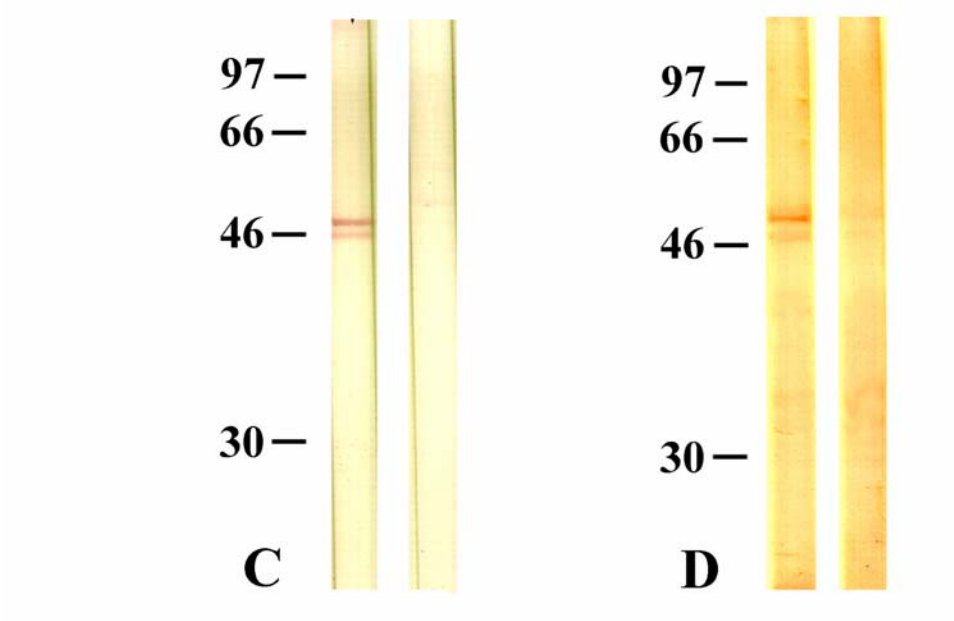

Fig. 15C,D: Specificity of anti-Kir2.4 antibodies. Western blots from transfected cells (C) displayed a double band (left lane), most probably due to the presence of phosphorylated species, within the expected range of molecular weights. Untransfected cells yielded blank blots (C, right lane). Western blots of heart homogenate (D) also show a protein band within the correct range.

3.2.6 Antibody specificity in brain sections

Immunocytochemical specificity was demonstrated using the olfactory bulb as an example (Fig. 16). The anti-Kir2 antibodies were applied to 20 µm rat brain sections. Each antibody showed a characteristic and individual distribution pattern. In all cases staining was abolished subsequent to preincubation with the cognate recombinant protein (not shown here, but see Fig. 23C). Chosen concentrations were used in all of the light microscopic screening experiments.

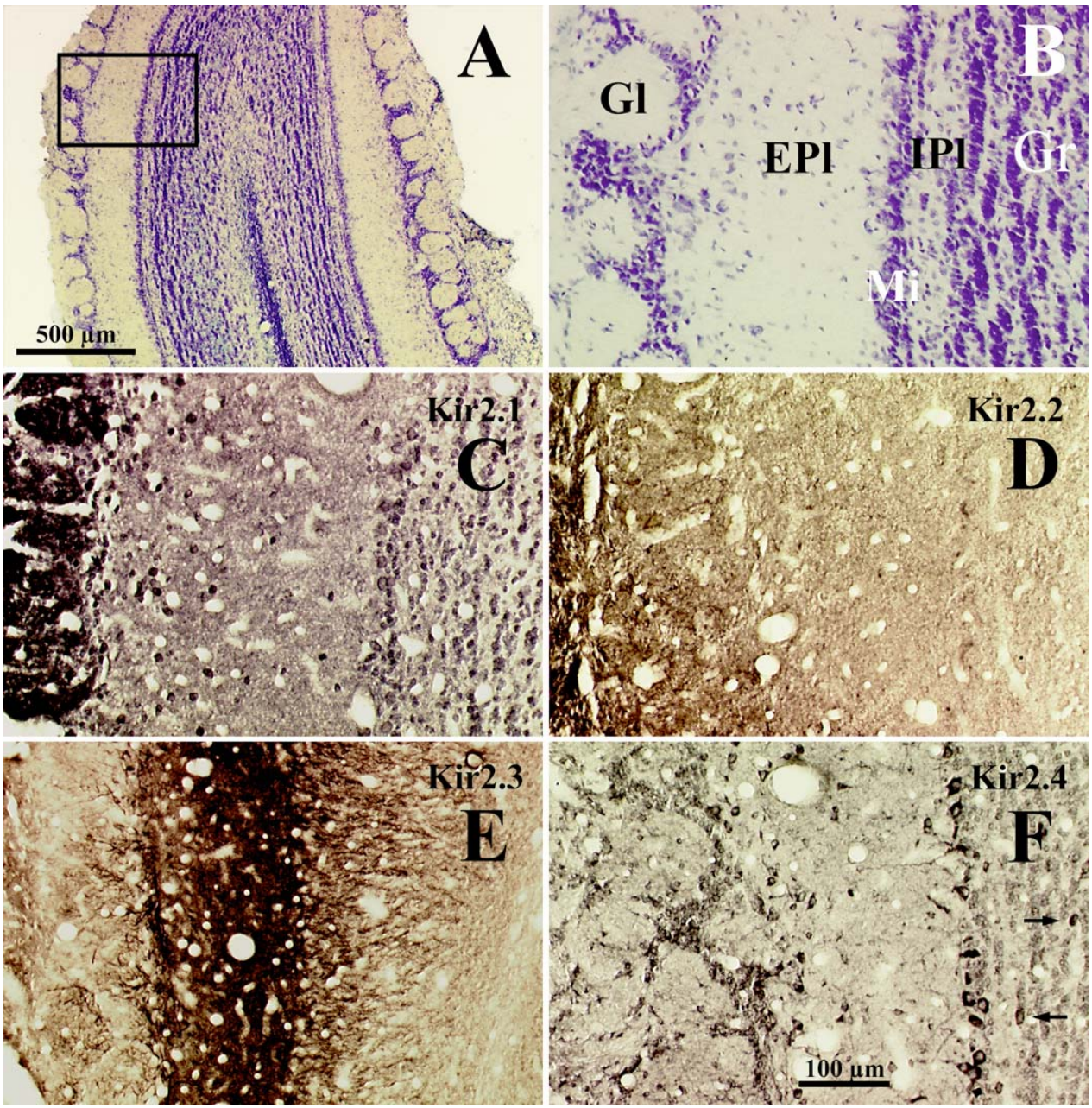

Fig. 16: Immunocytochemical labeling of the rat olfactory bulb confirms the specificity of the anti-Kir2 antibodies. For detailed analysis of the immunocytochemical specificities of the anti-Kir2 antibodies an area (boxed in A) containing the outer layers of the olfactory bulb was selected. Individual layers are evident at higher magnification in the section stained with cresyl violet (B). Immunoreactivities of individual members of the Kir2 subfamily (C-F) display specific and individual distribution patterns. Gl, glomerular layer; EPl, external plexiform layer; Mi, mitral cell layer; IPl, internal plexiform layer; Gr, granule cell layer.

The immunocytochemical localizations of the Kir channel proteins were in good agreement with *in situ* hybridization data[60]. Thus, Kir2.1 immunostaining was most prominent in the glomerular layer (Fig. 16C), where also Kir2.1 mRNA is intensively

expressed[61]. Again in agreement with mRNA findings, Kir2.2 immunoreactivity was most prominent in the glomerular layer and only weakly detectable in the mitral cell layer. Contrasting the other subfamily members, Kir2.3 channel proteins were predominantly expressed in the external plexiform layer of olfactory bulb and were virtually absent from the periglomerular cells (Fig. 16E). This is in perfect agreement with recent data from Kurachi's group[62]. Kir2.4 staining was found in most neurons, especially in the large cell bodies of mitral and tufted cells. Interestingly, in the granule cell layer, prominent immunostaining was displayed only by a small subset of granular cells (Fig. 16F, arrows).

3.3 Distribution of Kir2 channels in the rat brain

The expression of Kir2 mRNAs in the rat brain is known from *in situ* hybridization (ISH) experiments[63]. The corresponding proteins, however, may not necessarily be found in the same area, but may instead be sorted to the axons or their distant terminals. ISH data, therefore, do not necessarily display the subcellular and regional distribution of the channel protein and require complementary information from immunocytochemical experiments. Consequently, in a first step our experimental work focused on the general distribution of Kir2 channel proteins in different brain regions (Fig. 17-I – 17-IX).

3.3.1 Olfactory system

All four Kir2 subunits were expressed in the olfactory bulb (see detailed findings in chapter 3.2.6. and Fig. 16). Although all channels were expressed in the piriform cortex, the olfactory tubercle (Fig. 17-I) was labeled prominently by Kir2.1 and Kir2.3 antibodies and to a lesser extent by the other channel proteins. This finding is in excellent agreement with former data from *in situ* hybridization experiments[64].

[60] MORISHIGE, K.-I. 1993; HORIO, Y. 1996; KARSCHIN, C. 1999; BREDT, D.S. 1995; TÖPERT, C. 1998
[61] KARSCHIN, C. 1996
[62] INANOBE, A. 2002
[63] MORISHIGE, K.-I. 1993; HORIO, Y. 1996; KARSCHIN, C. 1999; BREDT, D.S. 1995; TÖPERT, C. 1998
[64] KARSCHIN, C. 1996

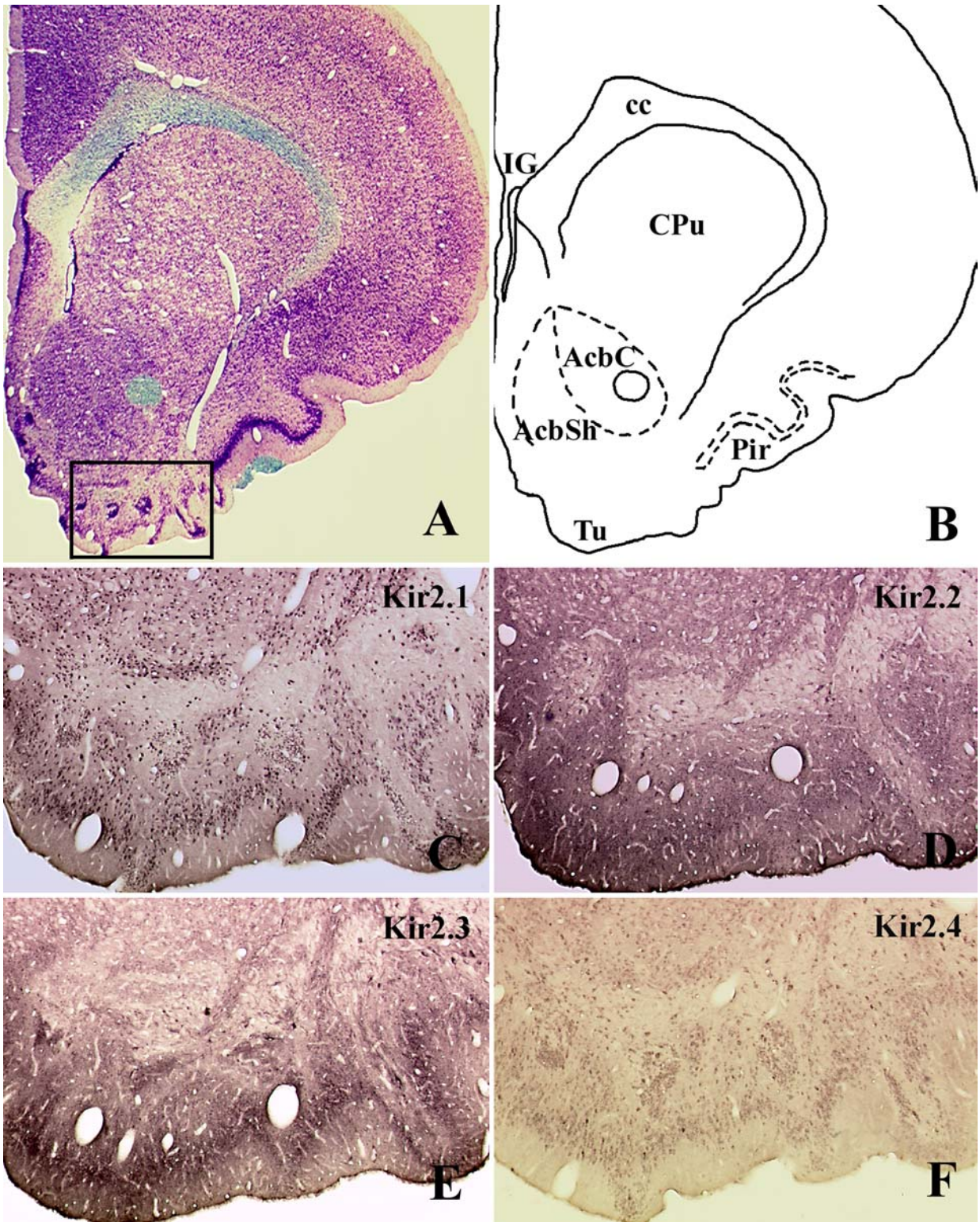

Fig. 17-I: Olfactory tubercle. For details see text. cc, corpus callosum; IG, induseum griseum; CPu, caudate putamen; AcbC, core part of the accumbens nucleus, AcbSh, shell part of the accumbens nucleus; Tu, olfactory tubercle; Pir, piriform cortex.

3.3.2 Hippocampus

The most prominent Kir2 channel expression was detected in the dentate gyrus (Fig. 17-II), although the Kir2.4 subunit was labeled to a lesser extent. Nevertheless, staining intensities varied also among the Kir2.1-2.3 members. Kir2.1 was present in the granule cell layer with particularly elevated levels, whereas the specific signal in all other hippocampal layers was very low, also including the neurons of the Ammon's horn. In contrast, the Kir2.2 subunit was found to be markedly elevated in the molecular layer of the dentate gyrus. Although all four Kir2 subunits were virtually absent from CA3 neurons, a prominent labeling of CA1 and CA2 neurons was detectable by Kir2.2 and Kir2.3 antibodies. Again the Kir2 channel distribution within the hippocampus is in good conformity with former *in situ* hybridization experiments[65].

3.3.3 Neocortex

Kir2.1-2.4 channels were expressed in all cortical areas (Fig. 17-III,B-E) and the antibody signal could be seen in most of the cortical cells, suggesting a possible co-expression of the different Kir2 channels. The labeling pattern reflects the laminar structure of the rat neocortex when compared with a Klüver-Barrera-stained section (Fig. 17-III,A). The strongest immunoreactivity was shown by Kir2.1 and Kir2.3 with a focal point on layer II and III neurons. Kir2.2 protein was present at moderate levels in all layers, with particularly elevated levels in layer V pyramidal cells. The Kir2.4 subunit was expressed in virtually all cortical neurons, but with only weak immunoreactivity. This latter finding partly differs from the distribution pattern described by Töpert[66], who reported the Kir2.4 subunit to be absent from the rat cortex (see also discussion).

[65] KARSCHIN, C. 1996
[66] TÖPERT, C. 1998

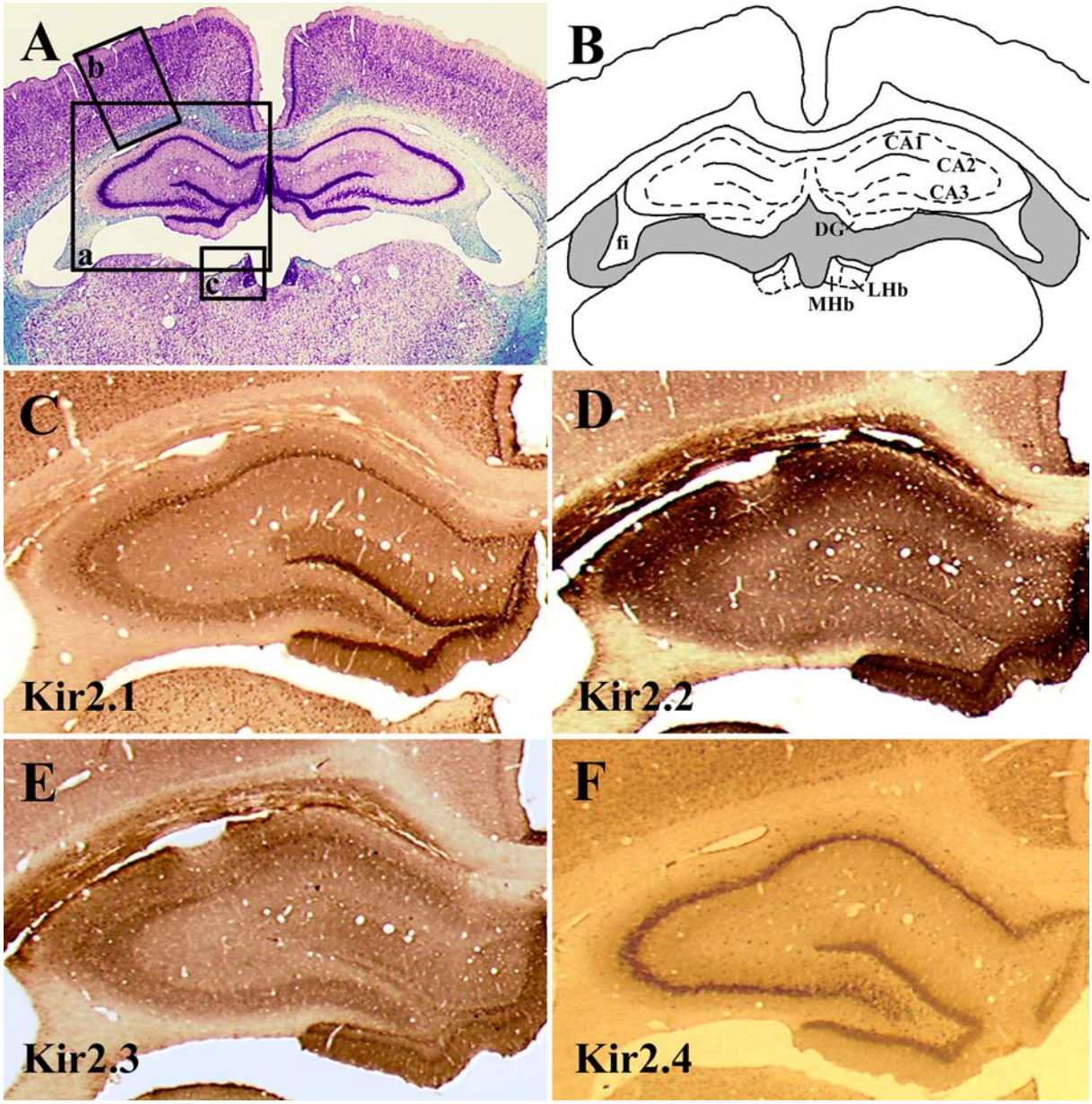

Fig. 17-II: Hippocampus. Areas C-F are boxed 'a' in A. For details see text. CA1-CA3, cornu ammonis 1-3; DG, dentate gyrus; fi, fimbriae; MHb, medial habenula; LHb lateral habenula.

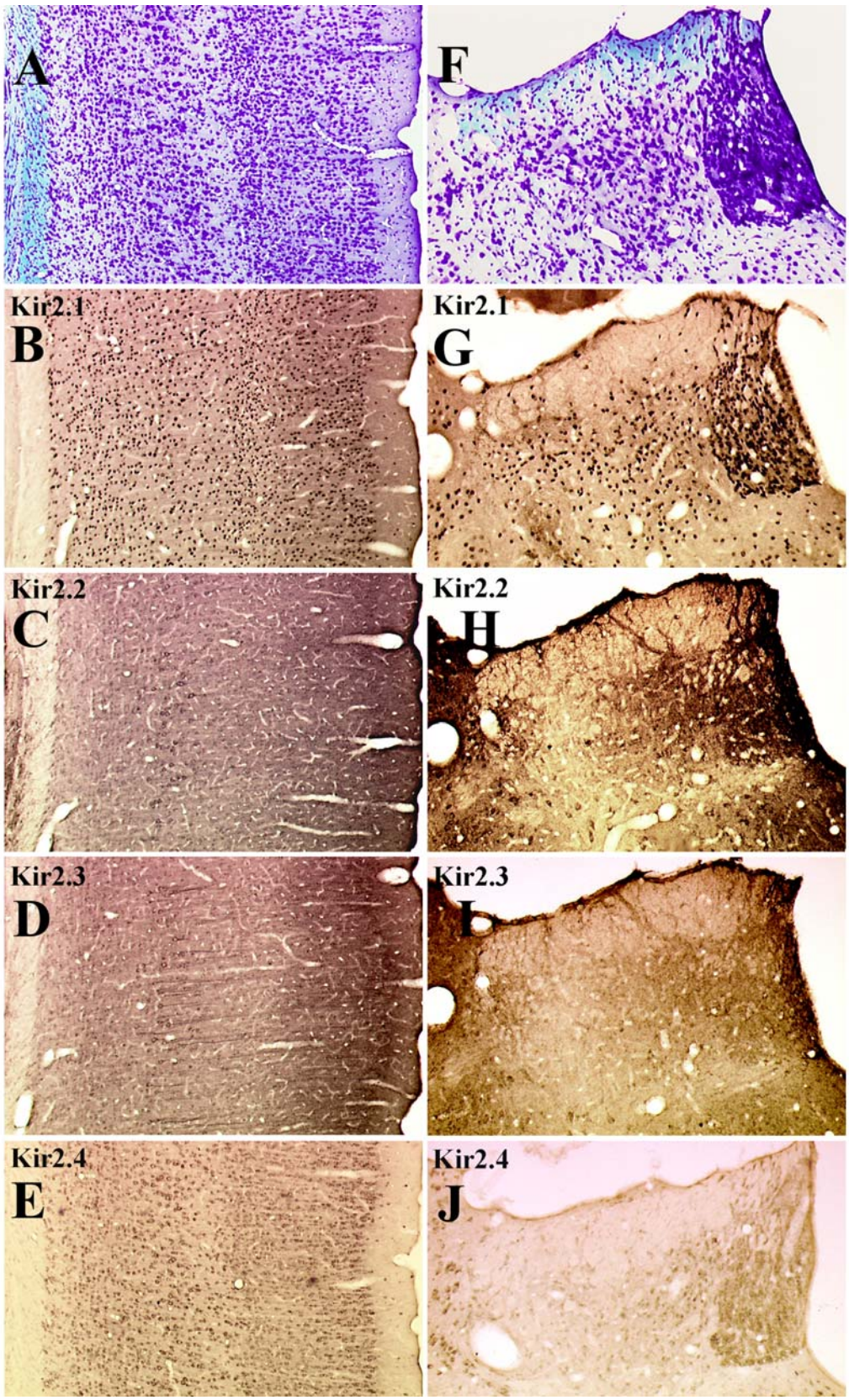

Fig. 17-III: Cortex (A-E), habenula (F-J). Areas A-E are boxed 'b' and F-J corresponds to 'c' in Fig. 17-IIA. For details see text.

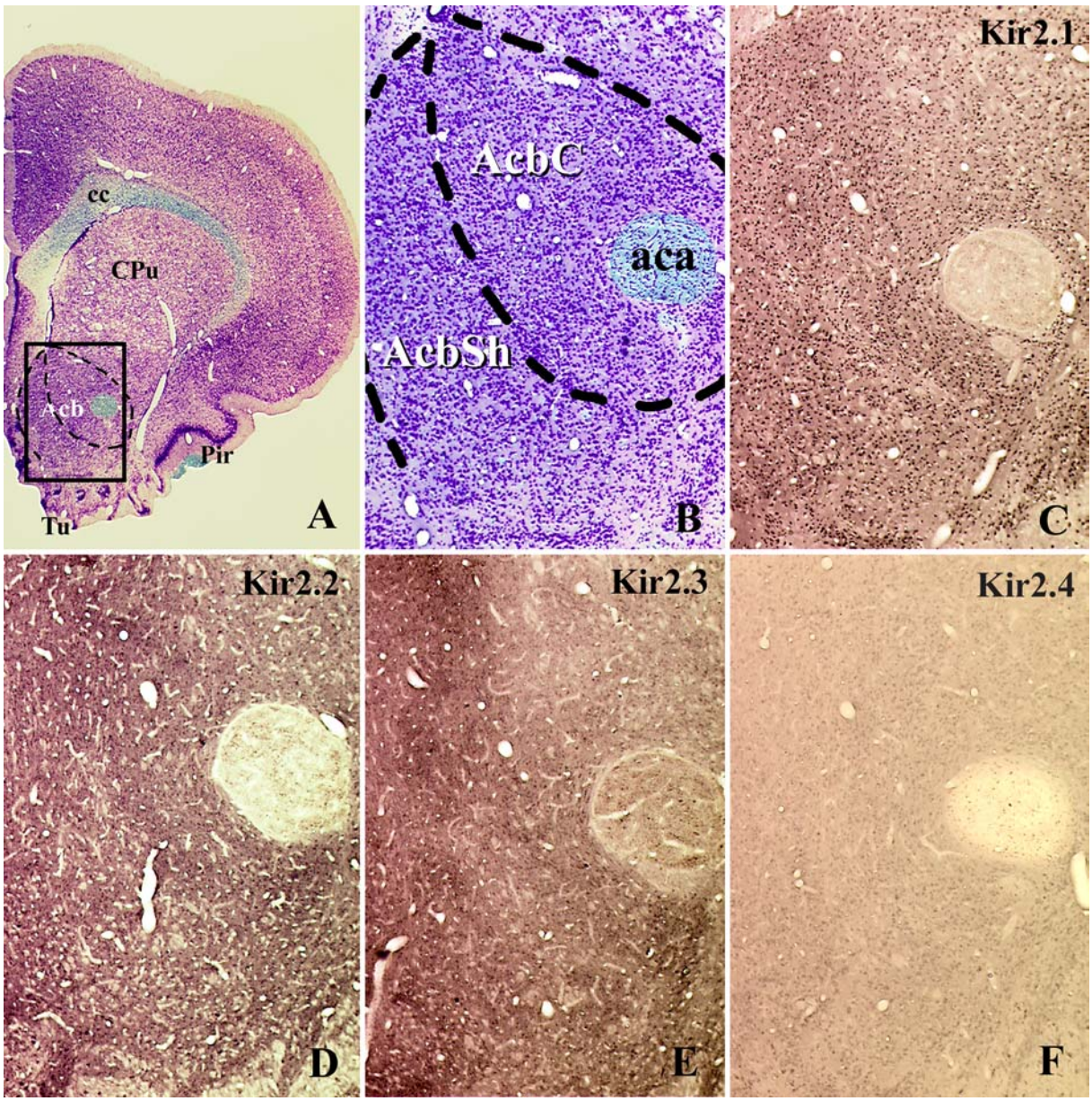

Fig. 17-IV: Nucleus accumbens. For details see text. cc, corpus callosum; CPu, caudate putamen; AcbC, core part of the accumbens nucleus, AcbSh, shell part of the accumbens nucleus; Tu, olfactory tubercle; Pir, piriform cortex; aca, anterior commissure.

3.3.4 Basal ganglia and amygdala

The caudate putamen and nucleus accumbens (Fig. 17-IV) were reported to be among the most prominently labeled brain structures when probed with Kir2.1 and Kir2.3 mRNAs[67], which is in good agreement with our antibody studies (the differential channel distribution in the striatum is summarized in chapter 3.4.1.).

[67] KARSCHIN, C. 1996; KARSCHIN, C. 1999

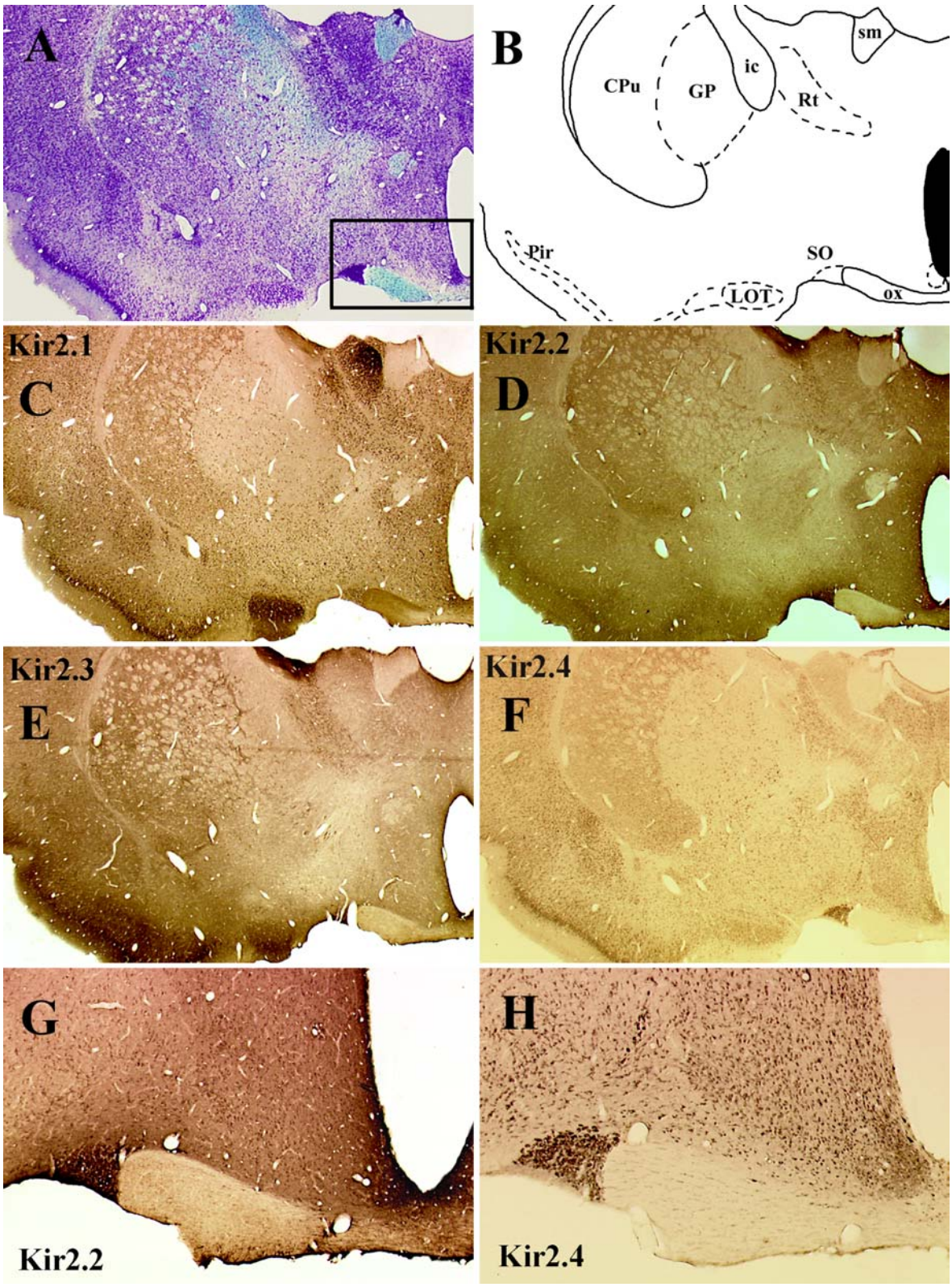

Fig. 17-V: Thalamus. For details see text. Areas G and H are boxed in A. CPu, caudate putamen; GP, globus pallidus; ic, internal capsule; Rt, reticular nucleus; sm, stria medullaris; Pir, piriform cortex; LOT, lateral olfactory tract nucleus; SO, supraoptic nucleus; ox, optic chiasma.

Kir2.4 was only weakly detectable in the nucleus accumbens, whereas all the other Kir2 channel subunits were abundantly expressed. Kir2.1 and Kir2.2 proteins were present in all accumbal parts at moderate levels, whereas a more differential signal was observed for Kir2.3, with particularly elevated levels in the shell part of the nucleus accumbens (Fig. 17-IV,E) and a patchy distribution resembling the expression pattern within the striatum (compare chapter 3.4.1.). Although Kir2.2-2.4 proteins were absent in amygdala nuclei and lateral olfactory tract nucleus, significant levels of Kir2.1 were found in the amygdala and strong Kir2.1 expression in the lateral olfactory tract nucleus (Fig. 17-V,C).

3.3.5 Thalamus

In the thalamus, all four Kir2 subunits displayed a differential distribution pattern. The Kir2.4 subunit was virtually absent in all thalamic nuclei. The Kir2.3 protein was also not detectable in most of the nuclei (anterior, lateral, paraventricular, posterior, medio-, laterodorsal, medial geniculate etc.), but it was expressed in the reticular thalamic nucleus (Fig. 17-V,E), which supports former mRNA studies[68]. The distribution of the Kir2.1 channel subunit, however, is in contrast to these *in situ* hybridization experiments, where the Kir2.1 protein is reported to be absent from all thalamic nuclei. The present study reveals a strong signal in the anterodorsal nucleus (Fig. 17-V,C) and still moderate levels for example in anteroventral, reticular and posterior thalamic nuclei. As previously described, the Kir2.2 subunit was abundant in many thalamic nuclei.

3.3.6 Hypothalamus and habenula

In conformity with earlier mRNA labeling[69], the Kir2.2 channel subunit was expressed most prominently in hypothalamic nuclei with the highest signal being observed in anterior area, preoptic nucleus and supraoptic nucleus (Fig. 17-V,G). The Kir2.3 protein was absent in the hypothalamus and only weak expression was observed with Kir2.4 and Kir2.1 antibodies. The exception was the Kir2.4 immunoreactivity in the supraoptic nucleus, where particularly elevated levels were found. Only one subunit, Kir2.2, was present at extremely high levels in the medial habenula, but not in the lateral habenula

[68] KARSCHIN, C. 1996

(Fig. 17-III,H). Kir2.1 protein was found throughout the habenula, but with significantly lower levels when compared with Kir2.2. In contrast, the Kir2.4 channel subunit was absent and the Kir2.3 protein was only weakly expressed in the medial habenula.

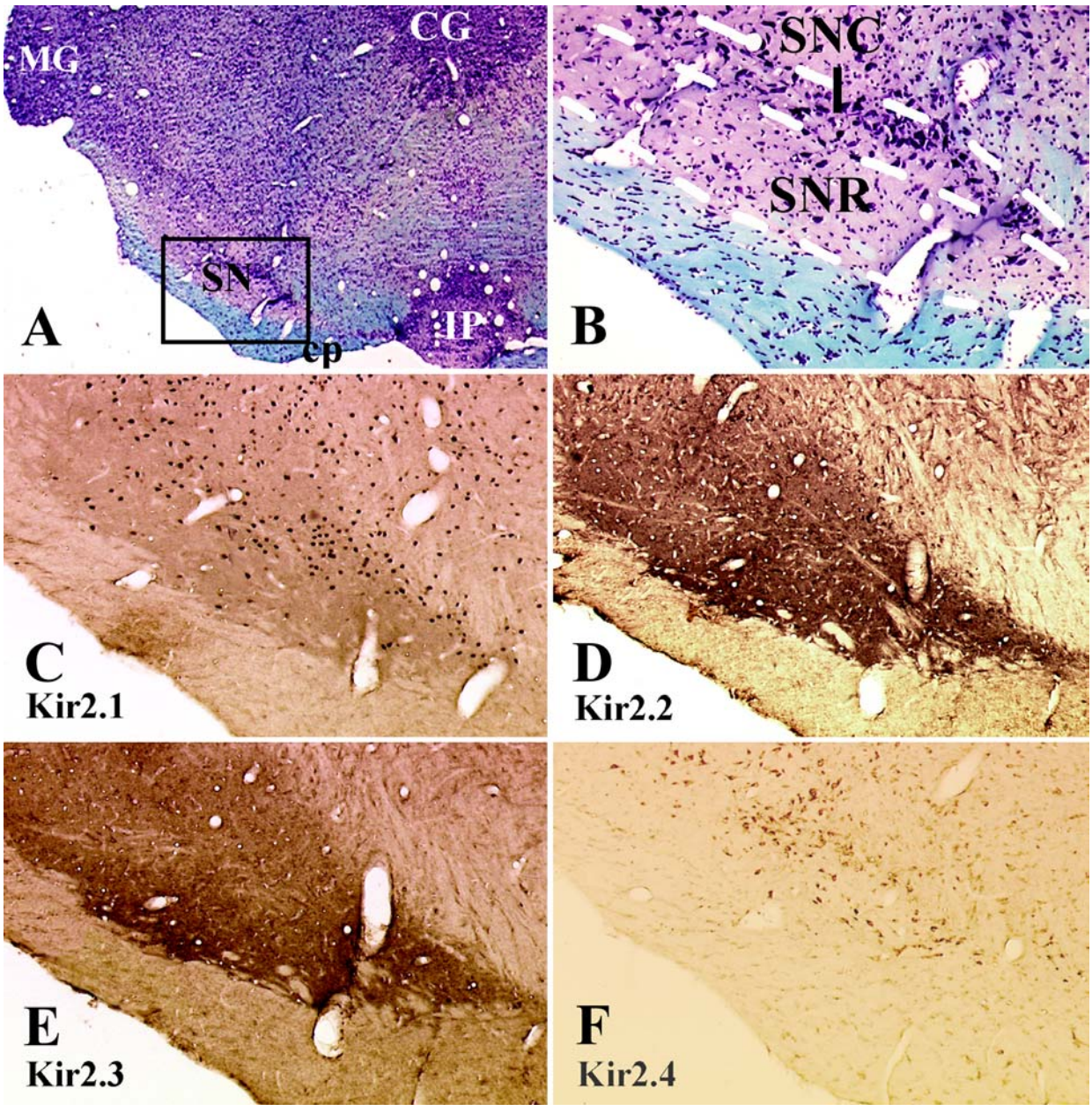

Fig. 17-VI: Substantia nigra. For details see text. MG, medial geniculate; CG, central gray; SNC, substantia nigra pars compacta; SNR, substantia nigra pars reticulata; cp, cerebral peduncle; IP, interpeduncular nucleus.

[69] HORIO, Y. 1996; KARSCHIN, C. 1999

3.3.7 Substantia nigra, ventral tegmental area (VTA), superior colliculus

All four Kir2 channel subunits were expressed by substantia nigra cells in a differential pattern (Fig. 17-VI). The Kir2.1 and Kir2.4 subunit was observed only in the SN pars compacta, whereas the Kir2.2 and Kir2.3 proteins were expressed in both parts auf SN with markedly elevated levels in the pars reticulate, Kir2.2 and Kir2.3 displaying a similar distribution pattern, indicating co-expression of these two subunits. Only one channel protein, Kir2.1, was present at low levels in the ventral tegmental area.

The superior colliculus (optic tectum) was among the most prominently labeled brain structures when labeled with Kir2.1 antibodies (Fig. 17-VII,C) and displayed also elevated signals for the Kir2.2 subunit protein. In contrast, the Kir2.3 subunit was only weakly expressed in this major target for retinal ganglion cells and the Kir2.4 channel protein was absent. Expression in the central gray was generally weak; however, few cells were expressing elevated levels of Kir2.2 protein. Otherwise, Kir2.2 and in this isolated case Kir2.4 channels were extensively expressed in the oculomotor nucleus (Fig. 17-VII,H/J), which is in line with with mRNA studies[70].

3.3.8 Cerebellum and spinal medulla

The Kir2 channel proteins present remarkable differences in the expression pattern throughout the cerebellum (Fig. 17-VIII). The Kir2.2 subunit expression was the strongest in the cerebellar cortex with restriction to the granule cell layer, thereby supporting the former data from *in situ* hybridization[71]. Contrasting this previously reported mRNA distribution, the Kir2.3 channel protein was entensively expressed by the large neurons in the deep cerebellar nuclei and by Purkinje cells, which is, however, in agreement with data from Falk's group[72]. The molecular layer contained low levels of Kir2.1 and Kir2.4 proteins. Both channels were also weakly expressed in the deep nuclei of the cerebellum. All Kir2 subunits were present in the motoneurons of the spinal cord with particularly

[70] TÖPERT, C. 1998; KARSCHIN, C. 1996
[71] KARSCHIN, C. 1999; BREDT, D.S. 1995
[72] FALK, T. 1995

elevated levels of the Kir2.2 channel protein.

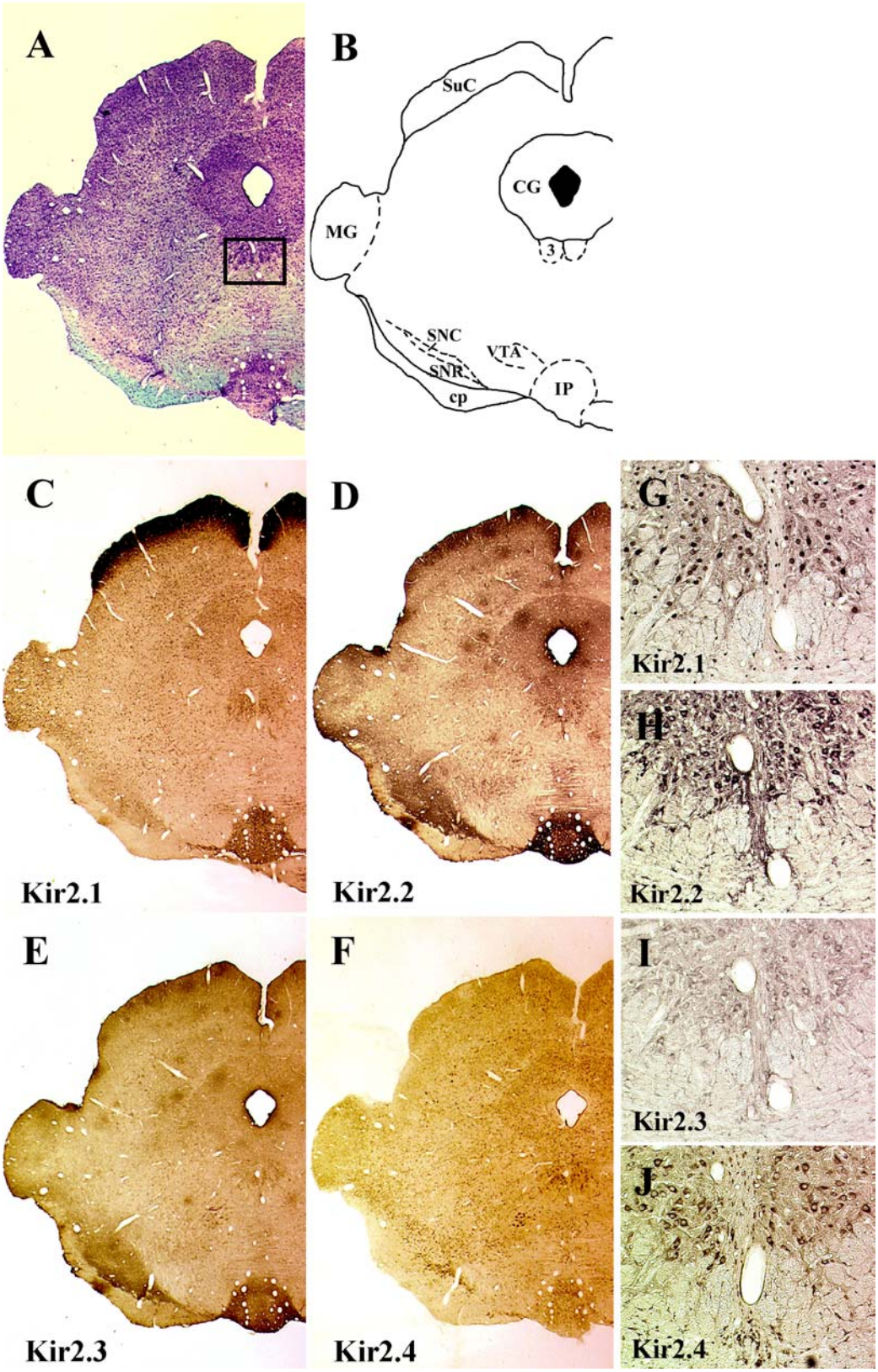

Fig. 17-VII: Mesencephalon. Adjacent sections of the oculomotor nucleus (G-J) are from the region boxed in A. For details see text. MG, medial geniculate; SuC, superior colliculus; CG, central gray; SNC, substantia nigra pars compacta; SNR, substantia nigra pars reticulata; VTA, ventral tegmental area; cp, cerebral peduncle; IP, interpeduncular nucleus; 3, oculomotor nucleus.

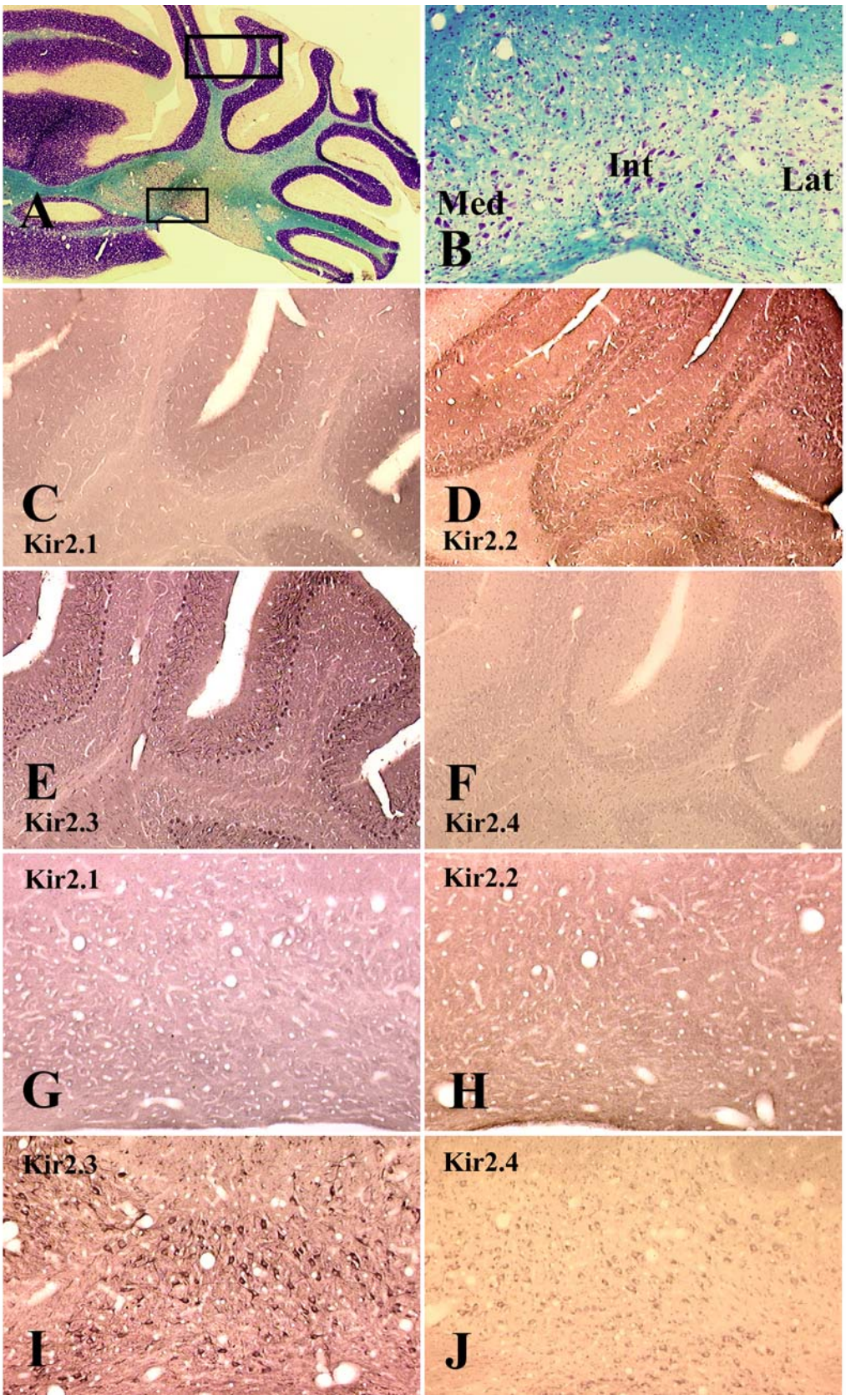

Fig. 17-VIII: Cerebellum. Adjacent sections from the cerebellar cortex (C-F) and deep nuclei (G-J). For details see text. Med, medial cerebellar nucleus; Int, interposed cerebellar nucleus; Lat, lateral cerebellar nucleus.

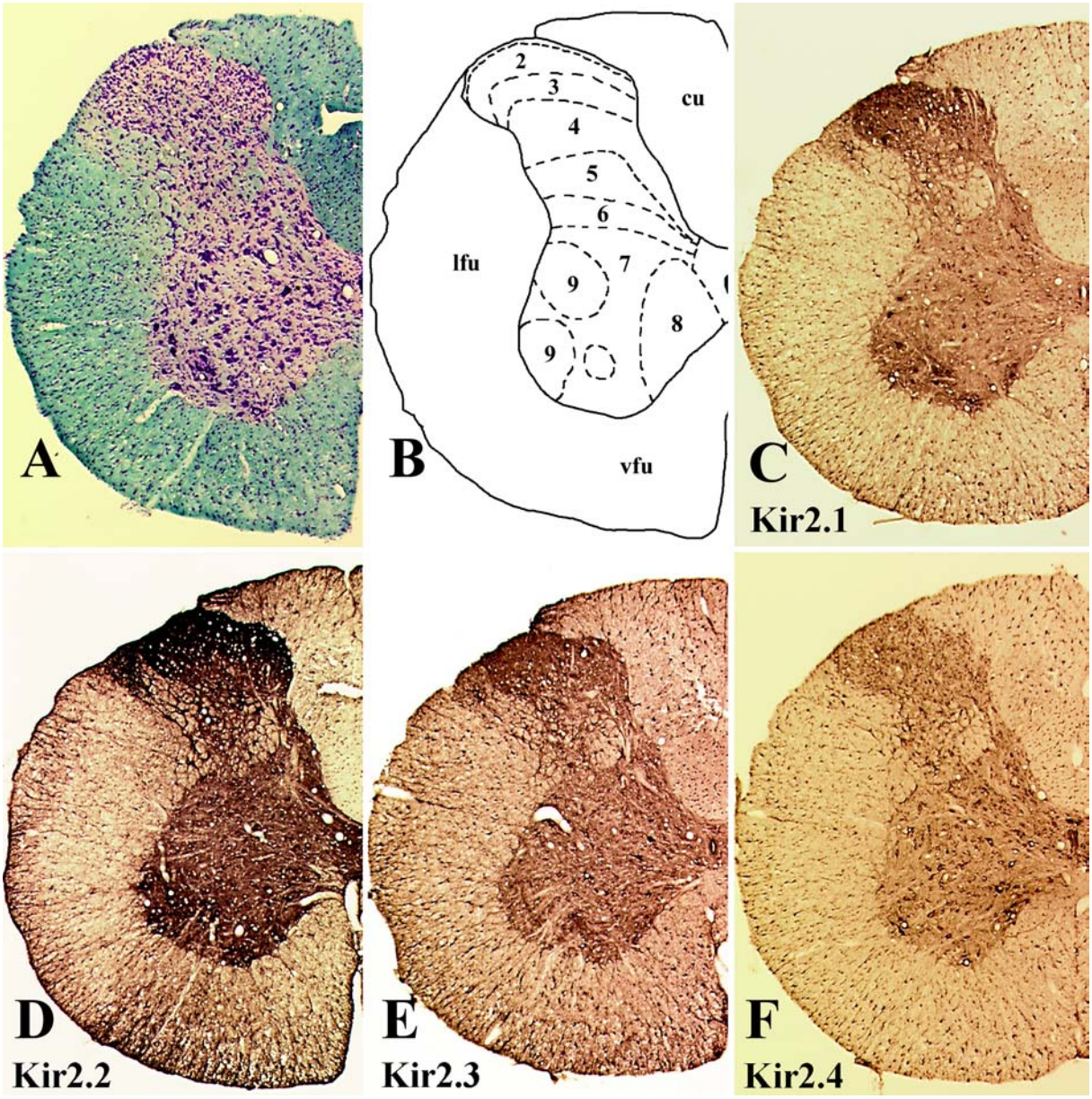

Fig. 17-IX: Medulla spinalis. For details see text. cu, cuneate fasciculus; lfu, lateral funiculus; vfu, ventral funiculus; 2-9, spinal cord layers.

The previously reported preference of hindbrain structures to express the Kir2.2 subunit[73] can be supported by the finding of Kir2.2 protein throughout the gray matter of the spinal cord with extremely high levels in the substantia gelatinosa.

[73] STONEHOUSE, A.H. 1999; KARSCHIN, C. 1996

Table 5: Distribution of individual Kir2 subunits in different brain regions

Brain region	Kir2.1	Kir2.2	Kir2.3	Kir2.4
Telencephalon				
Olfactory bulb				
Glomerular layer	++++	+	0	+
External plexiform layer	+	0	++++	0
Mitral cell layer	+	+	+	++
Granule cell layer	++	0	+	+
Olfactory tubercle	++	+	+++	0
Islands of Calleja	+	0	0	0
Piriform cortex	++	+	++	+
Neocortex				
Layer I	0	+	+	0
Layer II	+++	++	+++	++
Layer III	+++	++	+++	+
Layer IV	++	+	++	++
Layer V	++	+++	++	++
Layer VI	++	+	+	+
Hippocampus				
Dentate gyrus				
Molecular layer	+	+++	+	0
Granule cell layer, Lamina sup.	+++	++	++	+
Granule cell layer, Lamina inf.	0	+	+	0
Polymorphic layer				
CA1-CA2				
Oriens layer	0	+	++	+
Pyramidal cell layer	+	++	++	+
Radiate layer	0	+	++	0
Lacunosum moleculare layer	+	++	+	0
CA3				
Oriens layer	0	+	+	+
Pyramidal cell layer	+	+	+	+
Radiate layer	0	+	+	+
Basal forebrain				
Substantia innominata	0	+	0	+
Basal nucleus of Meynert	+	++	++	+
Basal ganglia				
Caudate putamen (Striatum)	++	+++	+++	+
Nucleus accumbens	++	++	++	+
Globus pallidus	+	++	++	+
Claustrum	0	+	0	+
Endopiriform nucleus	+	+	+	+
Lateral olfactory tract nucleus	+++	0	+	+
Amygdala				
Cortical nuclei	+	0	0	0
Medial nucleus	+	0	0	0
Basomedial nucleus	+	0	0	0
Diencephalon				
Thalamus				
Anterodorsal nucleus	+++	0	0	0
Anteroventral nucleus	++	0	0	0
Anteromedial nucleus	+	0	0	0
Laterodorsal nucleus	+	+	0	0
Mediodorsal nucleus	+	0	0	0
Centrolateral nucleus	0	++	0	+
Paraventricular nucleus	+	++	0	+
Reuniens nucleus	+	+	0	0

Reticular nucleus	++	++	++	+
Posterior nucleus	++	+	0	0
Medial geniculate nucleus	+	+	0	0
Paratenial nucleus	+	++	0	+
Hypothalamus				
Anterior area	+	++	0	+
Ventrolateral nucleus	0	+	0	+
Lateral area	+	+	0	0
Preoptic nucleus	+	++	0	+
Periventricular nucleus	+	+	0	0
Paraventricular nucleus	+	+	0	+
Supraoptic nucleus	+	++	0	++
Epithalamus				
Medial habenula	++	++++	+	0
Lateral habenula	+	+	0	0
Mesencephalon				
Red nucleus	0	+	+	+
Substantia nigra				
Pars compacta	+	++	+	+
Pars reticulata	0	+++	++	0
Ventral tegmental area	+	0	0	0
Interpeduncular nucleus	++	+++	++	0
Superior colliculus	++++	++	+	0
Central gray	+	++	0	+
Edinger-Westphal nucleus	+	+	0	+
Oculomotor nucleus (III)	+	++	0	+++
Metencephalon				
Cerebellum				
Deep nuclei	+	0	+++	+
Molecular layer	+	0	0	+
Granule cell layer	0	+++	0	+
Purkinje cells	0	0	++	0
Myelencephalon				
Spinal medulla				
Substantia gelatinosa	+	++++	+	0
Motoneurons	++	+++	+	+

3.4 Distribution of Kir2 channels in the striatum

The striatum plays a critical role in movement selection, motivated behavior and neural transmission via basal ganglia circuitry. To evaluate the possible involvement of Kir2 channels in the fine tuning of these pathways, it is important to know their exact distribution within the striatum. A distinct localization in either the patch compartment or the cholinergic interneuron would suggest that selective channel activation or inhibition could specifically influence the outcome of a movement and, perhaps, open new strategies for novel therapeutic regimes.

Table 6: Striatal Kir2 channel expression, results from in situ hybridization experiments

channel subunit	author	remarks
Kir2.1	Karschin, C. et al. 1996	abundant (Acb, CPu)
Kir2.2	Karschin, C. et al. 1996	moderate (Acb, CPu), large cells prominent
Kir2.3	Karschin, C. et al. 1996	abundant (Acb, CPu)
	Falk, T. et al. 1995	only few (VP, CPu)
	Bredt, D.S. et al. 1995	high (striatum)
Kir2.4	Töpert, C. et al. 1998	no expression

Abbreviations: *Acb* accumbens nucleus, *CPu* caudate putamen, *VP* ventral pallidum

3.4.1 Kir2 subunits are differentially distributed in the rat striatum

The expression of Kir2 mRNAs in the rat striatum is known from *in situ* hybridization experiments (table 5). Immunocytochemical experiments were performed to get more detailed information about the subcellular and regional Kir2 channel protein distribution.
Rat brain sections were stained with antibodies to all four Kir2 subunits using the routine conditions described above. Although distribution in some regions of the rat brain is very divergent, in the striatum there are remarkable similarities: Survey micrographs (Fig. 18) suggest that all four Kir2 channel proteins are expressed by medium-sized spiny neurons. Nevertheless, staining intensities varied among the members of the potassium channel subfamily. The strong Kir2.2 staining of the neuropil in the caudatoputamen (CPu) obscured the visualization of neuronal cell bodies (Fig. 18D). Indeed, many spiny projection neurons were moderately labeled with no obvious preference for a subset of cells. Interestingly, neurons with prominent Kir2.2-immunoreactivity (Fig. 18D, arrowheads) were grouped in the pallidum (GP). The same was true for the Kir2.3 channel (Fig. 18E). Not all neurons of the pallidum are stained with the same intensity, suggesting functional differences. Whether the strongly stained neurons represent a cell type similar to the newly described type II neurons in the internal pallidum[74] is unclear at present.

[74] PARENT, M. 2001

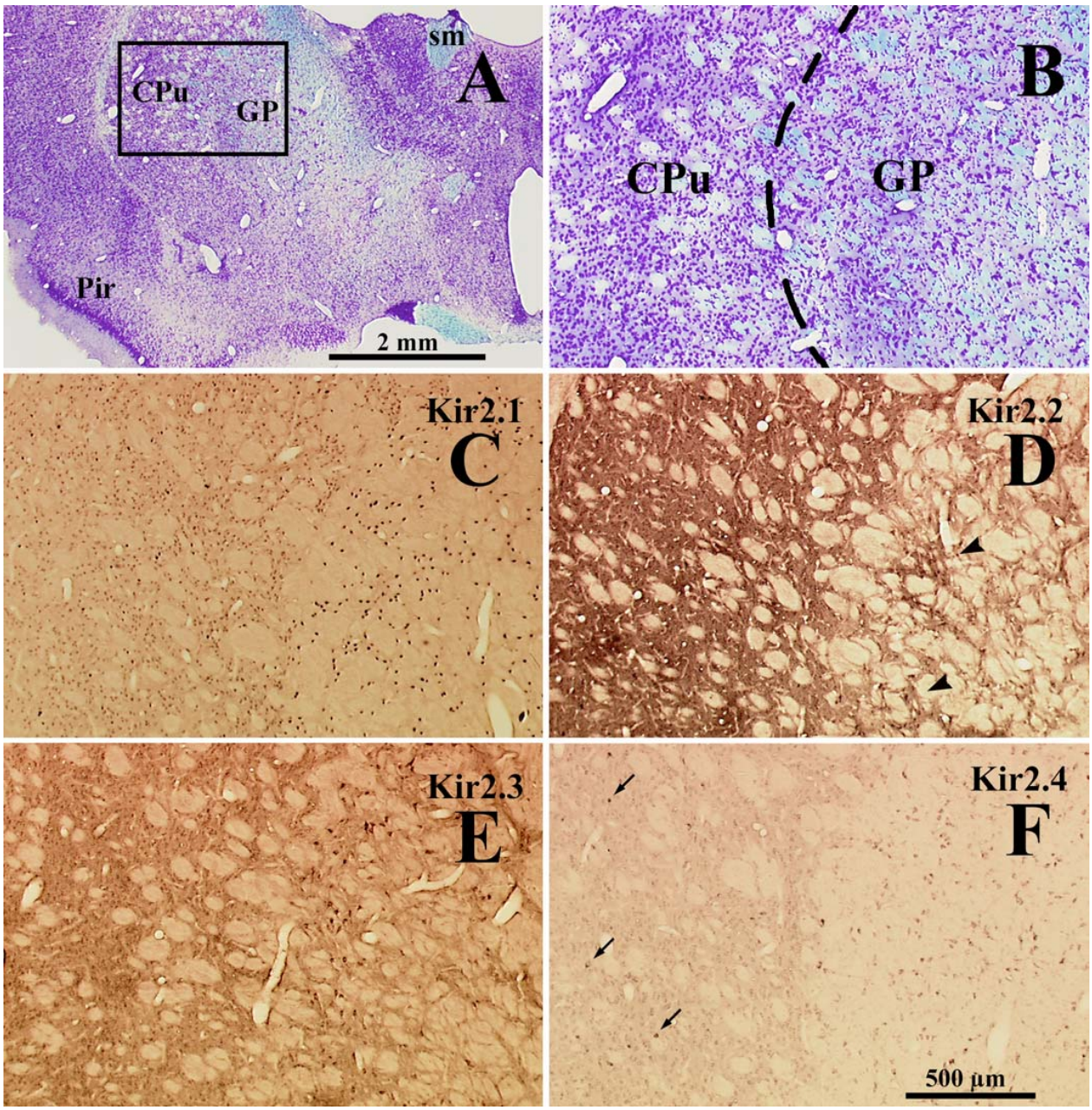

Fig. 18: Regional and cellular distribution of Kir2 subunits in the rat striatum. A series of six adjacent sections was used to analyze the immunocytochemical patterns of the individual members of the Kir2 family. Coronal sections were obtained shortly caudal to the optic chiasm and stained according to Klüver-Barrera for morphological examination (A,B). An area (boxed in A) containing parts of the caudate-putamen and the external pallidum was selected for further investigation. Distinct patterns of immunostaining were obtained for the individual Kir2 subunits (C-F). Note that Kir2.2-positive neurons are clustered in the pallidum (D, arrowheads) and that large neurons in the striatum display prominent staining (F, arrows) with the anti-Kir2.4 antibody. CPu, caudate-putamen; GP, globus pallidum externum; Pir, piriform cortex; sm, stria medullaris thalami.

The Kir2.1 subunit is apparently restricted to the somatodendritic compartment of many, if not all, spiny projection neurons leaving the neuropil unstained (Fig. 18C). Neurons of the pallidum also displayed homogeneous immunoreactivities. The Kir2.3 distribution pattern

of the caudatoputamen resembles that of the Kir2.1 subunit. Many projection neurons are labeled. In contrast to the other subunits, however, Kir2.3 immunoreactivity displayed stronger and weaker stained areas (see below). Finally, the Kir2.4 channel subunit showed a unique staining pattern with considerably less immunoreactivity as compared to the other Kir2 proteins (Fig. 18F). Probably all striatal and pallidal neurons could be detected with the anti-Kir2.4 antibodies. Some large neurons of the caudatoputamen, however, displayed especially strong Kir2.4 immunoreactivity (arrows).

3.4.2 Anti-Kir2.2 antibodies stain striatal fiber bundles

Aside from somatodendritic labeling of projection neurons, Kir2.2 immunoreactivity also produced a dense signal in the neuropil (Fig. 18). Under routine conditions (see methods) brain sections incubated with anti-Kir2.2 antibodies did not allow visual identification of stained fibers. However, a different image appeared when immunocytochemical conditions were optimized to focus on this special problem (Fig. 19). The lower concentration of anti-Kir2.2 antibodies hardly stained spiny projection neurons, but showed an extensive labeling of striatal fiber bundles, which was absent after preincubation with the Kir2.2 protein. This observation was consistent throughout rostral and caudal areas of the striatum and also in different animals. As an example, coronary sections of the striatum at the level of the anterior commissure (Fig. 19A, B) are depicted.

The sorting of the Kir2.2 protein to the axon compartment is supported by data obtained at the electron microscopic level. Gold dots represent Kir2.2 channel protein. They are highly concentrated within the fiber bundle (Fig. 19C), but only sparse in the surrounding neuropil.

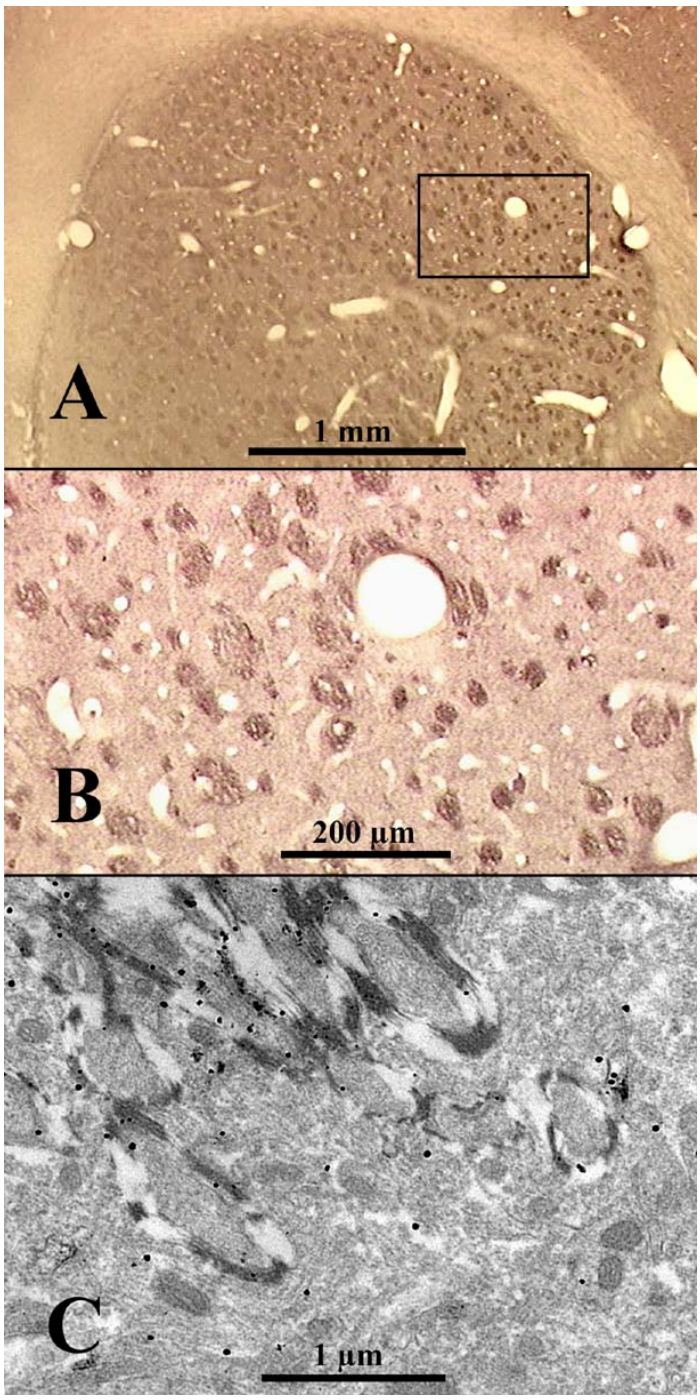

Fig. 19: Anti-Kir2.2 antibodies stain striatal fiber bundles. Using carefully selected conditions (for details see text) Kir2.2 immunoreactivity displayed a prominent labeling of fiber bundles within the striatum (A,B). At the electron microscopic level (C) the gold dots representing Kir2.2 channel distribution are found highly concentrated within the fiber bundles, suggesting the Kir2.2 subunit being sorted to the axonal membrane. Gold dots are sparse in the surrounding neuropil.

3.4.3 Kir2.3 channels are predominantly localized in the matrix compartment

The detailed analysis of the Kir2.3 protein distribution again required carefully selected antibody concentrations. These optimized conditions demonstrate that from the Kir2 family proteins only the Kir2.3 subunit is distributed inhomogeneously. Regions of low antibody binding are intermingled with areas of stronger immunoreactivity (Fig. 20A). This heterogeneity, which may be related to the compartmental organization, was detectable in all rats and extended throughout the whole striatum along the rostro-caudal axis.

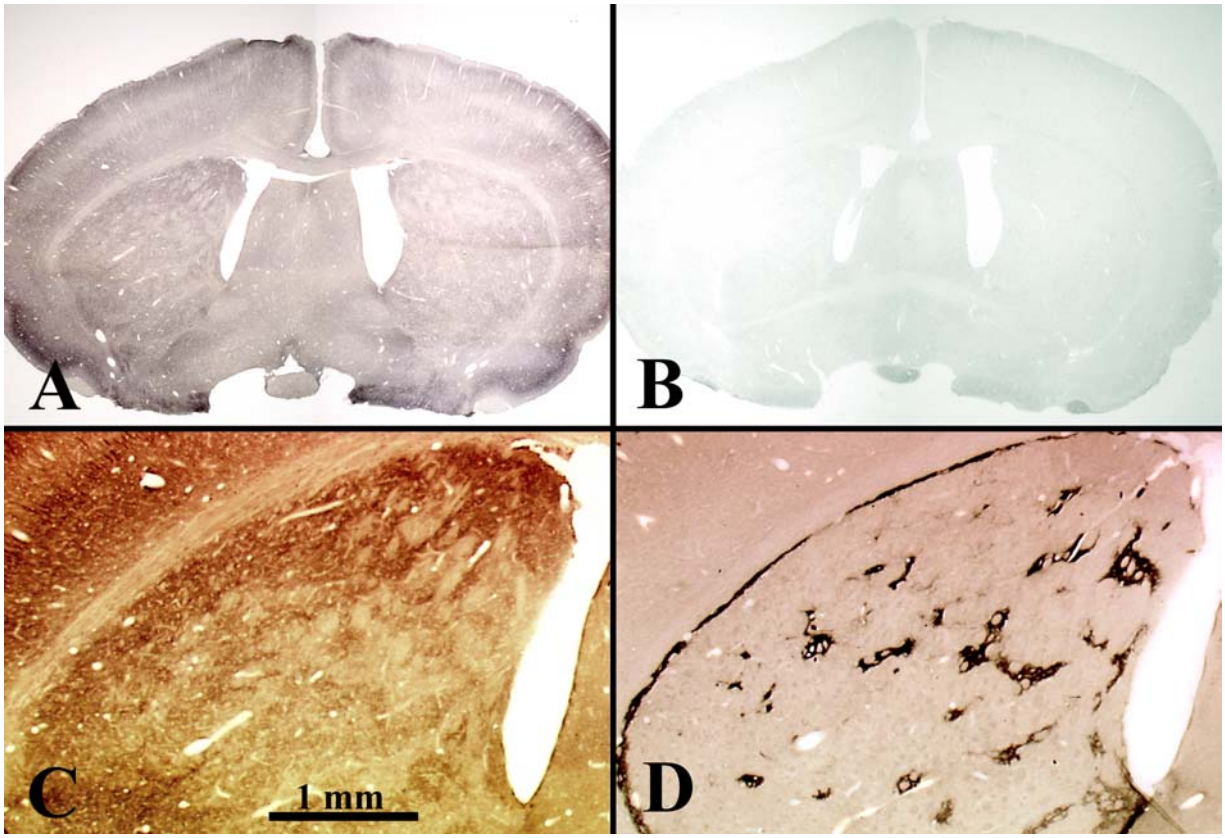

Fig. 20: Kir2.3 channel subunit protein is inhomogeneously distributed throughout the striatum. Complete immunostained sections (A) of the rat forebrain, unlike sections with antigen competition (B), show Kir2.3 immunoreactivity in the striatum. Using selected conditions, an inhomogeneous distribution of the Kir2.3 subunit in the striatum becomes obvious (C). The pattern of reduced Kir2.3 staining seems similar to that of the striatal patch compartment as visualized via the immunocytochemical localization of μ-opiate receptors (D).

Now one could argue that the patchy distribution of Kir2.3 immunoreactivity might be caused by the existence of cell-dense and cell-poor regions. To rule out this possibility the Kir2.3 localization was compared to an adjacent Klüver-Barrera stained section (Fig. 21).

The medium spiny neurons are rather homogeneously distributed between the prominent fiber bundles, a typical feature of the striatum. In regions of strong Kir2.3 reaction (Fig. 21A and B, arrowheads) and in poorly stained areas (arrows), cell density is similar. Consequently, the patchy distribution of Kir2.3 channel subunits cannot result from high or low cell densities. In contrast, it seemed to be roughly congruent with the distribution of μ-opiate receptors (Fig. 20D), the original[75] and well recognized marker of the striatal patch compartment.

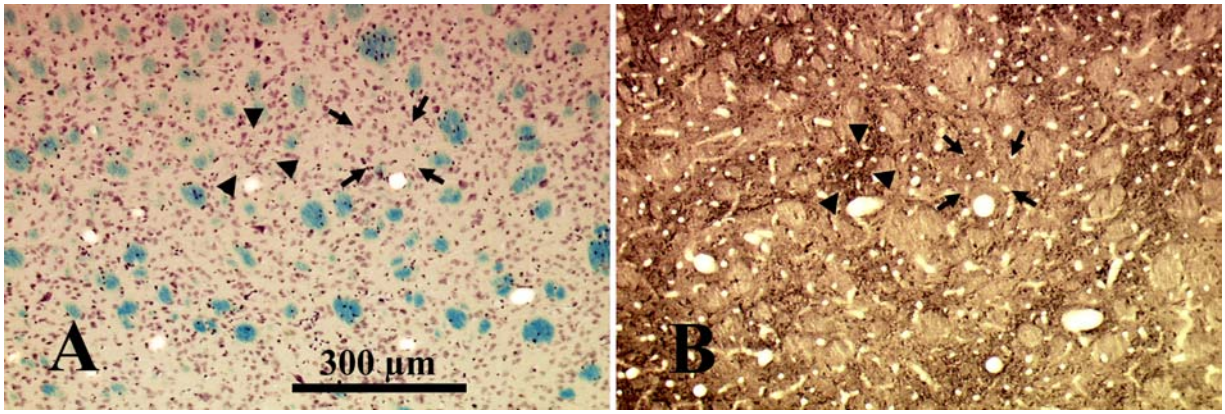

Fig. 21: Striatal cell density. Adjacent sections stained according to Klüver-Barrera (A) and for the Kir2.3 subunit (B) demonstrate that the increased Kir2.3 immunoreactivity is not simply due to an increased density of nerve cells at this location (compare areas between the three arrowheads or between the four arrows). Note the identical localization of capillaries in (A) and (B).

The identity of the Kir2.3-weak areas with the patch compartment became obvious when both distribution patterns were compared in adjacent sections (Fig. 22). The upper images (Figs. 22A, C) display the distribution of patch compartments using immunocytochemical visualization of μ-opiate receptor distribution. The same areas in an adjacent section are shown in the lower panel photographs (Figs. 22B, D) stained with anti-Kir2.3 antibodies. Striatal fiber bundles are hatched to make sure that the patchy Kir2.3 reactivity is not confused with unstained fibers.

In an overlay of striatal patches with the Kir2.3 image (Fig. 22B, D) the low Kir2.3 immunoreactivity inside the patch compartment is verified. The lines surrounding the patches nicely correspond to the borders between areas of different Kir2.3 staining

[75] PERT, C.B. 1976

intensities. Thus, there is a clear correlation between areas with increased Kir2.3 immunoreactivity and the striatal matrix compartment.

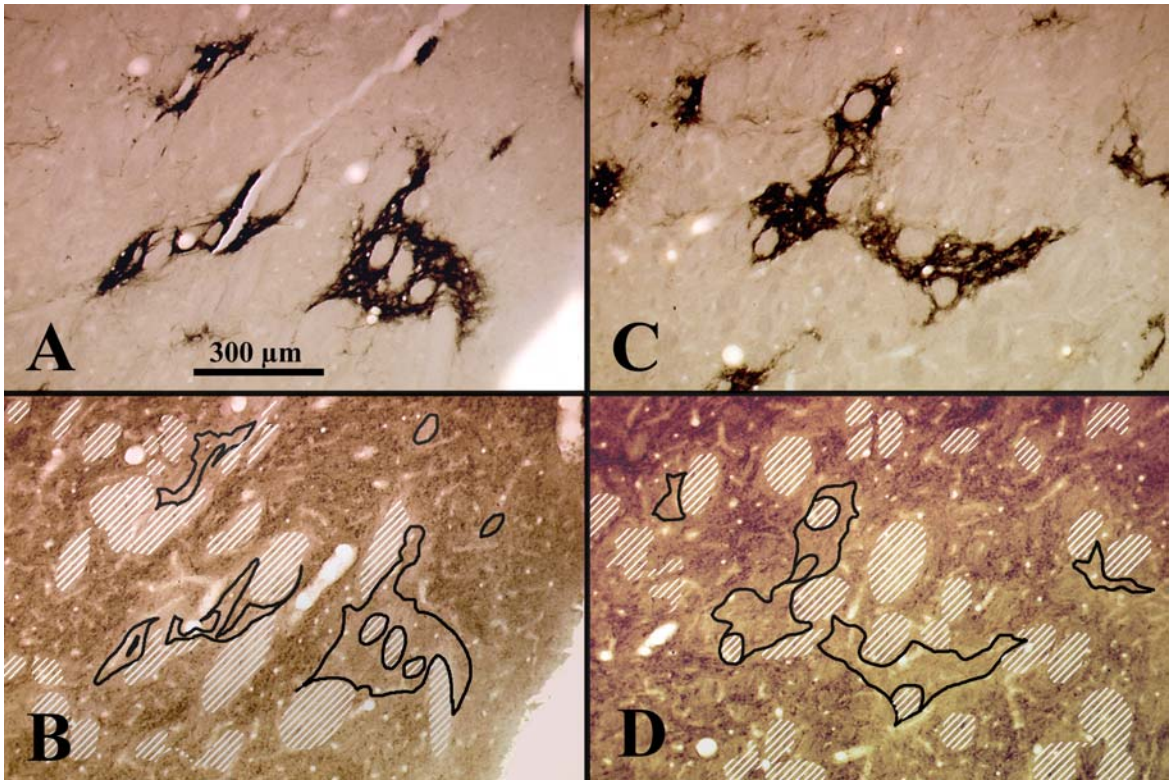

Fig. 22: Correspondence between the striatal patch compartments and areas with reduced Kir2.3 immunoreactivity. For direct correlation, areas of reduced Kir2.3 immunoreactivity (B,D) and the striatal patch compartment as visualized by µ-opiate receptor staining (A,C) are compared in adjacent sections. In (B,D) areas occupied by fiber bundles are hatched to avoid confusion. The patch compartment (as seen in A and C) is outlined in black to facilitate comparison.

3.4.4 Kir2.4 channel subunits are localized at cholinergic interneurons

In addition to the striatal patch compartment, cholinergic interneurons represent a major decision making component within the basal ganglia circuitry. Localization of one of the Kir2 channel subfamily members in these giant interneurons would imply their importance in the regulation of basal ganglia circuitry.

A survey micrograph (Fig. 23A) shows large Kir2.4-positive neurons (arrows) dominating the minor immunoreactivity of spiny projection neurons. Due to their large size and small number these cells most likely represent aspiny cholinergic interneurons. To verify this assumption, striatal cholinergic neurons were identified by the presence of choline

acetyltransferase (ChAT), the enzyme that catalyses the formation of acetylcholine from acetyl-CoA and choline.

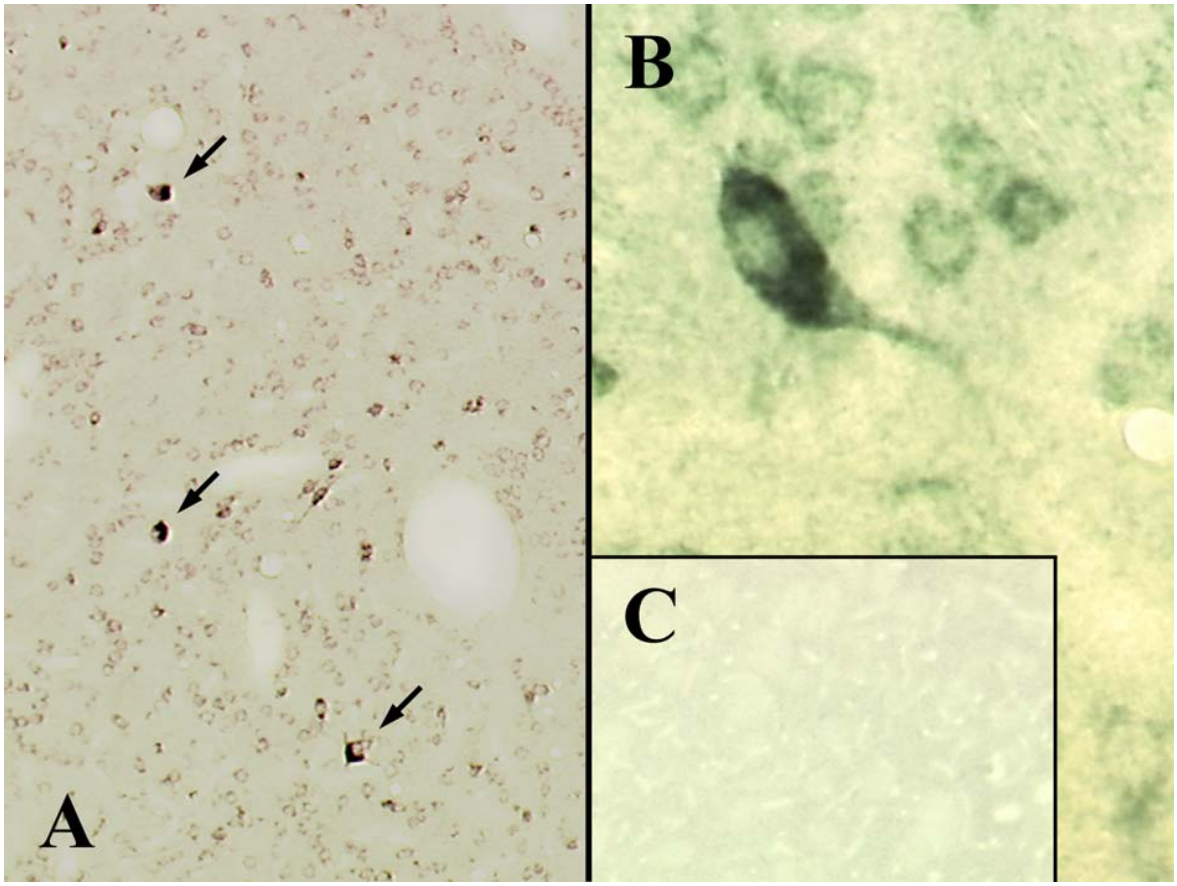

Fig. 23: Kir2.4 channel immunoreactivity is most prominent in large striatal interneurons. Immunoreactivity for the Kir2.4 subunit in the rat striatum is mostly somatodendritic and largely absent from the neuropil (A). Staining is weak, however, in the large population of small striatal neurons and prominent in only a few, very large cells (A, arrows; B), most likely representing the so-called 'giant' interneurons in the striatum. Immunoreactivity is abolished (C) subsequent to preincubation of anti-Kir2.4 antibodies with the cognate protein.

Double labeling experiments (Fig. 24) confirmed the staining of cholinergic interneurons by the anti-Kir2.4 antibody. Under red fluorescence the microscopic image displays about five different neurons expressing Kir2.4 channel proteins (Fig. 24B, arrowheads). Green ChAT immunoreactivity presents a similar distribution of neurons (Fig. 24A). One single small cell, weakly stained for Kir2.4 (arrow in B), remained immunonegative for ChAT. The expression of Kir2.4 channels at cholinergic interneurons is verified by the yellow color of labeled neurons in the overlay image (Fig. 24C). The single smaller cell displays a red fluorescence only (Fig. 24C, arrow). Most probably it represents a spiny striatal projection neuron devoid of ChAT immunoreactivity. In addition to the Kir2.4 channel

protein, the Kir2.2 subunit was also localized to cholinergic interneurons, confirming data from *in situ* hybridization experiments (see discussion).

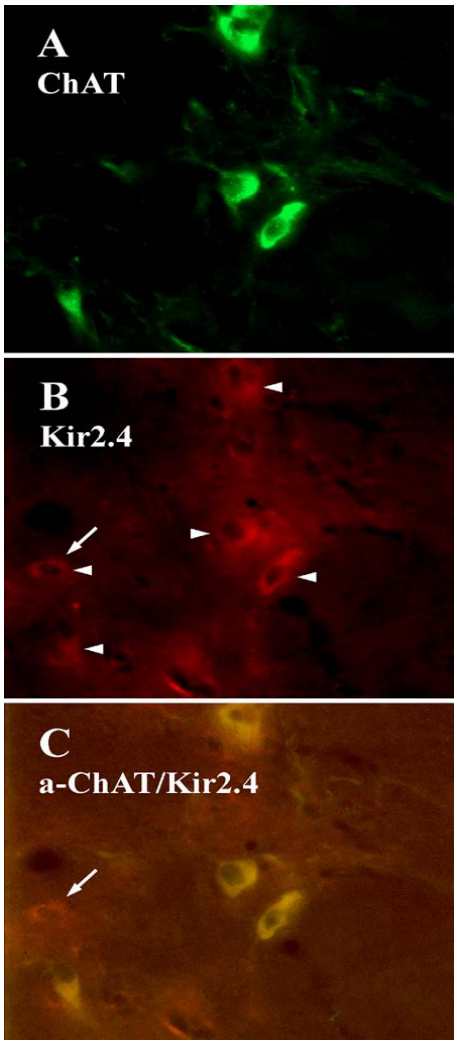

Fig. 24: Immunofluorescence double labeling of large striatal interneurons for choline acetyltransferase (ChAT) and Kir2.4 immunoreactivity. Sections were treated simultaneously with monoclonal mouse anti-ChAT- and rabbit anti-Kir2.4-antibodies, followed by visualization with Oregon Green-labeled goat anti-mouse and Texas Red-labeled goat anti-rabbit secondary antibodies. The four ChAT-positive cholinergic neurons (A) express Kir2.4-immunoreactivity (B, arrowheads) as judged from their yellowish appearance (C) after double exposition for green and red fluorescence.

The expression of Kir2 channels at ChAT neurons was confirmed at the electron microscopic level, also focusing on subcellular channel distribution. For this purpose cholinergic interneurons were labeled with anti-ChAT antibodies and visualized via peroxidase and diaminobenzidine. Anti-Kir2.2 and anti-Kir2.4 antibodies were detected using gold-labeled secondary antibodies. Both Kir2 subfamily members were localized at cholinergic interneurons (Fig. 25).

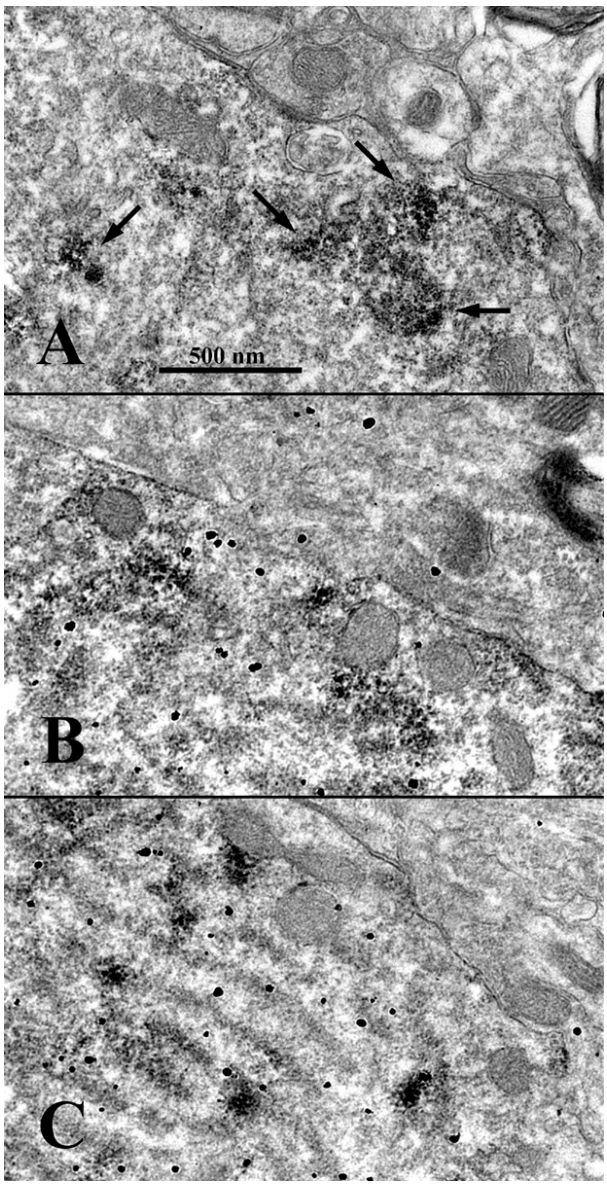

Fig. 25: Double labeling of Kir2.4 and choline acetyltransferase at the electron microscopic level. Cholinergic interneurons are identified by their amorphous diaminobenzidine reaction product (A, arrows) in single- (A) or double-stained sections. Kir2 immunoreactivity is visualized by silver-intensified ultrasmall gold particles (for details see methods). Cholinergic interneurons display Kir2.2 (B) as well as Kir2.4 (C) immunoreactivity.

DAB-positive cholinergic neurons were recognized by dark cytoplasmic deposits (Fig. 25A, arrows). In double labeling experiments, gold dots indicated the localization of Kir2.2 (Fig. 25B) and Kir2.4 (Fig. 25C) channel subunits. Note that there are some gold dots outside the cholinergic interneuron in anti-Kir2.2- but not in anti-Kir2.4-stained sections. Thus, only Kir2.4-immunoreactivity was found to be restricted to cholinergic inter-neurons, offering possibilities for specific, Kir2.4-based modulation of the striatal cholinergic system with potential therapeutic consequences.

4 Discussion

Potassium channels are important components of the signal transduction machinery of the nervous system and virtually all other cells of the mammalian body. They are involved in a wide variety of functions such as setting and stabilizing the resting potential of most cell types or regulating the depolarization time course in pacemaker cells. Other parameters like action potential duration, firing frequencies, and interspike intervals are also determined by the activity of potassium channels[76]. A functional channel is formed by the homomeric or heteromeric aggregation of four subunit proteins, usually from members of one channel family. The basic structural organisation of such a subunit consists of a short amino acid sequence, which forms a "loop" into the membrane and is flanked by two transmembrane domains (see Fig. 1B). The loop takes part in forming the channel pore. This basic structural unit may be supplemented by four additional membrane spanning domains, or two units may be combined to a single protein, thus forming three structural classes of potassium channels[77]. With respect to sequence homologies, each of these classes consists of at least six families, again each represented by one to nine members, each possibly represented by more than five splice variants. Summing up to about 90 individual genes with even more functional gene products from different splice variants and the formation of heterooligomers, there is an impressive amount of potassium channels, large enough to cover the complex range of channel functions in living cells.

This complexity explains the fact that a variety of quite distinct diseases can be traced back to ion channel defects. Thus, Andersen's syndrome (AS), a rare inherited disorder characterized by periodic paralysis, cardiac arrhythmias, and dysmorphic features, is due to mutations of the Kir2.1 potassium channel[78]. Furthermore, an increasing number of neurological diseases such as hereditary deafness syndromes, episodic ataxia type-1, acquired neuromyotonia, and others are the results of compromised potassium channel functions[79]. On the other hand, the large molecular diversity of the channels should allow the development of highly specific drugs, which may selectively target cell types, groups, or systems throughout the body, correcting or at least improving disturbed functions. The

[76] HILLE, B. 1995
[77] for more information see http://nt-salkoff.wustl.edu
[78] PLASTER, N.M. 2001, FELIX, R. 2000
[79] BENATAR, M. 2000

great potential of this approach is documented by the effective treatment of diabetes or cardiac arrhythmias with drugs, which are primarily directed to ATP-sensitive or HERG-type potassium channels, respectively. The impact of this strategy for improving neuropsychiatric pharmacotherapy is under consideration[80]. Systematic development of further neuroactive drugs, however, will depend on information about the involvement of molecularly defined potassium channels in identified neuronal circuits. In this respect it is important to understand the regional, cellular, and subcellular localizations of identified potassium channel subunits in clinically important brain nuclei such as the basal ganglia.
In the present study we generated highly specific, affinity-purified rabbit antibodies to study the detailed distribution of Kir2 inwardly rectifying potassium channel subunits in the striatum. With respect to a potential involvement of Kir2 channels in motor output of the basal ganglia, we focused on the striatal key structures for movement regulation. In particular, we asked whether any of the Kir2 channels are selectively distributed in the patch or matrix compartment of the striatum or preferentially localized at cholinergic interneurons.

4.1.1 Kir2 channel proteins are differentially expressed throughout the rat brain

The monospecific antibodies allowed the characterization of Kir2 protein localization in the rat central nervous system. The widespread presence of all four Kir2 channel subunits in the rat brain may indicate their important role in central signal processing and neural transmission. Our data agree with earlier *in situ* hybridization (ISH) experiments (see chapter 3.3.) and electrophysiological studies, confirming the basic distribution patterns of Kir2.1, Kir2.2 and Kir2.3 subunits. However, ISH experiments only indicate which neurons can synthesize these subunits. Our immunocytochemical experiments extend these data, presenting information on the subcellular localization in the different types of neurons. Exemplary in the basal ganglia, all Kir2 subunits are localized in the somata and dendrites of striatal neurons. Data obtained so far suggest that Kir2.2 is the only member of this channel family, which is additionally sorted to the axonal plasma membrane.

[80] ALLEN, J.W. and ETCHEBERRIGARAY, R. 1998

Regional and cellular localizations of the Kir2.4 subunit, as presented here, contrast an earlier *in situ* hybridization study by Töpert et al. 1998, where Kir2.4 mRNA was reported to be primarily expressed in neurons of cranial nerve motor nuclei. The present investigation reveals a widespread Kir2.4 immunoreactivity among neurons in many brain areas (see chapter 3.3.). In all areas the signal was blocked by preabsorption of antibodies with its cognate recombinant protein, ruling out background labeling. Another difference is the Kir2.4 localization in the rat striatum, where no Kir2.4 transcripts were detected by *in situ* hybridization[81]. We found a signal in most, if not all striatal neurons. With the exception of the cholinergic interneurons, however, Kir2.4 immunoreactivity is less intense as compared to the other members of the Kir2 subfamily.

The apparent contradiction may be, however, simply due to aspects of sensitivity. We also find very strong labeling of brain stem motor neurons (Fig. 17-VII,J), where Kir2.4 mRNA was reported to be primarily expressed, but we detect weaker expression in most neurons throughout the brain. Our data, therefore, support the prominent localization of Kir2.4 protein in motor nuclei. Interestingly enough, motor neurons are cholinergic as are the giant interneurons in the striatum. This raises the possibility that cholinergic neurons in general may preferentially use the Kir2.4 subunit to control their resting potentials. Further investigation of other cholinergic cell groups in the vertebrate CNS should provide more decisive information.

The sensitivity aspect is supported by experiments with the rat retina. Kir2.4 transcripts[82] and proteins[83] were clearly detected in the retina, while Töpert et al. did not find any Kir2.4 mRNA expression in this organ. These data strengthen our hypothesis of a more widespread Kir2.4 localization as supported by Töpert's study.

The detailed channel protein distribution of all members of the Kir2 subfamily in the rat brain is summarized in table 4. Excellent agreement of the Kir2.1-Kir2.3 subunit (for Kir2.4 see above mentioned comments) with former *in situ* hybridization experiments[84] was found in most brain regions, for example olfactory bulb, olfactory tubercle, neocortex, hippocampus, caudate putamen, nucleus accumbens, lateral olfactory tract nucleus, hypothalamus, habenula and superior colliculus (Fig. 17-I – 17-IX). But in some areas

[81] TÖPERT, C. 1998
[82] HUGHES, B.A. 2000
[83] SKATCHKOV, S.N. 2001
[84] MORISHIGE, K.-I. 1993; HORIO, Y. 1996; KARSCHIN, C. 1996; BREDT, D.S. 1995; FALK, T. 1995.

there are differing distribution patterns of mRNA and channel protein expression. The most obvious difference was observed in the hindbrain, where the Kir2.1 and Kir2.3 subunits were reported to be virtually absent[85]. In contrast to their report and in strong agreement with a previous mRNA study on the Kir2.3 subunit[86], we found the distribution of the Kir2.3 channel subunit extended to cerebellar Purkinje cells and to neurons of the deep cerebellar nuclei (Fig. 17-VIII,E/I). The Kir2.1 subunit was also detected in the cerebellum (molecular layer and deep nuclei), which is supported by a former localization study[87]. Nevertheless, the cerebellar expression of the Kir2.2 protein with very high signals in the granule cell layer is confirmed in our investigation.

Another difference was found in the thalamus (Fig. 17-V). Although the Kir2.2, Kir2.3 and Kir2.4 channel distribution is similar to the previously described mRNA localization pattern, the Kir2.1 protein was found at significant levels in various thalamic nuclei, thereby contrasting former investigations[88]. Finally, we observed expression of all four members of the Kir2 subfamily in the substantia nigra, where only the Kir2.2 subunit was reported to be expressed[89]. In fact, the Kir2.2 channel protein was present in markedly elevated levels, but also the Kir2.3 subunit displayed specific signals mainly in the pars reticulata.

4.1.2 The Kir2.3 subunit is preferentially expressed in striatal matrix neurons

All members of the Kir2 subfamily are differentially distributed throughout the rat striatum, thus confirming the fundamental localization pattern as reported from previous *in situ* hybridization experiments (see table 5). The broad distribution of all Kir2 channels suggests important roles for these channels in regulating neuronal excitation and transmission within the basal ganglia circuitry.

The present study demonstrates an inhomogeneous distribution of potassium channels in the striatum. Thus, one member of the inwardly rectifying Kir2 family, namely the Kir2.3 channel protein in the rat striatum, displays a heterogeneous pattern that can neither be explained by varying cell densities nor by the numerous fiber bundles. Instead, the density

[85] KARSCHIN, C. 1999; ISOMOTO, S. 1997
[86] FALK, T. 1995
[87] LIAO 1996; MIYASHITA and KUBO 1997; SIGNORINI 1997
[88] HORIO, Y. 1996; ISOMOTO, S. 1997.

of the inwardly rectifying potassium channels nicely correlates with the striatal compartments. The Kir2.3 channel tends to avoid the patch compartment and is predominantly expressed in the striatal matrix.

An inhomogeneous distribution of Kir2.3 channels in the striatum was inferred from Surmeier's group[90] using single-cell RT-PCR and whole-cell patch clamp techniques. They found a preferential expression of Kir2.1, Kir2.2 and Kir2.3 channels in either SubP-positive or Enk-positive medium spiny neurons. The Kir2.3 channel was expressed in all SubP-positive neurons but only in a minority of Enk-positive cells. Thus, the discovered distribution pattern refers to the distinction between direct and indirect pathway of striatal signal transduction (see chapter 1.2.3.). Extending these data, our results illuminate a difference between the striatal patch and matrix compartment.

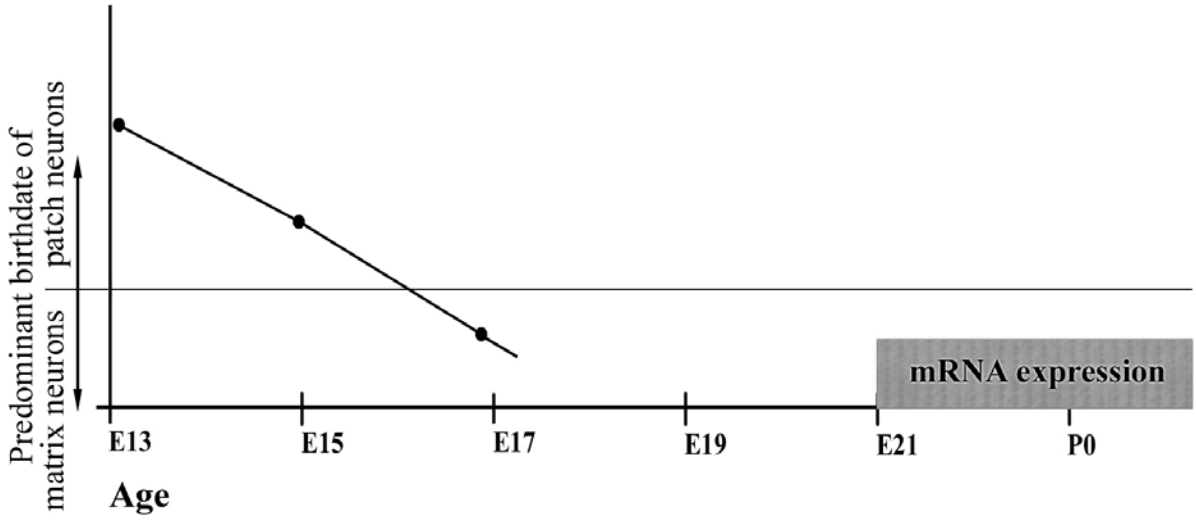

Fig. 26: Ratios of patch neurons to matrix neurons across embryonic ages. Ratios above the solid horizontal line indicate a predominance of patch neuron birthdates and ratios below the line indicate a predominance of matrix neuron birthdates. Consequently, at the time of beginning Kir2.3 mRNA expression most of the neurons end up in the matrix compartment.

The preferential localization of the Kir2.3 subunit in the striatal matrix compartment is in agreement with developmental studies. Thus, most of early born neurons (becoming postmitotic between E12-E16) end up in the patch, while the majority of later born neurons (E18-postnatal day P2) mature in the matrix compartment[91]. Correspondingly,

[89] KARSCHIN 1996
[90] MERMELSTEIN, P.G. 1998
[91] VAN VULPEN, E.H.S. 1998; VAN DER KOOY, D. 1987

onset of Kir2.3 channel expression begins late, and Kir2.3 mRNA is absent from the brain until E21[92]. Apparently, at the time when striatal neurons start expressing Kir2.3 channel proteins, these neurons are still in development and there is an extraordinarily high probability that they will end up in the matrix compartment (Fig. 26). Of course, not only developing neurons express Kir2.3 channels. But Kir's evident influence in development of trophic interaction and synaptogenesis[93] suggests an electrophysiological involvement as early as necessary.

Inwardly rectifying Kir2 channels dominate the electrophysiological behavior in the down-state of medium spiny neurons[94] (see chapter 1.2.1) by keeping the membrane potential close to the K^+ equilibrium potential. Based upon our studies, in matrix neurons this is mainly done by the Kir2.3 channel. Thus, the amount and activity of Kir2.3 channels determine the membrane conductance in matrix medium spiny cells. It is well known that the transition to the up-state and following spike generation depends on temporally coherent excitatory synaptic input. If the cells express a high number of Kir2.3 potassium channels, massive convergent input is necessary to generate the up-state. Consequently, it may be expected that pharmacologically blocked Kir2.3 channels fail to stabilize the neuronal down-state.

The matrix-related basal ganglia loops are thought to transmit effectory signals, i.e. the motor output. In contrast, patch-related circuitry mainly accounts for the regulation of the motor effects. Application of a selective Kir2.3 channel blocking drug could facilitate spiking within the matrix compartment by excitatory input while the patch might be virtually unaffected due to their absent Kir2.3 expression. Therefore, blocking of Kir2.3 channels may specifically improve the motor outcome (for example bradykinesia) in Parkinson's disease.

4.1.3 Kir2.4 immunoreactivity in the striatum is most prominently displayed by the giant cholinergic interneurons

Although anti-Kir2.4 antibodies react with many neurons in the striatum, they most intensely stain the giant interneurons. The cholinergic nature of these neurons was

[92] KARSCHIN, C. 1997
[93] KARSCHIN, C. 1999

confirmed by double labeling experiments at the light and electron microscopic level. Cholinergic interneurons also display the Kir2.2 subunit, but only at a level comparable to that in the spiny projection neurons. Our results are supported by the Kir2.2 mRNA distribution as reported recently[95].

Bearing in mind the pivotal role of cholinergic neurons for the motor outcome of neuronal computations in basal ganglia, Kir2.4 subunit containing potassium channels, due to their restricted localization, may be especially important. They will take part not only in controlling the activity of the interneurons, but may be further involved in regulating the fine tuning between the two basal ganglia pathways. Thus, cholinergic interneurons are known[96] to activate the spiny projection neurons of the indirect pathway via M1 receptors (see introduction). M1-based stimulation of these neurons should be additionally facilitated by the concomitant destabilization of the resting potential due to an inhibition of Kir2.3 channel activity inherent to M1 receptor activation[97].

4.1.4 Can Kir channel subunits be targets for novel therapeutic strategies?

As mentioned above, a variety of distinct diseases can be traced back to ion channel defects. This is also confirmed in the special case of inwardly rectifying potassium channels. Mutations in genes encoding Kir channels have been shown to cause hereditary diseases. Salt-wasting and metabolic acidosis in Bartter's syndrome[98] often is due to the malfunction of ROMK1 (Kir1.1) channels in the kidney. Degeneration of cerebellar granule cells with resulting ataxia is due to Kir3.2 missense mutations in *weaver* mice[99]. However, only little progress has been made in supporting recent therapeutic strategies by targeting Kir channel subunits. This may be primarily due to the fact that our knowledge on the detailed biological functions of Kir channels in the nervous system is still limited. Some natural drugs affecting Kir channel activity like the Kir1.1/Kir3.1-specific channel inhibitor tertiapin[100] and the spermine-like Kir blocker Philanthotoxin[101] are available.

---

[94] MERMELSTEIN, P.G. 1998, NICOLA, S.M. 2000
[95] KARSCHIN, C. 1996
[96] DI CHIARA, G. 1994; CALABRESI, P. 2000
[97] CHUANG, H. 1997
[98] SCHEINMAN, S.J. 1999
[99] PATIL, N. 1995
[100] JIN, W. and LU, Z. 1998
[101] LEE, J.K. 1999

These are hopeful beginnings on the way to specifically treating Kir channel-based diseases.

Inwardly rectifying potassium channels can be attractive candidates for novel therapeutic regimes only if the channels are selectively expressed in those nervous structures that are important for any neuropsychiatric disorder or for side effects during established treatment. In that case, activation or inhibition of Kir channels may influence the clinical situation of affected patients. The present study reports the Kir2 channel localization to defined structures of the basal ganglia circuits, which are basically involved in the regulation of movements. Patch and matrix striatal compartments as well as the cholinergic interneurons represent these key structures and display a specific distribution pattern of Kir2 channel subunits.

Pharmacological manipulations of potassium channels will extend available interactions with transmitter systems. Thus, selective activation of Kir2.4-subunit containing channels in the striatum will stabilize the resting potential of giant cholinergic interneurons. Consequently, action potential firing and cholinergic transmission will be reduced in a manner comparable with the application of an anticholinergic drug. Because of the influence restricted to the interneuron, however, diverse side effects of anticholinergic therapy may be absent or reduced. It could not be expected, of course, that simply targeting Kir2.4 channels in the striatum by channel openers or blockers would affect only motor behavior without side effects on other neurons. However, it is conceivable to use such drugs at subthreshold doses. Thus, on their own, such treatments may remain without obvious pharmacological effects. Combination with again subthreshold doses of a second drug, however, which affect striatal ChAT neurons via a distinct mechanism, for instance other channels[102], should cause an effect above threshold.

Pharmacological intervention with neurotransmission within the matrix and patch compartments of the striatum seems to be more complex with respect to the predominant Kir2.3 expression in the matrix. Increasing membrane excitability by inhibiting Kir channels may partly compensate the problems of dopamine-deficiency such as akinesia, tremor, or rigor in parkinsonian states.

Matrix inputs in most areas of the striatum are predominantly related to sensorimotor processing, whereas patch input has a strong relation to the limbic system. Keeping in

[102] THOMZIG, A. 2003

mind these functional compartmental differences, a Kir2.3-mediated activation or inhibition of matrix neurons may predominantly influence motor circuits within the basal ganglia, leaving limbic circuits mainly unaffected. Thus, targeting Kir2.3 channels may participate in an improved neuroleptic therapy. Aiming at motor and not at limbic circuits may disconnect the antipsychotic effects of neuroleptics from their severe motor side effects, such as early and late dyskinesias as well as parkinsonoid syndromes.

Additional examination of limbic circuits will be required to provide further information. The nucleus accumbens seems to connect motor outcome with the limbic system ("limbic/motor interface") and plays a major role in mediating motivation and reward[103]. It contains two subdivisions, shell and core, which are cytoarchitectonically and pharmacologically distinct and differ also in their afferent and efferent connections[104]. The present investigation revealed the expression of all four Kir2 subfamily members in the nucleus accumbens (Fig. 17-IV). Interestingly, the Kir2.3 subunit displayed a patchy distribution in the core part resembling the striatal expression pattern and supporting the strong histochemical relation between core and striatum[105]. Moreover, particularly elevated signals of the Kir2.3 channel protein in the shell part of the nucleus accumbens suggest profound involvement in the neuronal excitability and regulation at this site of limbic/motor interaction. Therefore, a more detailed analysis of ventromedial striatal areas and the nucleus accumbens is in progress in our laboratory.

[103] HABER, S.N. 2000; WHITE, N. 1998
[104] VOORN, P. 1996; HABER, S.N. 2000; GROENEWEGEN, H.J. 1996; JOEL, D. 2000; JONGEN-RÊLO, A.L. 1994
[105] GROENEWEGEN, H.J. 1996; HABER, S.N. 2000

Summary

Parkinson's disease is the most frequent movement disorder caused by loss of dopaminergic neurons in the midbrain. Intentions to avoid side effects of conventional therapy should aim to identify additional targets for potential pharmacological intervention. In principle, every step of a signal transduction cascade, such as presynaptic transmitter release, type and occupation of postsynaptic receptors, G protein-mediated effector mechanisms, and the alterations of pre- or postsynaptic potentials as determined by the local ion channel composition, have to be considered. Due to their diversity and their widespread but distinct localizations, potassium channels represent interesting candidates for new therapeutic strategies.

As a first step, the present report aimed to study the cellular and subcellular distribution of the individual members of the Kir2 family in the striatum, a group of proteins forming inwardly rectifying potassium channels. For this purpose polyclonal, monospecific, affinity purified antibodies against the less conserved carboxyterminal sequences from the Kir2.1, Kir2.2, Kir2.3, and Kir2.4 proteins were prepared. All subunits of the Kir2 family were detected on somata and dendrites of most striatal neurons. However, the distribution of two of them was not homogeneous. Striatal patch areas were largely devoid of the Kir2.3 protein, and the Kir2.4 subunit was most prominently expressed on the tonically active, giant cholinergic interneurons of the striatum. These two structures are among the key players in regulating dopaminergic and cholinergic neurotransmission within the striatum, and therefore are of major importance for the output of the basal ganglia. The heterogeneous localization of the Kir2.3 and the Kir2.4 subunits with respect to these strategic structures pinpoints these channel proteins as promising targets for future pharmacological efforts.

References

Aizman, O. et al. 2000. Anatomical and physiological evidence for D1 and D2 dopamine receptor colocalization in neostriatal neurons. Nat. Neurosci. 3: 226-230.

Alexander, G.E., DeLong, M.R., Strick, P.L. 1986. Parallel organization of functionally segregated circuits linking basal ganglia and cortex. Ann Rev Neurosci: 9: 357-381.

Alexander, G.E. and Crutcher, M.D. 1990. Functional architecture of basal ganglia circuits: Neural substrates of parallel processing. TINS 13: 266-271.

Alexander, G.E., Crutcher, M.D., DeLong, M.R. 1990. Basal ganglia-thalamocortical circuits: parallel substrates for motor, oculomotor, 'prefrontal' and 'limbic' functions. Progr. Brain Res. 85:119-146.

Allen, J.W., Etcheberrigaray, R. 1998. Potassium channels in neuropsychiatric disorders: potential for pharmacological intervention. CNS Drugs 10: 61-82.

Baev, K.V. 1995. Disturbances of learning processes in the basal ganglia in the pathogenesis of Parkinson´s disease: a novel theory. Neurological Research 17: 38-48.

Benatar, M. 2000. Neurological potassium channelopathies. Q. J. Med. 93: 787-797.

Bennett, B.D., Callaway, J.C., and Wilson, C.J. 2000. Intrinsic membrane properties underlying spontaneous tonic firing in neostriatal cholinergic interneurons. The Journal of Neuroscience 20: 8493–8503.

Bergmann, H., Feingold, A., Nini, A., Raz, A., Slovin, H., Abeles, M., and Vaadia, E. 1998. Physiological aspects of information processing in the basal ganglia of normal and parkinsonian primates. TINS 21, 32-38.

Biggin, P.C., Roosild, T., and Choe, S. 2000. Potassium channel structure: domain by domain. Current Opinion in Structural Biology 10: 456-461.

Bolam, J. et.al. 1988. Cellular substrate of the histochemically defined striosome/matrix system of the caudate nucleus: a combined Golgi and immunocytochemical study in cat and ferret. Neuroscience 24, 853-875.

Bolam, J.P. et.al. 1984. Characterization of cholinergic neurons in the rat neostriatum. A combination of choline acetyltransferase immunocytochemistry, Golgi-impregnation and electron microscopy. Neuroscience 12: 711-718.

Bredt, D.S., Wang, T.-L., Cohen, N.A., Guggino, W.B., and Snyder, S.H. 1995. Cloning and expression of two brain-specific inwardly rectifying potassium channels. Proc. Natl. Acad. Sci. USA 92: 6753-6757.

Caboche, J., Rogard, M., and Besson, M.J. 1991. Comparative development of D1-dopamine and μ-opiate receptors in normal an in 6-hydroxydopamine-lesioned neonatal rat striatum: dopaminergic fibers regulate μ but not D1 receptor distribution. Devl Brain Res. 58: 111-122.

Calabresi, P., Pisani, A., Mercuri, N.B., Bernardi, G. 2000. ACh-mediated modulation of striatal function. TINS 23, 120-126.

Cepeda, C., Levine, M.S. 1998. Dopamine and N-methyl-D-aspartate receptor interactions in the neostriatum. Dev Neurosci 20: 1-18.

Chandy, K.G. and Gutman, G.A. 1993. Nomenclature for mammalian potassium channel genes. Trends in Pharmacological Sciences 434.

Chen, H., Kubo, Y., Hoshi, T., Heinemann, S.H. 1998. Cyclosporin A selectively reduces the functional expression of Kir2.1 potassium channels in Xenopus oocytes. FEBS Letters 422: 307-310.

Chuang, H., Jan, Y.N. and Jan, L.Y. 1997. Regulation of IRK3 inward rectifier K+ channel by m1 acetylcholine receptor and intracellular magnesium. Cell 89: 1121–1132.

Cohen, N.A., Brenman, J.E., Snyder, S.H., and Bredt, D.S. 1996a. Binding of the inward rectifier K+ channel Kir2.3 to PSD-95 is regulated by protein kinase A phosphorylation. Neuron 17: 759-67.

Cohen, N.A., Sha, O., Makhina, E.N., Lopatin, A.N., Linder, M.E., Snyder, S.H., Nichols, C.G. 1996b. Inhibition of an inward rectifier potassium channel (Kir2.3) by G-protein □□ Subunits. Journal of biological chemistry 271: 32301-32305.

Collins, A., German, M.S., Jan, Y.N., Jan L.Y., and Zhao, B. 1996. A strongly inwardly rectifying K+ channel that is sensitive to ATP. J Neurosci 16: 1-9.

Coulter, K.L., Périer, F., Radeke, C.M., and Vandenberg, C.A. 1995. Identification and molecular localization of a pH-sensing domain for the inward rectifier potassium channel HIR. Neuron 15: 1157-1168.

Dahlstrom, A. and Fuxe, K. 1964. Evidence for the existence of monoamines containing neurons in the central nervous system. 1. Demonstration of monoamines in the cell bodies of brain stem neurons. Acta physiol. scand. 62: 1-55.

Desban, M., Kemel, M.L., Glowinski, J., and Gauchy, C. 1993. Spatial organization of patch and matrix compartments in the rat striatum. Neuroscience 57: 661-671.

Di Chiara, G., Morelli, M., Consolo, S. 1994. Modulatory functions of neurotransmitters in the striatum: ACh/DA/NMDA interactions. TINS 17, 228-233.

Doupnik, C.A., Davidson, N., and Lester, H.A. 1995. The inward rectifier potassium channel family. Current Opinion in Neurobiology 5: 268-277.

Doyle, D.A. et al. 1998. The structure of the potassium channel: molecular basis of K+ conduction and selectivity. Science 280: 69-77.

Eblen, F. and Graybiel, A.M. 1995. Highly restricted origin of prefrontal cortical inputs to striosomes in the macaque monkey. J. Neurosci. 15: 5999-6013.

Fakler, B., Brändle, U., Glowatzki, E., Weidemann, S., Zenner, H.-P., and Ruppersberg, J.P. 1995. Strong voltage-dependent inward rectification of inward rectifier K+ channels is caused by intracellular spermine. Cell 80: 149-154.

Fakler, B., Ruppersberg, J.P. 1996. Functional and molecular diversity classifies the family of inward-rectifier K+ channels. Cell Physiol Biochem 6: 195-209.

Falk, T., Meyerhof, W., Corrette, B.J., Schäfer, J., Bauer, C.K., Schwarz, J.R., Richter, D. 1995. Cloning, functional expression and mRNA distribution of an inwardly rectifying potassium channel protein. FEBS Letters 367: 127-131.

Felix, R. 2000. Channelopathies: ion channel defects linked to heritable clinical disorders. J. Med. Gen. 37: 729-740.

Flaherty, A.W. and Graybiel, A.M. 1991. Corticostriatal transformations in the primate somatosensory system. Projections from physiologically mapped body-part representations. J. Neurophysiol. 66: 1249-1263.

Gerfen, C.R. 1992. The neostriatal mosaic: multiple levels of compartmental organization. TINS 15, 133-138.

Gerfen, C.R. 1989. The neostriatal mosaic. Striatal patch-matrix organization is related to cortical lamination. Science 246: 385-388.

Glowatzki, E., Fakler, G., Brandle, U., Rexhaausen, U., Zenner, H.P., Ruppersberg, J.P., and Fakler, B. 1995. Subunit-dependent assembly of inward-rectifier K+ channels. Proc R Soc Lond B Biol Sci 261: 251-261.

Graybiel, A. M. 1990. Neurotransmitters and neuromodulators in the basal ganglia. TINS 13, 244-254.

Groenewegen, H.J., Wright, C.I., and Beijer, A.V.J. 1996. The nucleus accumbens: gateway for limbic structures to reach the motor system? Progress in Brain Research 107: 485-511.

Groves, P.M. et al.1995. In: Models of information processing in the basal ganglia (Houk, J.C., Davis, J.L., and Beiser, D.G., eds), pp. 51-96, MIT Press.

Haber, S.N., Fudge, J.L., and McFarland, N.R. 2000. Striatonigrostriatal pathways in primates form an ascending spiral from the shell to the dorsolateral striatum. The Journal of Neuroscience 20: 2369–2382.

Herkenham, M. and Pert, C.B. 1981. Mosaic distribution of opiate receptors, parafascicular projections and acetylcholinesterase in the rat striatum. Nature 291: 415-418.

Hibino, H., Horio, Y., Inanobe, A., Doi, K., Ito, M., Yamada, M., Gotow, T., Uchiyama, Y., Kawamura, M., Kubo, T., Kurachi, Y. 1997. An ATP-dependent inwardly rectifying potassium channel, KAB-2 (Kir4.1), in cochlear stria vascularis of inner ear: its specific subcellular localization and correlation with the formation of endocochlear potential. J Neurosci 17: 4711-4721.

Hille, B. (Ed.) 1995. Ionic channels of excitable membranes. Sinauer Associates, Sunderland, MA.

Ho, K., Nichols, C.G., Lederer, W.J., Lytton, J., Vassilev, P.M., Kanazirska, M.V., Hebert, S.C. 1993. Cloning and expression of an inwardly rectifying ATP-regulated potassium channel. Nature 362: 31-38.

Hodgkin, A.L., Huxley, A.F., and Katz, B. 1952. Measurements of current-voltage relations in the

membrane of the giant axon of Laligo. J Physiol (Lond) 116: 424-448.

Horio, Y., Morishige, K.-I., Takahashi, N., and Kurachi, Y. 1996. Differential distribution of classical inwardly rectifying potassium channel mRNAs in the brain: Comparison of IRK2 with IRK1 and IRK3. FEBS Lett. 379: 239-243.

Huang, C.L., Feng, S., and Hilgemann, D.W. 1998. Direct activation of inward rectifier potassium channels by PIP2 and its stabilization by Gbg. Nature 391: 803-806.

Hughes, B.A., Kumar, G., Yuan, Y., Swaminathan, A., Yan, D., Sharma, A., Plumley, L., Yang-Feng, T.L., Swaroop, A. 2000. Cloning and functional expression of human retinal Kir2.4, a pH-sensitive inwardly rectifying K+ channel. Am J Physiol Cell Physiol 279: C771-C784.

Inanobe, A., Fujita, A., Ito, M., Tomoike, H., Inageda, K., Kurachi, Y. 2002. Inward rectifier K+ channel Kir2.3 is localized at the postsynaptic membrane of excitatory synapses. Am. J. Physiol. 282: C1396-C1403.

Ishii, M., Horio, Y., Tada, Y., Hibino, H., Inanobe, A., Ito, M., Yamada, M., Gotow, T., Uchiyama, Y., Kurachi, Y. 1997. Expression and clustered distribution of an inwardly rectifying potassium channel, KAB-2/Kir4.1, on mammalian retinal Müller cell membrane: their regulation by insulin and laminin signals. J Neurosci 17: 7725-7735.

Isomoto, S., Kondo, C., and Kurachi, Y. 1997. Inwardly rectifying potassium channels: their molecular heterogeneity and function. Japanese Journal of Physiology 47: 11-39.

Jan, L.Y. and Jan, Y.N. 1997. Cloned potassium channels from eucaryotes and procaryotes. Annu. Rev. Neurosci. 20: 91–123.

Jin, W. and Lu, Z. 1998. A novel high-affinity inhibitor for inward-rectifier K+ channels. Biochemistry 37: 13291-13299.

Joel, D. and Weiner, I. 2000. The connections of the dopaminergic system with the striatum in rats and primates: an analysis with respect to the functional and compartmental organization of the striatum. Neuroscience 96: 451–474.

Jongen-Rêlo, A.L., Voorn, P., and Groenewegen, H.J. 1994. Immunohistochemical characterization of the shell and core territories of the nucleus accumbens in the rat. Eur. J. Neurosci. 6: 1255-1264.

Karschin, C., Dissmann, E., Stuhmer, W., and Karschin, A. 1996. IRK(1-3) and GIRK(1-4) inwardly rectifying K+ channel mRNAs are differentially expressed in the adult rat brain. J. Neurosci. 16, 3559-3570.

Karschin, C. and Karschin, A. 1997. Ontogeny of gene expression of Kir channel subunits in the rat. Molecular and Cellular Neuroscience 10: 131–148.

Karschin, C. and Karschin, A. 1999. Distribution of inwardly rectifying potassium channels in the brain. Current Topics in Membranes 46: 273-292.

Katz, B. 1949. Les constantes électriques de la membrane du muscle. Arch. Sci. Physiol. 2: 285-299.

Kawaguchi, Y., Wilson, C.J., and Emson, P.C. 1990. Projection subtypes of rat neostriatal matrix

cells revealed by intracellular injection of biocytin. J. Neurosci. 10: 3421-3438.

Kawaguchi, Y., Wilson, C.J., Augood, S.J., and Emson, P.C. 1995. Striatal interneurons: chemical, physiological and morphological characterization. Trends Neurosci. 18: 527-535.

Kita, H. and Kitai, S.T. 1988. Glutamate decarboxylase immunoreactive neurons in rat neostriatum: Their morphological types and populations. Brain Res. 447: 346-352.

Kooy, D. van d., Fishell, G. 1987. Neuronal birthdate underlies the development of striatal compartments. Brain Research 401: 155-161.

Koyama, H., Morishige, K.I., Takahashi, N., Zanelli, J.S., Fass, D.N., Kurachi, Y. 1994. Molecular cloning, functional expression and localization of a novel inward rectifier potassium channel in the rat brain. FEBS Letters 341: 303-307.

Krapivinsky, G., Gordon, E.A., Wickman, K., Velimirovic, B., Krapivinsky, L., Clapham, D.E. 1995. The G-protein-gated atrial K+ channel IKACh is a heteromultimer of two inwardly rectifying K+ channel proteins. Nature 374: 135-141.

Kubo, Y., Baldwin, T.J., Jan, Y.N., and Jan, L.Y. 1993. Primary structure and functional expression of a mouse inward rectifier potassium channel. Nature 362: 127-133.

Kubo, Y. and Murata, Y. 2001. Control of rectification and permeation by two distinct sites after the second transmembrane region in Kir2.1K+ channel. Journal of Physiology 531.3: 645–660.

Laemmli, U.K. 1970. Cleavage of structural proteins during the assembly of the head of bacteriophage T4. Nature 227:680-685.

Lee, J.K., John, S.A., Weiss, J.N. 1999. Novel gating mechanism of polyamine block in the strong inward rectifier K+ channel Kir2.1. J. Gen. Physiol. 113: 555-563.

Liao, Y.J., Jan, Y.N., and Jan, L.Y. 1996. Heteromultimerization of G-protein-gated inwardly rectifying K+ channel proteins GIRK1 and GIRK2 and their altered expression in weaver brain. J. Neurosci. 16: 7137-7150.

Liu, G.X., Derst, C., Schlichthörl, G., Heinen, S., Seebohm, G., Brüggemann, A., Kummer, W., Veh, R.W., Daut, J., and Preisig-Müller, R. 2001. Comparison of cloned Kir2 channels with native inward rectifier K+ channels from guinea-pig cardiomyocytes. J. Physiol. 532.1: 115-126.

Lopatin, A.N., Makhina, E.N., and Nichols, C.G. 1994. Potassium channel block by cytoplasmic polyamines as the mechanism of intrinsic rectification. Nature 372: 366-369.

Lu, Z. and MacKinnon, R. 1994. Electrostatic tuning of Mg2+ affinity in an inward-rectifier K+ channel. Nature 371: 243-246.

MacKinnon, R., Cohen, S.L., Kuo, A., Lee, A., Chait, B.T. 1998. Structural conservation in prokaryotic and eukaryotic potassium channels. Science 280: 106-109.

Minor, D.L., Masseling, S.J., Jan, Y.N., and Jan, L.Y. 1999. Transmembrane structure of an inwardly rectifying potassium channel. Cell 96: 879–891.

Mermelstein, P.G., Song, W.-J., Tkatch, T., Yan, Z., and Surmeier, D.J. 1998. Inwardly rectifying

potassium (IRK) currents are correlated with IRK subunit expression in rat nucleus accumbens medium spiny neurons. Journal of Neuroscience 18: 6650-6661.

Miyashita, T., and Kubo, Y. 1997. Localization and developmental changes of the expression of two inward rectifying K+ channel proteins in the rat brain. Brain Res. 750: 251-263.

Morishige, K.-I., Takahashi, N., Findlay, I., Koyama, H., Zanelli, J.S., Peterson, C., Jenkins, N.A., Copeland, N.G., Mori, N., and Kurachi, Y. 1993. Molecular cloning, functional expression and localization of an inward rectifier potassium channel in the mouse brain. FEBS Letters 336: 375-380.

Namba, N., Inagaki, N., Gonoi, T., Seino, Y., Seino, S. 1996. Kir2.2v: a possible negative regulator of the inwardly rectifying K+ channel Kir2.2. FEBS Letters 386: 211-214.

Nicola, S.M., Surmeier, D.J., Malenka, R.C. 2000. Dopaminergic modulation of neuronal excitability in the striatum and nucleus accumbens. Annu Rev Neurosci 23: 185-215.

Nishida, M., MacKinnon, R. 2002. Structural Basis of Inward Rectification: Cytoplasmic Pore of the G Protein-Gated Inward Rectifier GIRK1 at 1.8 Å Resolution. Cell 111: 957–965.

Nisenbaum, E.S., Wilson, C.J. 1995. Potassium currents responsible for inward and outward rectification in rat neostriatal spiny projection neurons. Journal of Neuroscience 15: 4449-4463.

Parent, A. 1990. Extrinsic connections of the basal ganglia. TINS 13, 254-258.

Parent, A., Sato, F., Wu, Y., Gauthier, J., Lévesque, M., and Parent, M. 2000. Organization of the basal ganglia: the importance of axonal collateralization. TINS 23, S20-S27.

Parent, M., Levesque, M., Parent, A. 2001. Two types of projection neurons in the internal pallidum of primates: single-axon tracing and three-dimensional reconstruction. J. Comp. Neurol. 439: 162-175.

Patil, N., Cox, D.R., Bhat, D., Faham, M., Myers, R.M., Peterson, A.S. 1995. A potassium channel mutation in weaver mice implicates membrane excitability in granule cell differentiation. Nat. Genet. 11: 126-129.

Paxinos, G. and Watson, Ch. 1998. The rat brain in stereotaxic coordinates. 4th edition. Academic press, San Diego.

Penny, G.R. et.al. 1986. The glutamate decarboxylase immunoreactive, met-enkephalin-immunoreactive and substance P-immunoreactive neurons in the neostriatum of the rat and cat. Evidence for partial population overlap. Neuroscience 17: 1011-1045.

Perillán, P.R., Li, X., Potts, E.A., Chen, M., Bredt, D.S., and Simard, J.M. 2000. Inward rectifier K+ channel Kir2.3 in reactive astrocytes from adult rat brain. Glia 31: 181-192.

Pert, C.B., Kuhar, M.J., and Snyder, S.H. 1976. Opiate receptor: autoradiographic localization in rat brain. Proc. Natl. Acad. Sci. USA 73: 3729-3733.

Pitt, J.C., Lindemeier, J., Habbes, H.W., Veh, R.W. 1998. Haptenylation of antibodies during affinity purification: a novel and convenient procedure to obtain labeled antibodies for quantification and double labeling. Histochem. Cell Biol. 110: 311-322.

Plaster, N.M., Ptáček, L.J. et al. 2001. Mutations in Kir2.1 Cause the Developmental and Episodic Electrical Phenotypes of Andersen's Syndrome. Cell 105: 511–519.

Pompéia, C., Ortis, F., Armelin, M.C.S. 1996. Immunopurification of polyclonal antibodies to recombinant proteins of the same family. Biotechniques 21: 986.

Prüss, H., Wenzel, M., Eulitz, D., Thomzig, A., Karschin, A., Veh, R.W. 2003. Kir2 potassium channels in rat striatum are strategically localized to control basal ganglia function. Mol. Brain Res. 110: 203-219.

Qu, Z., Zhu, G., Yang, Z., Cui, N., Li, Y., Chanchevalap, S., Sulaiman, S., Haynie, H., and Jiang, C. 1999. Identification of a critical motif responsible for gating of Kir2.3 channel by intracellular protons. The Journal of Biological Chemistry 274: 13783-13789.

Qu, Z., Yang, Z., Cui, N., Zhu, G., Liu, C., Xu, H., Chanchevalap, S., Shen, W., Wu, J., Li, Y., and Jiang, C. 2000. Gating of inward rectifier K+ channels by proton-mediated interactions of N- and C-terminal domains. Journal of Biological Chemistry 275: 31573-31580.

Raab-Graham, K.F. and Vandenberg, C.A. 1998. Tetrameric subunit structure of the native brain inwardly rectifying potassium channel Kir 2.2. The Journal of Biological Chemistry 273: 19699-19707.

Raz, A., Feingold, A., Zelanskaya, V., Vaadia, E., Bergmann, H. 1996. Neuronal synchronization of tonically active neurons in the striatum of normal and parkinsonian primates. Journal of Neurophysiology 76: 2083-2088.

Reimann, F. and Ashcroft, F.M. 1999. Inwardly rectifying potassium channels. Current Opinion in Cell Biology 11:503–508.

Ruppersberg, J.P. 2000. Intracellular regulation of inward rectifier K+ channels. Pflügers Arch – Eur J Physiol 441: 1-11.

Sakura, H., Ammala, C., Smith, P.A., Gribble, F.M., and Ashcroft, F.M. 1995. Cloning and functional expression of the cDNA encoding a novel ATP-sensitive potassium channel subunit expressed in pancreatic beta-cells, brain, heart and skeletal muscle. FEBS Letters 377: 338-344.

Sanguinetti, M.C. and Spector, P.S. 1997. Potassium Channelopathies. Neuropharmacology 36: 755-762.

Scheinman, S.J., Guay-Woodford, L.M., Thakker, R.V., Warnock, D.G. 1999. Genetic disorders of renal electrolyte transport. New Engl. J. Med. 340: 1177-1187.

Signorini, S., Liao, Y.J., Duncan, S.A., Jan, L.Y., and Stoffel, M. 1997. Normal cerebellar development but susceptibility to seizures in mice lacking G protein-coupled, inwardly rectifying K+ channel GIRK2. Proc. Natl. Acad. Sci. USA 94: 923-927.

Skatchkov, S.N., Thomzig, A., Eaton, M.J., Biedermann, B., Eulitz, D., Bringmann, A., Pannike, T., Veh, R.W., Reichenbach, A. 2001. Kir subfamily in frog retina: specific spatial distribution of Kir6.1 in glial (Müller) cells. NeuroReport 12: 1437-1441.

Stanfield, P.R., Nakajima, Y., and Yamaguchi, K. 1985. Substance P raises neuronal membrane

excitability by reducing inward rectification. Nature 315: 498-501.

Stanfield, P.R., Davies, N.W., Shelton, P.A., Sutcliffe, M.J., Khan, I.A., Brammer, W.J., and Conley, E.C. 1994. A single aspartate residue is involved in both intrinsic gating and blockage by Mg2+ of the inward rectifier Kir2.1. Journal of Physiology: 478: 1-6.

Stockklausner, C., Ludwig, L., Ruppersberg, J.P., Klöcker, N. 2001. A sequence motif responsible for ER export and surface expression of Kir2.0 inward rectifier K+ channels. FEBS Letters 493: 129-133.

Stonehouse, A.H., Pringle, J.H., Norman, R.I., Stanfield, P.R., Conley, E.C., Brammar, W.J. 1999. Characterisation of Kir2.0 proteins in the rat cerebellum and hippocampus by polyclonal antibodies. Histochem. Cell. Biol. 112: 457-465.

Surmeier, D.J. et.al. 1996. Coordinated expression of dopamine receptors in neostriatal medium spiny neurons. J. Neurosci. 16: 6579-6591.

Taglialatela, M., Wible, B.A., Caporaso, R., Brown, A.M. 1994. Specification or pore properties by the carboxyl terminus of inwardly rectifying K+ channels. Science 264: 844-847.

Thomzig, A., Wenzel, M., Karschin, C., Eaton, M.J., Skatchkov, S.N., Karschin, A., Veh, R.W. 2001. Kir6.1 is the principal pore-forming subunit of astrocyte but not neuronal plasma membrane K-ATP channels. Mol. Cell. Neurosci. 18: 671-690.

Thomzig, A., Prüss, H., Veh, R.W. 2003. The Kir6.1-protein, a pore-forming subunit of ATP-sensitive potassium channels, is prominently expressed by giant cholinergic interneurons in the striatum of the rat brain. Brain Res. 986: 132-138.

Töpert, C., Döring, F., Wischmeyer, E., Karschin, C., Brockhaus, J., Ballanyi, K., Derst, C., and Karschin, A. 1998. Kir2.4: A novel K+ inward rectifier channel associated with motoneurons of cranial nerve nuclei. The Journal of Neuroscience 18: 4096–4105.

Töpert, C., Döring, F., Derst, C., Daut, J., Grzeschik, K.H., and Karschin, A. 2000. Cloning, structure and assignment to Chromosome 19q13 of the human Kir2.4 inwardly rectifying potassium channel gene (KCNJ14). Mammalian Genome 11: 247-249.

Trytek, E.S., White, I.M., Schroeder, D.M., Heidenreich, B.A., Rebec, G.V. 1996. Localization of motor- and nonmotor-related neurons within the matrix-striosome organization of rat striatum. Brain Research 707: 221-227.

Veh, R.W., Lichtinghagen, R., Sewing, S., Wunder, F., Grumbach, I.M., Pongs, O. 1995. Immunohistochemical localization of five members of the Kv1 channel subunits: Contrasting subcellular locations and neuron-specific co-localizations in rat brain. Eur. J. Neurosci. 7: 2189-2205.

Voorn, P., Brady, L.S., Berendse, H.W., and Richfield, E.K. 1996. Densitometrical analysis of opioid receptor ligand binding in the human striatum –I. Distribution of μ opioid receptor defines shell and core of the ventral striatum. Neuroscience 75: 777-792.

Vulpen, E.H.S. van, van der Kooy, D. 1998. Striatal cholinergic interneurons: birthdates predict compartmental localization. Developmental Brain Research 109: 51–58.

Watanabe, K., Kimura, M. 1998. Dopamine receptor-mediated mechanisms involved in the expression of learned activity of primate striatal neurons. J Neurophysiol 79: 2568-2580.

White, N. and Hiroi, N. 1998, Preferential localization of self-stimulation sites in striosomes/patches in the rat striatum. Neurobiology 95, 6486-6491.

Wilson, C.J. 1993. The generation of natural firing patterns in neostriatal neurons. Prog. Brain Res. 99:277–97.

Wilson, C. in Shepherd, G. 1998. The synaptic organization of the brain, Oxford University Press.

Wilson, C.J., Chang, H.T., and Kitai, S.T. 1990. Firing patterns and synaptic potentials of identified giant aspiny interneurons in the rat neostriatum. J. Neurosci. 10: 508-519.

Wilson, C.J. and Kawaguchi, Y. 1996. The origins of two-state spontaneous membrane potential fluctuations of neostriatal spiny neurons. J. Neurosci. 16:2397–410.

Wischmeyer, E., Döring, F., and Karschin, A. 1998. Acute suppression of inwardly rectifying Kir2.1 channels by direct tyrosine kinase phosphorylation. The Journal of biological chemistry 273: 34063-34068.

Yamashita, T., Horio, Y., Yamada, M., Takahashi, N., Kondo, C., and Kurachi, Y. 1996. Competition between Mg2+ and spermine for a cloned IRK2 channel expressed in a human cell line. J Physiol (Lond) 493: 143-156.

Yang, J., Jan, Y.N., and Jan, L.Y. 1995. Control of rectification and permeation by residues in two distinct domains in an inward rectifier K+ channel. Neuron 14: 1047-1054.

Zhu, G., Chanchevalap, S., Cui, N., and Jiang, C. 1999a. Effects of intra- and extracellular acidifications on single channel Kir2.3 currents. Journal of Physiology 516.3: 699-710.

Zhu, G., Qu, Z., Cui, N, and Jiang, C. 1999b. Suppression of Kir2.3 activity by protein kinase C phosphorylation of the channel protein at threonine 53. The Journal of biological chemistry 274: 11643-11646.

Curriculum vitae

Persönliche Daten

Name:	Harald Prüß
Geburtsdatum, -ort	10. 02. 1977, Güstrow
Anschrift:	Seidelstraße 5 D – 18273 Güstrow
Telefon:	+ 49 / (0) 38 43 - 68 47 11
E-Mail:	harald.pruess@gmx.de
Staatsangehörigkeit:	Bundesrepublik Deutschland
Familienstand:	ledig

Ausbildung

Schulausbildung:

1995	Abitur (Gesamtnote 1,0)

Studium:

seit 10/96	Studium der Humanmedizin an der medizinischen Fakultät der Humboldt-Universität zu Berlin (Charité)
1998	Staatliche Vorprüfung (Physikum)
2000	1. Staatsexamen (Note 1,0)
2001	Amerikanisches Staatsexamen USMLE Step 1
2002	2. Staatsexamen (Note 1,0) Amerikanisches Staatsexamen USMLE Step 2
2003	3. Staatsexamen (Note 1,0)
Dissertation (1998-2003)	„Kir2-Kaliumkanäle besetzen selektiv die Schlüsselpositionen für die Kontrolle der Basalganglien-Schleifen in der Ratte“ Experimentelle Doktorarbeit in der Arbeitsgruppe Prof. Veh, Institut für Molekulare Neuroanatomie und Elektronenmikroskopie, Charité

Wehr-/Zivildienst

1995-96	Grundwehrdienst im Sanitätsdienst der Bundeswehr, Giebelstadt und Kronskamp

Famulaturen

03-04/1999	Chirurgie / Traumatologie, Kreiskrankenhaus Güstrow
08-10/1999	Allgemeinmedizin / Family Practice, Scottdale, PA, USA
08-09/2000	Neurologie, St.-Josef-Krankenhaus Oberhausen

Praktisches Jahr

2002-2003	Innere Medizin, St. Gallen, Schweiz Neurochirurgie, St. Louis, MO, USA Chirurgie, Inverness, Scotland, UK Neurologie, Charité Berlin

Weitere Tätigkeiten

1999-2000	Studentische Hilfskraft am Lehrstuhl für Elektronenmikroskopie und Molekulare Neuroanatomie von Prof. Dr. R.W. Veh an der Charité
1997-2003	Tutor am Institut für Anatomie der Charité: Studentenbetreuung im Präparier- und Hirnkurs

Posterpräsentationen und

Vorträge

2000	European Neuroscience Meeting, Brighton, UK
	European Students Conference, Berlin
	Jahrestagung der Deutschen Gesellschaft für Anatomie, Würzburg
2001	DFG Schwerpunkttreffen, Berlin
	Jahrestagung der Deutschen Gesellschaft für Anatomie, Würzburg
	Society of Neuroscience Meeting, San Diego, USA

Zusätzliche Qualifikationen

Fremdsprachen:	Englisch: Abitur (Leistungskurs), mehrmonatige Auslandsaufenthalte in USA und UK
	Russisch: Abitur (Klasse 3-10)
EDV-Kenntnisse:	Anwendungssoftware: Microsoft Office
	Betriebssysteme: Windows 95/98/00/XP
	Programmiersprache: Turbo Pascal
Führerschein:	Klassen 1, 3, 4, 5

Private Interessen

Ornithologie/Naturschutz, künstlerisches Gestalten, Schwimmen, Belletristik

Harald Prüß

Publications

Full Papers:

Prüss H, Wenzel M, Eulitz D, Thomzig A, Karschin A, Veh RW (2003) Kir2 potassium channels in rat striatum are strategically localized to control basal ganglia function. Mol Brain Res 110:203-219

Thomzig A, **Prüss H**, Veh RW (2003) The Kir6.1 Protein, a Pore-Forming Subunit of K-ATP Channels, is Prominently Expressed by Giant Cholinergic Interneurons of the Striatum in the Rat Brain. Brain Res 986: 132-138.

Lectures:

Prüss H, Wenzel M, Karschin A, Veh RW (2001) Kir2 inwardly rectifying potassium channels occupy key positions for regulation of basal ganglia circuits. 18. Arbeitstagung der Anatomischen Gesellschaft, 26.-28. September 2001, Würzburg

Prüss H, Wenzel M, Karschin A, Veh RW (2001) Kir2 potassium channels in rat striatum are strategically localized to control basal ganglia function. DFG-Schwerpunkttreffen, Kalium-Kanäle, Berlin

Abstracts:

Prüss H, Lemcke J, Brune A, Wenzel M, Veh RW (2000) Localization of Kir2.2 and Kir2.3 proteins in rat substantia nigra, VTA and raphe nuclei. European Journal of Neuroscience 12 (suppl): 453

Prüss H, Lemcke J, Brune A, Wenzel M, Veh RW (2000) Cellular and subcellular distribution of Kir2.2 and Kir2.3 proteins in rat striatum, cerebellum and raphe nuclei. Ann Anat 183 (suppl): 276

Prüss H, Lemcke J, Brune A, Wenzel M, Veh RW (2001) Differential distribution of Kir2.2 and Kir2.3 proteins in rat substantia nigra, VTA, cerebellum and raphe nuclei. European Students Conference, Berlin, 2001

Prüss H, Wenzel M, Stroh T, Veh RW (2001) Kir2 Inwardly Rectifying Potassium Channels are Differentially Expressed in Striatal Compartments. Soc Neurosci Abstr 27:182

Wenzel M, **Prüss H**, Thomzig A, Goertzen A, Veh RW (2001) Cholinergic Striatal Neurons Express the Kir2.4 Subunit of Inwardly Rectifying Potassium Channels. Soc Neurosci Abstr 27:182

Prüss H, Wenzel M, Karschin A, Veh RW (2002) Kir2 inwardly rectifying potassium channels occupy key positions for regulation of basal ganglia circuits. Ann Anat 184 (suppl):179

Danksagung

Für die langjährige ganzheitliche Betreuung und Anleitung meiner Arbeit im Institut für Anatomie möchte ich mich herzlich bei Prof. Dr. R.W. Veh bedanken. Sowohl die Bereitstellung des vorliegenden spannenden Forschungsthemas als auch die zahlreichen interessanten Gespräche haben mein Interesse an der Wissenschaft und dem ärztlichen Beruf erweitert und dabei Impulse gegeben, die weit über die Arbeit im Institut hinausgingen.

Ebenso gilt mein aufrichtiger Dank den zahlreichen wissenschaftlichen und technischen Mitarbeitern, durch deren Hilfe so manche Hürde der Laborarbeit genommen werden konnte. Die durch Freundlichkeit und wechselseitige Hilfe gekennzeichnete Atmosphäre behalte ich in dankbarer Erinnerung und sehe sie als Maßstab für meinen weiteren beruflichen und privaten Weg.

Darüber hinaus fühle ich mich besonders meiner Familie und allen Freunden sehr verbunden, die mich auf diesem Weg begleitet haben, meinen Enthusiasmus stets unterstützten und durch Motivation und Rückhalt den nötigen Raum für mein Arbeiten gaben.

Eidesstattliche Erklärung

Hiermit erkläre ich an Eides Statt, dass die Dissertation von mir selbst und ohne die unzulässige Hilfe Dritter verfasst wurde, auch in Teilen keine Kopie anderer Arbeiten darstellt und die benutzten Hilfsmittel sowie die Literatur vollständig angegeben sind.

Harald Prüß